TOOL WEAR MONITORING IN END MILLING OF MOULD STEEL USING ACOUSTIC EMISSION

OLUFAYO, OLUWOLE AYODEJI

(S210026162)

2011

Copyright Statement

TOOL WEAR MONITORING IN END MILLING OF MOULD STEEL USING ACOUSTIC EMISSION

By

Olufayo, Oluwole Ayodeji

Submitted in fulfilment/partial fulfilment of the requirements for the degree of Masters of Engineering at the Nelson Mandela Metropolitan University

December 2011

Promoter/Supervisor: Prof. Khaled Abou-El-Hossein

Co-Promoter/Co-Supervisor: Prof. Theo Ian van Niekerk

Author's Declaration

I, Olufayo, Oluwole Ayodeji hereby declare that:

- The work done in this thesis is my own;
- All sources used or referred to have been documented and recognized; and
- This thesis has not been previously submitted in full or partial fulfilment of the requirements for an equivalent or higher qualification at any other educational institution.

Author Signature Date: December 2011

Dedication

This treatise is dedicated to the **ALMIGHTY GOD**, who gave me the will and enablement to accomplish the goals for this phase of my academic development

My Lord and Saviour, Jesus Christ.

Acknowledgement

Sincere gratitude and appreciation goes to my promoter, Prof Khaled Abou-El-Hossein, for his support, guidance and mentorship and throughout the period of study. Furthermore, I am grateful to my co-supervisor, Prof Theo Van-Niekerk for all the assistance, guidance and the experience opportunities; AMTC for the facilities offered to me during my studies. I would like to acknowledge eNtsa, under the leadership of Prof D. G. Hattingh, Mr A. Young and Mr J. Cizek for all the technical assistance in the use of the CNC machine, Mr G. C. Erasmus for his assistance in the Metallurgy lab. I would also like to thank my fellow researchers – the currently registered Degree and Masters Students for their moral support.

I also would like to acknowledge Technology Innovation Agency / Department of Science and Technology of South Africa and Research Capacity development of NMMU for the financial support provided for this research.

Special gratitude also goes to my parents, Prof. and Dr (Mrs) Olufayo, who have instilled in me a deep love for the academics. You encouraged me and to be an engineer like you. Thank you dad! To my big auntie, Dr (Mrs) Esther Titilayo Akinlabi, I say a big “Thank you”, for your support and mentorship. Also, my appreciation goes to my uncle Mr Akinlabi, Akinkunmi, Stephanie, - Dr and Mrs F. A. Emuze, Dr and Mrs K. A. Olowu, Mr and Mrs R. A. Jimoh, Mrs Olutobi, Liliane Creppy and my closest best pal, my dear sister Motunrayo Olufayo.

I remain grateful to all my friends – John Fernandes, Christiaan Pretorius, Sarel Bezuidenhout, Tim Otieno Hennie Van Rooyen, Akshay Lakhani, Kayode Oyedemi, Ama Boateng, Ikho Bambiso and colleagues who in one way or another have assisted me in being who I am. Thank you.

Abstract

Today's production industry is faced with the challenge of maximising its resources and productivity. Tool condition monitoring (TCM) is an important diagnostic tool and if integrated in manufacturing, machining efficiency will increase as a result of reducing downtime resulting from tool failures by intensive wear.

The research work presented in the study highlights the principles in tool condition monitoring and identifies acoustic emission (AE) as a reliable sensing technique for the detection of wear conditions. It reviews the importance of acoustic emission as an efficient technique and proposes a TCM model for the prediction of tool wear. The study presents a TCM framework to monitor an end-milling operation of H13 tool steel at different cutting speeds and feed rates. For this, three industrial acoustic sensors were positioned on the workpiece. The framework identifies a feature selection, extraction and conditioning process and classifies AE signals using an artificial neural network algorithm to create an autonomous system. It concludes by recognizing the mean and rms features as viable features in the identification of tool state and observes that chip coloration provides direct correlation to the temperature of machining as well as tool condition.

This proposed model is aimed at creating a timing schedule for tool change in industries. This model ultimately links the rate of wear formation to characteristic AE features.

Table of Contents

List of Tables

List of Figures

Chapter 1 Introduction

1.1 Preface

Due to the rapid growth in cutting edge technology the need for a healthy manufacturing sector is essential to meet the market demand. Machining is an important process to consider in large scale industrial production. Numerous cutting operations are employed in a machining environment. These operations are aimed at the removal of material by power-driven machine tools to mechanically cut the material or generate required geometry. Modern day machining is controlled by the use of computers. Computer Numerical Control (CNC) machine tools are driven by abstractly programmed commands which automate machining to facilitate the cutting process.

The influence of the CNC machining on the automation of the manufacturing process is substantial but this innovation fails to monitor the quality of its operations. The challenge of wear formation on the edges of the tools, which causes defects on the workpiece, poses a threat to total automation. Thus, the introduction of an adequate tool condition monitoring system is vital.

TCM as a modern diagnostic tool provides an opportunity to orthodox routine manufacturing systems to adequately and efficiently control their operations. It provides the building blocks for intelligent futuristic and autonomous manufacturing.

This study creates and evaluates a TCM model with evolutionary techniques for improved productivity in manufacturing.

1.2 Tool condition monitoring in industry

The industrial revolution of today's manufacturing industries is anchored around various cutting operations. Such processes range from milling, cutting, drilling, turning and grinding operations. These operations which form a potent underlying factor in the production of engineering products are constrained by low efficiency and high cost. Due to these challenges an adequate monitoring system is essential to ensure optimal yield.

Tool Condition monitoring is a modern monitoring approach used in the industrial sector for various processing operations including machining. This monitoring process oversees the state of the cutting tool during machining operations to help predict tool life and alert for tool replacement in time to avoid downtime condition.

TCM in machining operations of today's manufacturing is also paramount for high productivity. This system of monitoring of machining operation is used to determine the overall system effectiveness (OOE) of the production line [1].

The OOE largely depends on the amount of downtimes caused by the machine breakdown as a result of tool failure. In monitoring on-line downtime conditions, two problem sources are identified. One problem is caused by the transfer of work piece between machines and the other by excessive wear and breakage generated on tools during machining [2]. The downtime generated from transfer of work pieces is unfortunately unavoidable during operation, but tool wear can be monitored and controlled successfully.

TCM could be performed on various cutting operations to determine the wear rates. Operations such as cutting, grinding, milling and drilling are common industrial

machining operations that could be successfully monitored. Numerous research efforts have been conducted in this field. There has been significant interest in the monitoring and study of face-milling and turning operations. The reasons why these research efforts are delineated towards these conventional cutting operations is because of the ease of monitoring, low expenses involved and high quality of obtained signals.

In this study, downtime conditions caused by wear on tool flank are monitored. The research also focuses on the widely researched milling operation, which is heavily used in industries.

1.3 Study objectives

This research aims at monitoring tool wear during a milling operation through acoustic signals captured by a multi-sensor data acquisition system.

The research will monitor milling machining operation at different combinations of process parameters when cutting tool steel to link the rate of wear generated on the tools to the AE data. The developed monitoring technique will help to determine the necessary time interval between successive tool changes. The work is expected to produce a model that can describe the behaviour of cutting tools based on the characteristics of the AE signal.

1.4 Study scope

The scope of this research was identified accordingly:

- To carry out a feasibility study which highlights the principles of tool condition monitoring processes using AE sensing technologies
- To monitor tool steel metals on milling machining operations at high speed utilising three industrial AE sensors at different positioning arrangements.
- To analyse signal parameters obtained through an artificial intelligent network.
- To create a model which links the rate of wear generated on the tool to the AE data for an optimal tool change timing sequence.

1.5 Hypothesis

The integration of a data acquisition system with a multi-sensing technology on machining operations during the real time usage may be realised to monitor wear formation on tool inserts, and produce efficient tool change timing schedule.

For that we may use a simultaneous sampling multifunction data acquisition system, based on computer architecture and driven by a graphical programming language to develop an acquisition framework which harmonizes sensor acquisition, monitors and analyses signals.

1.6 Delimitations

This research is intended to provide a guided practice to the use of AE data to determine wear rate in machining operations. However, the scope of this research is limited to its implementation on the milling machining process and the use of the machine tools having rigidity and stiffness close to the one used in this experimental work. The factors considered for the estimation of the wear values are limited to the speed of rotation and feed.

In addition, the results could be generalised for cases where the cutting tool and workpiece are made from carbides and mould steels respectively.

1.7 Significance of research

The benefits gained from automating manufacturing process are challenged by the high cost and reduced efficiency incurred from sudden tool damages as a result of excessive tool wear. Tool wear monitoring technique based on an artificial intelligence structure addresses the challenges in tool condition monitoring.

The importance of acoustic emission in machining as a sensing parameter is under-emphasized. Acoustic emission as a sensing parameter is an adequate source of information on the real-time operations. Its continuous source generation aids to classify the system responses and information to create a monitoring impression of the machining process.

Major manufacturing industries in South Africa, such as the automobile industries, concerned with massive machining operations could reduce their production costs and improve the yearly turn-out by the implementation of an optimal tool change timing sequence using this solution.

This study would create a conceptual and fundamental model which could be extended to numerous cutting operations, workpiece material and adjusted to fit the manufacturing need in each industrial sector.

1.8 Structure of thesis

Chapter 2 of the thesis describes the relevant theoretical concepts, which underline TCM. It includes a progressive evolution and areas of study. Chapter 3 expands the

acoustic emission concept as a sensing technique and reviews signal processing and processing techniques employed in TCM. Chapter 4 provides a detailed description of the experimental setup and system process flow. It exposes the implementation methodology and equipment used. Chapter 5 presents the various results observed and discusses the observations. It also presents the correlation of AE features to tool wear and proposes a model for predicting wear formation.

Chapter 2 Literature Review- T.C.M

Tool condition monitoring is a diagnostic process which overviews the state of the tool during machining operations to alert when tool is damaged. TCM in manufacturing is used as a feedback system to obtain information of the cutting process. It enhances manufacturing by creating a platform via which a closed loop control of industrial machines is conceivable. It also gives grounding for modern technological evolutionary techniques such as artificial intelligence.

Advanced capabilities such as a quality control and machine tool diagnostic control are important features postulated in future machine tool designs. Therefore an adequate control of the machining process which reduces unnecessary costs, increasing productivity over time and optimizing process parameters is a desirable trait in manufacturing.

The main disadvantages in TCM range from the costs of sensing for optimal results to the influence of noise from machining environment. The vast choice in sensor and parameter has made TCM ambiguous in application. Some cutting operations have been observed to only perform optimally with distinct TCM models since the manufacturing environment forms a factor for consideration in design. Focused research on specific sensing techniques is also based on costs or ease of data manipulation.

TCM is employed in automotive, tool manufacturing, electrical and mechanical product manufacture and other industries. It is applied in drilling, milling, lathe turning, turning, grinding and other machining operations.

The design of TCM as a precautionary means in machining can be viewed as a categorization model. The classification of the evolving state of the tool is the main concept in TCM. The framework in Figure 2.1 shows the various phases employed, from the signal acquisition to the classifications of features.

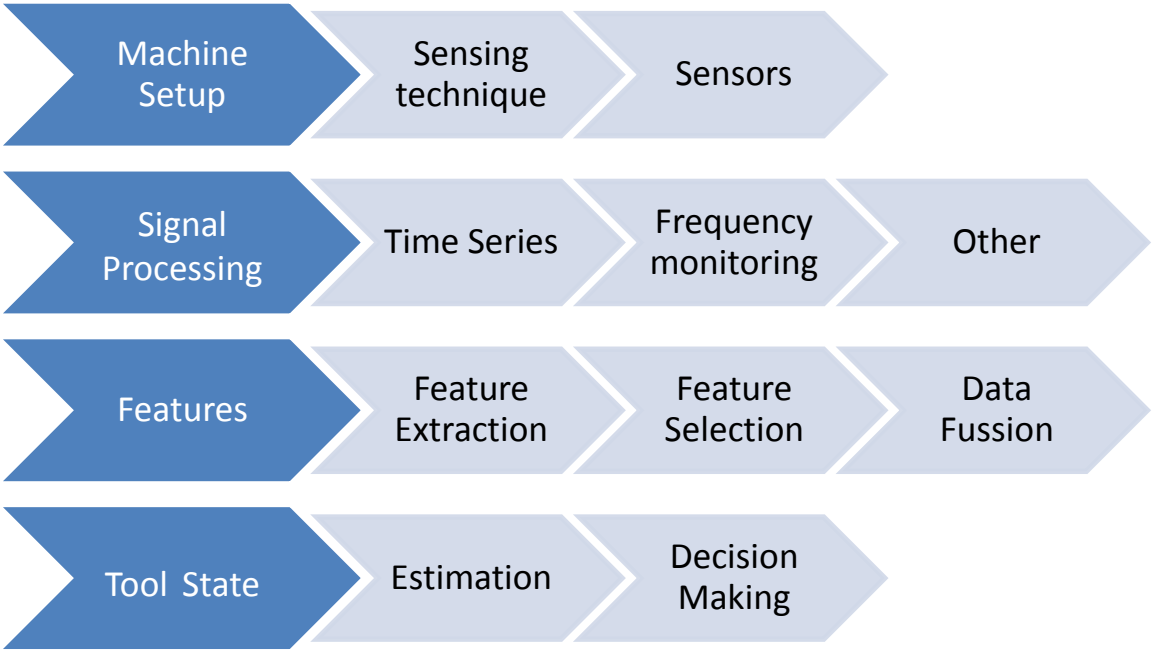

Figure 2.1 Framework of TCM

2.1 Tool life

Tool life is defined as the time elapsed to produce an acceptable workpiece before tool failure [3]. The time of usability of the tool is influenced by the rate of wear formation on its surface. This wear weakens the tool yielding to a catastrophic tool failure. The life of a cutting tool can thus be determined by the amount of wear that has occurred on the tool profile. This wear state reduces the efficiency of cutting tool to an intolerable level or until eventual tool failure occurs [4].

Several definitions have been postulated for tool life. These definitions are founded on the time criterion of usability, output production of the tool or even wear rate standards. One of the most common tool life models are Taylors equations.

Taylor's equation

$$TL = \frac{At}{V_{bt}} \tag{2.1}$$

Where TL is the tool life, V the cutting speed, At and bt are constants [5]

Extended Taylor's equation

$$TL = f(a_{p,}, f, v, VB) = G \cdot a_p^a \cdot f^b \cdot vc \cdot VB^d \tag{2.2}$$

Where f is the feed, v the speed of cutting, a the depth of cut and VB is the flank wear width. G, a, b, c, d are extended Taylor's equation coefficients. Taylor's extended equation is based on the determination of tool life using all cutting parameters and the amount of wear formed whereas its predecessor emphases only on significant parameters i.e. the cutting speed. Although Taylor's equation provides the simple relationship between tool life and certain cutting parameters, as well as possesses an easy implementation process, nonetheless it is limited only to information about tool life [6]. The use of empirical equations to calculate tool life based on cutting parameters such as the depth of cut, feed rate and speed of cutting has been greatly a common practice in many research works [5] [3]. Other empirical relations have related the tool life to tool temperature [5] and also modelled tool life as a stochastic process [7].

2.2 Mechanisms of tool wear

Wear formed on the tool could occur based on some certain modes of formation. The formation modes are termed as the mechanisms of wear. Some common wear mechanisms normally found in the machining environment are as follows:

Abrasion wear: Abrasion occurs as a result of the interaction between the face of the tool and the workpiece. This is characterised by a loss of relief on the flank of the tool. Abrasive wear occurs due to the dissimilarity of the hardness of the two mating materials.

Adhesive wear: Adhesion occurs in metal when the force elements of the material are not as strong as the interactive forces with the workpiece. This yields to the transference of material between the metals. Adhesive wear causes the build-up or welding of the machine chips on the tool cutting edge.

Attrition wear: Attrition is a form of erosive wear effect occurring on cutting tools. It is caused by the impact of particles (liquid, gaseous, solid) on the metal surface which gradually erode fragments of the surface due to its momentum effect.

Fatigue wear: The wear resulting from fatigue is described as the weakening of the material surface by the cyclic loading and unloading during machining. This is noticed in interrupted operations such as milling. Generally, cracks announce the presence of fatigue wear on the tool surface, which eventually leads to total fracture.

Diffusion wear: Diffusion, also known as dissolution wear is an outcome of the gradual dissemination of solid element from one material to the other due to extreme heat and high friction conditions. It involves the decomposition of part the surface of one material and its integration into its opposing mating surface. This normally

occurs at a slow sliding velocity. Diffusion wear is greatly dependent on the material composition of the machined surface. The affinity of some elements in the material towards opposing elements could enhance the rate of diffusion wear experienced in machining. This wear mechanism is mostly experienced in the machining of ceramic materials with diamond tools.

Corrosive wear: Corrosion resulting in chemical wear is brought about by chemical attack on the surface of the tool. Continuous friction on the tool depletes the protective oxidation films on that surface. This oxidation may accelerate the wear formation on the tool. The effect of high temperature and frictional forces over a long term would eventually alter material composition.

Fracture wear: Severe fracture wear is commonly experienced in interrupted machining. Fracture wear occurs as the gradual chipping and cracking of solid surface due to the sudden loading and collision of both materials.

These wear mechanisms could be encountered in various combinations during machining. Dominant wear mechanisms are influenced by various factors, such as the cutting parameters, geometry of the tool, temperature, and speed of cutting operations, and other controllable and uncontrollable conditions.

2.3 Forms of wear on the tool edge

Tool wear generally occurs as a result of a combination of wear modes. Dominant wear modes depend on cutting conditions and process specifications. These dominant features are mainly responsible for wear formation. Some common identified wear forms are [8]:

- flank wear
- crater wear
- chipping
- breakage
- nose wear
- plastic deformation
- cracking
- notch wear

Four of the above listed forms are generally more rampant in cutting operations. These are flank wear, crater wear, nose wear and notch wear. Figure 2.2 and Figure 2.3 show the various wear zones, region of wear and measurement parameters.

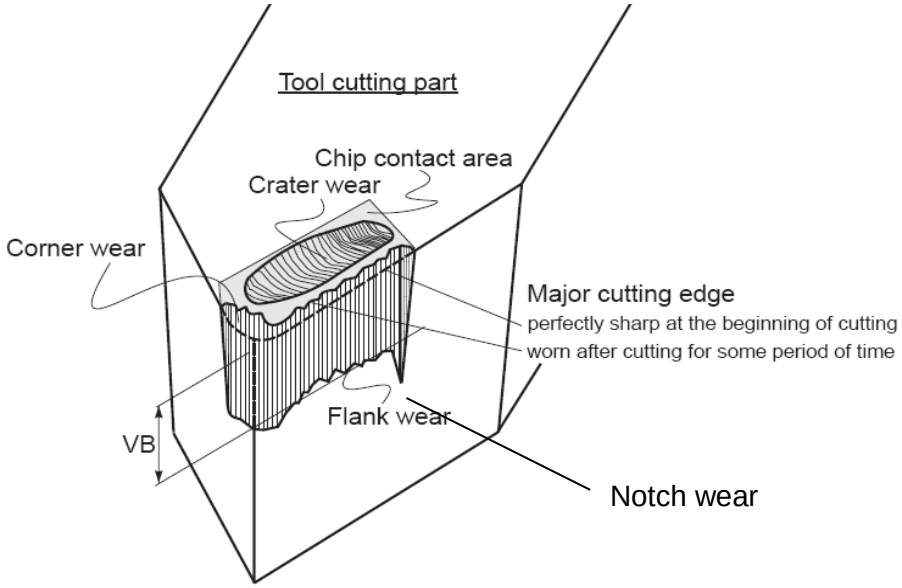

Figure 2.2 Wear zones at cutting tool tip [4]

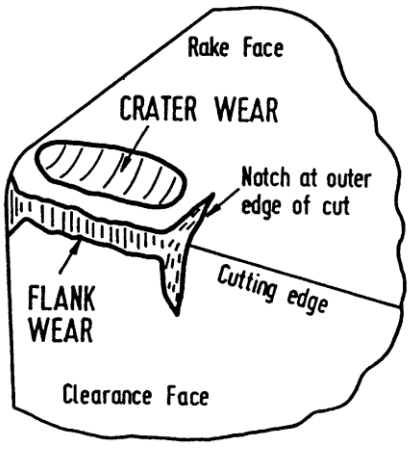

(a)

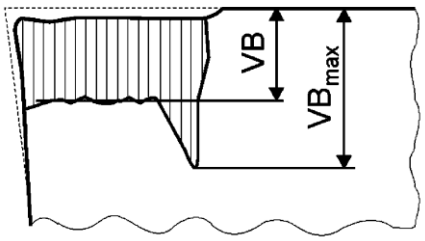

VB - Flank Wear
VB $_{max}$ - Maximal Wear

(b)

Figure 2.3 Regions of wear (side view); (b) measurement of flank [9]

Flank Wear: Wear on the flank is dominated by abrasion. It arises due to both abrasive and adhesive wear mechanism from the intensive rubbing action of the two surfaces in contact i.e. the clearance face of the cutting tool and the newly formed surface of the workpiece. This action leads to increase in surface contact area and heat generation which in turns impair the surface quality. The rate of flank wear generated during machining operations varies along the cutting process [10].

Nose Wear: Nose wear is found on the nose point of the cutting tool. It occurs predominantly due to abrasive effects on the edges of the tool yielding to an increase in the negative rake angle. At high cutting speed, the cutting tool edge deforms plastically and may result in the loss of the entire nose. Wear formed on the nose affects the quality of the surface finish [8].

Crater Wear: Wear on the crater surface arises due to the combination of wear mechanisms: adhesion, abrasion, diffusion, thermal softening and plastic deformation. This form of wear is generally formed on the rake face some distance away from the tool edge as a crater. The crater wear is quantified by its depth and cross-sectional area of the crater for measurement. The most important factors influencing crater wear are temperature at the tool–chip interface and the chemical affinity between tool and workpiece materials [11].

Notch Wear: Abrasion and adhesion modes of wear are the main mechanisms involved in notch wear. Notch wear is formed at the boundary of the machined surface with no chip contact during cutting. This mode of wear also known as groove wear, is predominant in ceramic cutting tools with low toughness. [11]

Amidst the groups, the flank wear is often selected as the tool life criterion because it determines the diametric accuracy of machining, its stability and reliability [12].

2.4 Tool wear progression

Research has shown that tool wear evolves at different rates in cutting operations. The rate of wear formation on the tool is largely dependent on the wear mechanisms occurring in the process. In flank wear, abrasion and adhesion cause a rapid rise in tool material loss at the initial stage followed by a relatively slow increase in wear rate and ends with another rapid formation of wear before fracture. This curve form is generally accepted by numerous researchers. Three basic stages of wear are identified from this curve: the initial stage, the regular stage and the fast stage. However, Ertunc [13] mentioned that tool wear progresses through five stages, shown in Figure 2.4.

1. Initial wear;
2. Slight wear (regular stage of wear);
3. Moderate wear (micro breakage stage of wear);
4. Severe wear (fast wear stage); and
5. Worn-out (or tool breakage).

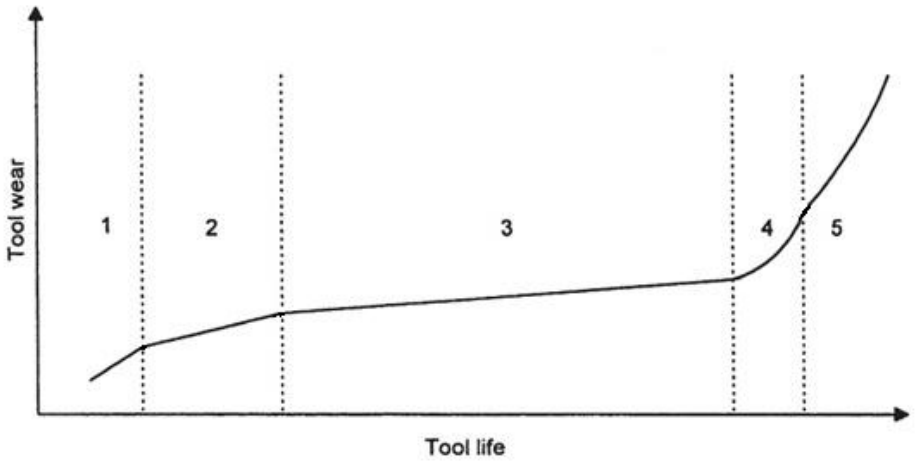

Figure 2.4 Tool life progression curve [13]

2.5 Factors influencing tool life

Tool wear formation is subjective to some machining parameters. The parameters, which affect the rate of tool wear, are

- Cutting conditions (cutting speed v, feed f, depth of cut d)
- Cutting tool geometry (tool rake, cutting edge and clearance angles)
- Properties of work and tool material.
- Properties of lubricants or coolant
- Rigidity of machine tool

It is generally known that the life of a tool is directly related to its rate of wear. Therefore the parameters influencing tool wear would as well adversely affect its tool life. The Tool life of a cutting tool is not only dependent on the wear but can be influenced by numerous other factors relating to the microstructural properties of the material.

The following factors affect the life of a cutting tool:

- type of material being cut
- microstructure of the material
- hardness of the material
- type of surface on the metal (smooth or scaly)
- material of the cutting tool
- profile of the cutting tool
- type of machining operation being performed
- speed, feed and depth of cut [8]

In their research, Dimla and Lister conclude that the cutting speed has the strongest influence amidst these. They postulate that “regardless of the differences in the values and trends of the normal and shear stresses at the contact interfaces, minimum tool wear occurs and apparent friction coefficient reaches its lowest value at the optimum cutting speed”. [14]

2.6 Cutting tool materials

There are various cutting tool materials employed in the machining process. Ranging from high-speed steel to ceramics many of these cutting tool materials are used in the manufacturing industry today. These materials are classified based on the following properties:

- Resistance to heat
- Resistance to abrasion (hardness)
- Resistance to fracture (toughness)

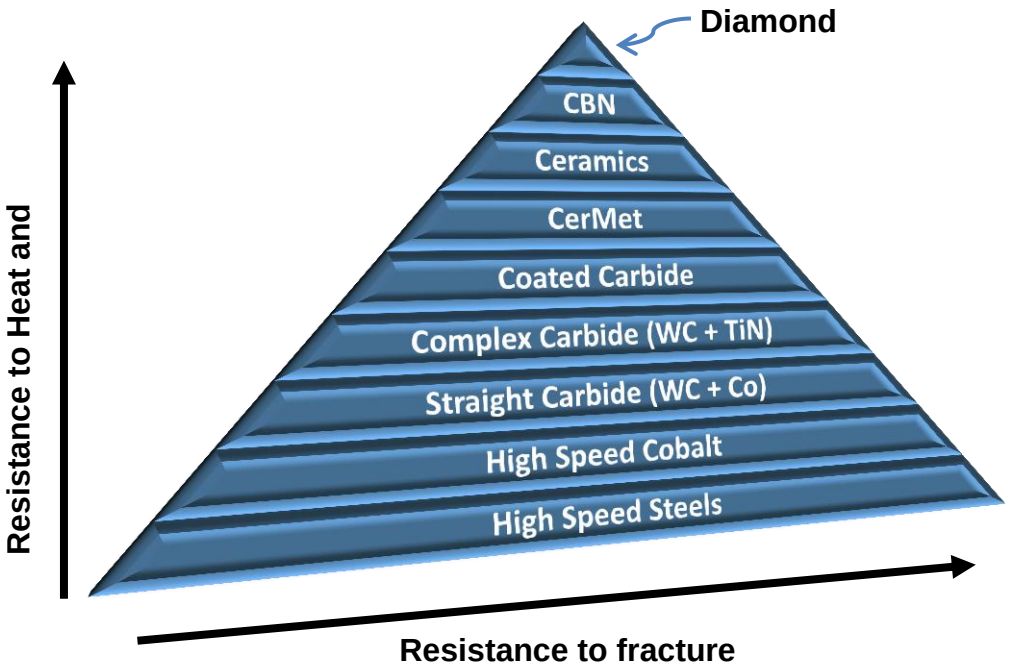

Figure 2.5 Cutting tool material chart

2.6.1 Tool steels

Steels are created from the addition of a small percentage of carbon to iron-ore. The carbon percentage content present in steels is the fundamental factor in steel classification but at levels above 3%, steel undergoes a transformation to cast-iron. Table 2.1 below, shows the classification of steel and their various percentage composition.

Table 2.1 Classification of steels

Class of Steel	Percentage
Low carbon Steel	0.08% - 0.25 %
Medium Carbon Steel	0.25% - 0.60 %
High Carbon Steel	0.60% - 2.40 %

2.6.2 High speed steels (HSS)

High Speed Steels (HSS) form an important classification of cutting material. This class has been greatly utilised in most industrial manufacturing processes globally. Numerous types of tool steels have been formulated to vary the distinct properties of hardness, toughness wear resistance and hardness retention. These HSS are classified based on their chemical compositions. Various elements such as carbon, silicon, manganese chromium, molybdenum, nickel, vanadium, tungsten and cobalt are alloyed to produce tool steels with controlled properties.

Table 2.2 displays the effect of alloying elements on the properties of tool steels.

Table 2.2 Effects of alloying elements

	C	Cr	Mo	V	W	Co
Hardness	***Increase***	***Increase***	***Increase***	***Increase***	***Increase***	***Greatly increases***
Toughness	***No Change***	***No Change***	***Increase***	***No change***	***No change***	***Decrease***
Heat Resistance	***Increase***	***Decrease***	***Increase***	***Increase***	***Increase***	***Greatly increases***
Abrasion Resistance	***Increase***	***Increase***	***Increase***	***Greatly increases***	***Increase***	***Increase***

2.7 Tool monitoring techniques

Various tool wear monitoring methods have been proposed. However, due to the complexity of machining process, monitoring methods always undergo new developments and modifications. An ideal model has not yet been found. Scheffer [15] classifies the various techniques based on the type of sensor used, the parameter monitored and the state of machine process. Based on sensing style, ranging from sound, temperature, force and current methods sensing parameters have been classified into direct and indirect sensing methods [16].

Direct sensing: This method directly monitors actual quantity of wear variable during operation [17]. It is less utilised in the industrial sector due to its cost implication and intricacy of implementation. Direct sensing is greatly affected by environmental machining factors such as illumination, the use of cutting fluid, chips formation and material temperature. Some examples of sensing technologies employing this method are the optical sensing, radioactive, laser beams and electrical resistance.

Indirect sensing: Indirect sensing has been greatly utilised in the industry despite its lower accuracy due to its ease of implementation and cost-effectiveness [15]. Unlike direct sensing, this method monitors the process parameters correlated with tool wear. Indirect methods employ the heavy usage of statistical and analytical models on the tool wear correlations to draw conclusions. Some of the sensing methods used in the indirect method are Acoustic Emission (AE), spindle motor current, cutting force, vibration, cutting temperature etc…

The monitoring techniques could be employed based on real-time or off-line conditions. Continuous monitoring permits the instant recognition of wear formation and provides a corrective methodology of wear identification. Despite these advantages, on-line tool wear monitoring has been a challenging area of research and industrial implementation due to the various influences from the machining environment and technical set-up.

AE technologies are one of the most effective sensing technologies in monitoring tool wear [16]. AE signals are very effective in indirect method due to its non-intrusiveness, ease of operation and fast dynamic response [18].

This study evaluates AE as a sensing technique due to its ease of acquisition. Its high frequency and continuous waveform provides substantial information of the whole process while unaffected by environmental noise from machining.

From Table 2.3 the importance of these advantages in AE sensing can be inferred by the amount of research.

Table 2.3 Summary of sensing methods used for different machine technology

	Drilling	Forging	Gear	Grinding	Milling	Reaming	Turning
Acoustic Emission	[19-21]	[22]	[23]	[24-28]	[18] [29-38]	[39]	[29] [40-52]
Current	[53]				[54]		[55]
Cutting Force	[19-20] [53] [56]	[22]			[30-31] [33-37] [54] [57-64]		[44-45] [49] [52] [65-68]
Gap Sensor					[30]		
Image Sensor							[69-70]
Sound	[56]						[69]
Spindle Power				[26]	[36]		
Vibration	[56]				[30] [33] [35-36] [60] [71]		[29] [47-48] [55] [67]

2.8 Sensor fusion

Other segregations of research are based on the sensing technology and analysis methodologies employed. Some sensors employed in today's manufacturing industry are:

- Sound sensor
- Acoustic sensors
- Ultrasonic sensors
- Laser sensor
- Force sensors
- Eddy current sensor
- Temperature sensor
- Magnetic field sensors
- Electro-optical sensors
- Holographic sensors
- Thermocouple sensors
- Vibration sensors
- Velocity sensors
- Displacement sensors
- and acceleration sensors

Sensors are positioned at various stages of the machine process to:

- ascertain the performance of the machines
- observe the process evolution
- evaluate the quality of the output
- and supervise and control process parameters utilised

Research proves that sensor positioning affects data quality [72]. Sensors are most often found placed on the machine, tool or the workpiece.

Numerous articles enumerate various merits of Acoustic Emission based on monitoring methodology. These were based on its frequency range which prevents the intrusion of environmental noises, ease of placement of sensors, low cost

involvement and its sampling speed which does not interfere with the cutting operations. [32] [50] [73] [74] [75]. From the findings, AE is termed one of the most efficient TCM sensing methods which can be applied to machining processes [38].

The use of a sensor fusion approach was conducted in this study to further optimize AE as a viable technique. Three acoustic AE sensors were positioned at different ends of the workpiece. The influence of sensor positioning and averaging signal values postulates to further increase sensitivity of AE signals and this could be applied via a fusion process.

Sensor fusion or multisensory fusion techniques are greatly used in TCM. Dimla [10] describes the utilisation of more than one sensor signal from different sources to detect the same parameter as sensor fusion. Noise from the process infiltrates signals and influences the correlation efficiencies of signals. Thus, signal to noise ratio forms a decisive parameter to estimate whether the measurement provides significant correlation to the anticipated quantity. In multisensory fusion techniques, signal features from different sensors determine the output state of the tool. This technique however, executes the fusion process at the decision level of the TCM framework.

The integration of the many sensory correlated features with a single or different process parameters gives a more sensitive and reliable prediction than a single sensory feature [76] [77]. This led Sick [17] to conclude that only the technique of sensor fusion can provide sufficient information in a monitoring system. However, practice has shown that in some cases a multisensory fusion with neural networks may produce worse results than a single sensor approach. This situation scenario may occur due to over-generalisation of the output by an excessive pattern learning

[17].In general, most of research show conversely a higher efficiency when operating on multisensory fusion techniques [30] [36] [78].

2.9 Acoustic emission (AE)

Acoustic emission originates from the strain energy released as the rubbing process of cutting takes place. This is caused by the considerable amount of plastic deformation which occurs in metal cutting. Acoustic emission signal refers to transient elastic waves due to the rapid energy release from a localised source within a material [79].

A Comprehensive survey on the use of acoustic emission in TCM was conducted by Li [16].In his survey Li reiterates the efficiency and reliability of acoustic emission as a viable TCM sensing technique. The impressive amount of research in the last decade also indicates the increased interest in using AE in machining monitoring [21] [32] [42-43] [51] [72] [79]. Li in his review [16] reiterates the basic sources of acoustic emission during tool monitoring as the following:

- Plastic deformation during the cutting process in the work piece;
- Plastic deformation in the chip;
- Frictional contact between the tool flank face and the work piece which results in flank wear;
- Frictional contact between the tool rack face and the chip which result in crater wear;
- Collisions between chip and tool;
- Chip breakage;
- Tool fracture.

Figure 2.6 shows the various wear zones which are the AE sources, generated during the cutting operation and how they relate to the various faces of the tool. The interaction of these various AE sources is responsible for the noisy signal generation of AE waves.

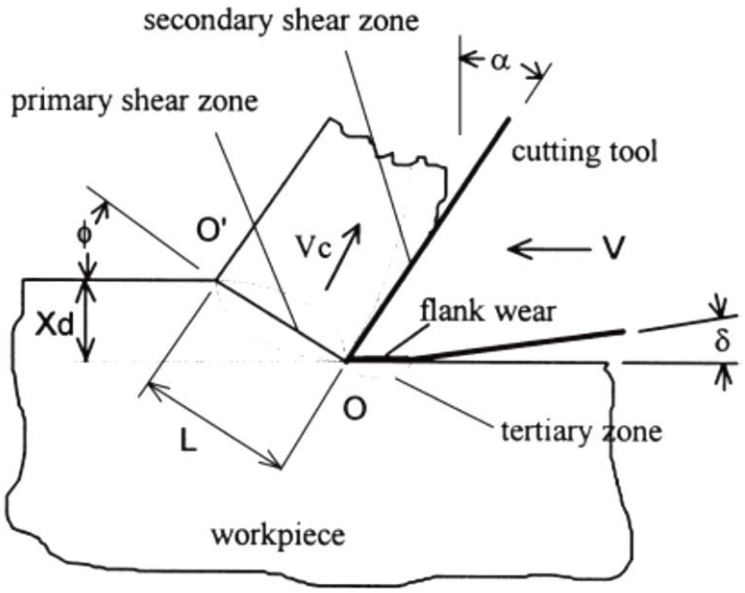

Figure 2.6 Zones of AE generation during metal cutting process [43]

2.9.1 Types of AE signals

There are numerous types of AE signals produced in the course of machining. These are continuous and burst type. Continuous AE signals are associated with plastic deformation in ductile materials [72]. This form of AE signal represents the gradual wear which is generated on the tool. Burst AE signals have been observed to determine tough collisions and fractures during metal working. These burst signal are generated owing to the engagement and disengagement of the tool with the workpiece [46]. It is generally acknowledged that AE signals are generated due to plastic deformation of crack growth in the material. Burst AE signals are more

efficient in identifying fractures while continuous AE signals are more successful in evaluating progressive machining operations.

Due to the frequent nature of entry and exit of the cutting tool, AE sensing faces challenges in adequately monitoring intermittent machining process such as milling. These collisions during cutting generate confusing data values about the present tool state. Numerous research work also identify a link between the magnitudes of the high peak AE parameters with catastrophic tool failure detection [46].

2.9.2 More on AE sensors

AE signals are easily identified in machining due to their higher frequency compared to machine vibrations. The application of non-destructive sensors therefore plays a major role in the monitoring process. The basic advantages of using acoustic signals in determining tool wear originate from its high frequency and sensitivity as well as its ease of placement and affordability. These sensors are of different types and are sensitive to the property of the material involved [24]. AE sensors could be placed on the workpiece to provide uninterrupted elastic energy signal. In the positioning of the sensor, further research on the properties of the transducers confirms a dominant relationship between the choice of location and the quality of the observed signals [80]. Inasaki [72] in his experiment proved the effect of sensor positioning in machining. He affixed an AE sensor on the cutting fluid supply nozzle, using the fluid as a medium for the generated signals. This system was conceived to avoid fluctuation in signal magnitude caused by the variation of the distance connecting the spindle head and the cutting point. His research reaffirmed the need to enhance the reliability of a monitoring process by ensuring high sensitivity of AE sensing technology.

Piezoelectric devices are suitable in the measurement of AE stress waves on the workpiece. Piezoelectric devices convert mechanical stress waves into electrical AE signals. They are resilient in structure and operate at higher sensitivity to most other sensors i.e. capacitive sensors and sensors based on electrodynamics and laser optical processes [81]. Piezoelectric possess sensitivities as high as 1000 V/µm which makes them suitable for measuring noise. The AE transducer operates with a flexible range of 20kHz to 1Mhz [38] which can be used to detect most significant machining conditions, but most research works were conducted in the range of 100kHz – 800kHz [21] [28] [82]. Many recent articles concerned with tool wear monitoring use piezoelectric sensors to establish the wear rate production on flank face of the tool [16] [38] [48] [83].

AE sensing technology can be based on numerous principles for data acquisition. Capacitance based AE sensors possess a high accuracy and are used to calibrate other AE sensors. Unfortunately, capacitance type displacement sensors are very sensitive to sensor position and surface mounting and thus not suitable for machining process monitoring [80].

Hao, Ramalingam and Klamecki say that the AE waveform is a material-dependent quantity and suffers attenuation and dispersion in its propagation to the transducer. The specimen geometry is continuously changing during deformation. Material property and shape changes also affect the interference, rejection and mode conversion of AE waves [82]. Their research investigated the relation of AE signal to the complexity of the nature of work material. This was conducted on a systematic study and evaluation of AE signal on cup drawing experiments during plastic deformations stages.

2.10 AE signal parameters

Some feature parameters and empirical models are used in AE analysis to determine tool state. Features such as skewness, kurtosis, ring-down count, rise time, event duration; frequency and RMS value are investigated. Jemielniak et al [46] in their article statistically analysed the AE signal from the sensor to determine the catastrophic tool failure. They considered skewness value to measure the symmetry of the distribution about its mean value but the kurtosis is a measure of the sharpness of its peak.

Chapter 3 reviews AE signal processing and parameters. Table 2.4 displays a summary of AE signal parameters employed in statistical signal processing:

Table 2.4 AE signal parameters [32]

Symbols	Definitions
AE_{AV}	The average value
AE_{RMS}	The RMS value
AE_{SD}	The standard deviation
AE_{MX}	The maximum value above which was 5% of all values
AE_{MI}	The minimum value below which was 5% of all values
AE_{RG}	The range (max–min)
AE_{MX-AV}	The maximum minus average
AE_{MI-AV}	The minimum minus average
AE_{dY}	The absolute difference between subsequent signal values

Chapter 3 Signal Processing

3.1 AE signal correction

During machining processes, due to the external load pressure applied from the tool, mechanical stress waves of high frequency are generated on the material. This source of AE stress waves observed operates at high frequency ranges and serves in acquiring information about the machining process. The behaviour of the machined material is also subjective to other factors such as environmental conditions and temperature.

The need to process AE signal is necessary to delimit the acquisition to needed values. AE signal correction can be implemented by the design certain processing blocks. Filtering, amplification and conversion are stages implemented during signal correction. AE couplers are stand-alone modules which could be integrated to perform these correctional stages. Despite their ease of integration, PC-based signal application presents a more efficient method for correctional signal processing. Figure 3.1 shows the AE process chain.

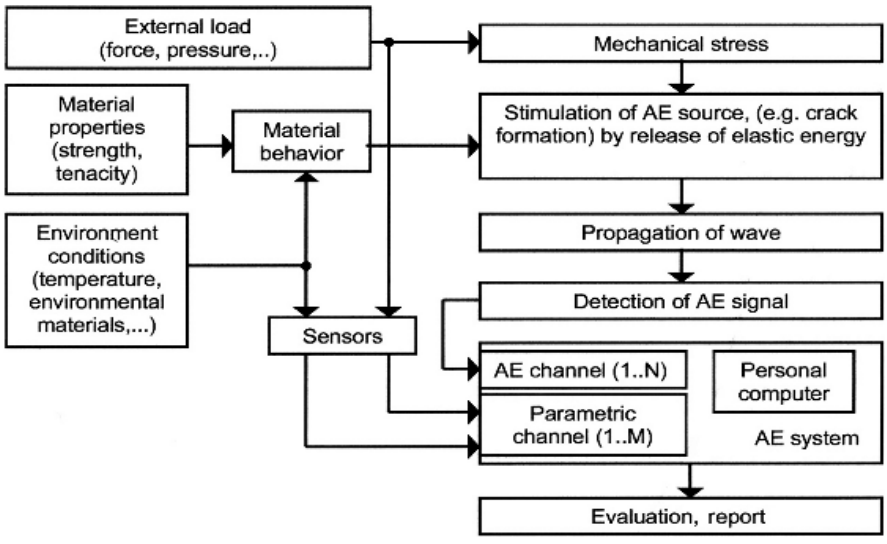

Figure 3.1 The AE process chain [81]

Signal processing forms the core of TCM. It forms the stage intended for the in-depth analysis of the acquired data. Due to the non-stationary characteristics and erratic transient nature of AE signal, extensive processing of waveforms is required. In this section of TCM, signal features are discussed. This phase of the research seeks to identify a processing technique suitable for the analysis of AE signals. It also presents and appraises the use of an artificial evolutionary technique to classify the wear in distinct states.

Signal features provide valuable information on the signal. The use for high computational and analytical know-how is desirable at this level [1]. Signal processing is also characterised with the variation of numerous model parameters in data evaluation. The selection of parameter values during computation have shown to have effect on processing time, efficiency as well as performance. The selection criteria for parameter choice is susceptible to the methodology employed. There are three basic stages identified in processing; they are:

- feature extraction
- feature selection
- decision making

3.2 Feature extraction

AE signals are complex in nature. They consist of overlapping transients and are very sensitive to environmental noise. Due to the complexity of the signal composition, it is essential to decompose the signal into features which provide information which directly correlates to the important machining conditions. Features generated serve as parameters from statistical mock-ups for visual analyses of

trends as well as inputs to decision making models such as neural networks. Sick [17] categorized classes of methods of feature extraction into the following:

- Time-domain feature extraction
- Frequency domain
- Time-frequency domain
- Statistical Feature extraction
- Other methods

3.2.1 Statistical time series

One of the most common tools in the analysis of AE data is the time series model [1]. Time series is a collection of numerical observations arranged in a natural order. Usually each observation is associated with a particular interval of time [84].Time series analysis encompasses approaches for analysing time series data to extract significant characteristics and information from the data. The most employed methodologies of this statistical tool are the Autoregressive (AR) and Autoregressive Moving-Average (ARMA) model.

An important factor to consider when modelling the end milling process is that the process can be divided into two independent models: a deterministic model and a stochastic model. The deterministic model is based around known dynamic characteristics of the milling process such as radial depth of cut, axial depth of cut, spindle speed, number of cutting teeth and spindle position. The stochastic model consists of the random variations contained within the overall signal [1].

The model coefficient of AR, Moving-average (MA), and ARMA are utilised as features for signal processing. Models can differ from one another in order. Higher

order models split signal into more distinct bands and can analyse distinctively noise embedded. The order of a time series model therefore determines the number of features that can be obtained from that model. Ravindra et al [85] in their study evaluated AR parameters, power of the AE signal and AR residual signals as features for TCM and found them to be effective in tool condition monitoring.

The AR model can be defined as

$$\bar{x}(n) = a_1 x(n-1) + a_2 x(n-1) + \cdots + a_p x(n-p) \tag{3.1}$$

Where $\bar{x}(n)$ is the AR predicted value, $x(n), n = 1,2,3, \ldots, N$ is the time series (acoustic emission), p is the AR order, $a_1, a_2, \ldots, a_p$ are the AR parameters and the residual component is $R(n) = x(n+p) - \bar{x}(n+p)$ [85]

The MA model is defined as:

$$\bar{u}(n) = b_1 u(n-1) + a_2 u(n-1) + \cdots + a_q u(n-q) \tag{3.2}$$

Where $\bar{u}(n)$ is the MA predicted value, $u(n), n = 1,2,3, \ldots, N$ is the time series (acoustic emission), q is the MA order, $b_1, b_2, \ldots, b_p$ are the MA parameters and the residual component is $R(n) = u(n+q) - \bar{u}(n+q)$

The ARMA (p, q) notation model represents time series with p autoregressive terms and q moving-average terms. This model contains the AR (p) and MA (q) models.

$$x(n) = -\sum_{k=1}^{p} a_k \left(x(n-1)\right) + \sum_{k=1}^{q} (b_1 u(n-1)\ ) \tag{3.3}$$

Xaoli's review [16] projects how experimental results have shown that the power of the AR residual signal in AE monitoring, increases with increase of the flank wear of tool cutter during turning operations. Pontuale et al [40] used the histograms of the

absolute value of time series amplitudes taken from measurements of new and worn tools. From this method, they identified some power law characteristics through the use of log-log histograms.

3.2.2 Time domain

Time domain involves the analysis of signal features, computational functions and economic data with respect to time. Time domain features are greatly used in TCM [85-86]. Jemielniak et al [86] in an attempt to find optimal features combination during an analysis of numerous signal features identified five time domain features from signals (Effective value, standard deviation, skewness, kurtosis, and crest factor) for examination. Explained below are some time domain signals features [36].

The mean of amplitude values of raw data signal is found by

$$M = \mu = \frac{1}{n}\sum_{i=1}^{n} x_i \tag{3.4}$$

The RMS for a collection of n values in the raw data is defined as

$$RMS = \sqrt{\frac{1}{n}\sum_{i=1}^{n} x_i^2} \tag{3.5}$$

The variance for a collection of values in the raw data is defined as

$$V = \sigma^2 = \frac{1}{n}\frac{\sum_{i=1}^{n}(x_i-\mu)^2}{n-1} \tag{3.6}$$

where σ is the standard deviation.

Skewness (S_k): The 3rd central moment is a measure of the “peakness” of the asymmetry of the distribution of the signal raw data. It is expressed as

$$Sk = \frac{1}{n}\frac{\sum_{i=1}^{n}(x_i-\mu)^3}{\sigma^3} \quad (3.7)$$

Kurtosis (K_u): Fourth central moment is a measure of the “peakness” of the probability distribution of the signal raw data

$$K_u = \frac{1}{n}\frac{\sum_{i=1}^{n}(x_i-\mu)^4}{\sigma^4} \quad (3.8)$$

Power (P): Signal power is defined as the measured area under the rectified signal envelope. This is another measurement of the signal amplitude; however, it is sensitive to amplitude as well as duration, and it is less dependent on operating frequency. Power is defined as

$$P = \frac{1}{n}\sum_{i=1}^{n} x_i^2 \quad (3.9)$$

Peak-to-peak amplitude (pp) is found by determining the difference between the highest peak values minus the lowest peak value attained by a signal. This peak-to-peak is expressed depending on the signal. For force it is expressed in Newton, for vibration and acoustics in microvolt, and for spindle power signal in kilowatts.

Crest factor (CF): the crest factor of a waveform is equal to the peak amplitude of a waveform divided by the RMS value. The crest factor calculation is used to provide an idea of the degree of impacting in a waveform. It is defined by the following formula:

$$CF = \frac{peak}{RMS} \quad (3.10)$$

The burst rate (Br): Sometimes called the pulse rate is the number of times the signal exceeds pre-set thresholds per second. This feature is only applied to vibration and AE signals. The pre-set threshold is usually set to 300μV [36].

3.2.3 Frequency and time-frequency domain

Frequency band acquired during frequency domain analysis differ in spectral energy distribution. Spectral energy provides ample information on the state of the machining process. It is obtained by computing the power spectral density (PSD) of the signal and increases or decreases based on wear level.

Fourier transform is used to decompose an energy-signal into its Fourier transform components. Specifically, a hanning window is applied as windowing method to the raw data before Fast Fourier transforms (FFT) to prevent leakage. Then, the power spectral density is obtained where it is formed by a plot of the frequency components on the x-axis and attendant power in that frequency on the y-axis [36].

Sum of total band power (STPB): The power spectrum does not directly give us the total power in the signal, only power in a particular spectral component. To obtain the total power in the signal or in a particular range, the integral of the PSD over the range of frequencies of interest must be obtained. The following formula defines STPB:

$$STPB = \int_{F1}^{F2} S(f)df \tag{3.11}$$

Where $S(f)$, represents the power at a specific frequency component and $(F1, F2)$ is the frequency band. Some frequency domain features are shown in Table 3.1 below [87].

Table 3.1 Some frequency domain features [87]

Some Frequency domain features	**Description**
Mean of band power spectrum (MBP)	$MBP = \frac{1}{n}\sum_{i=1}^{n} S(f)_i$
Variance of band power spectrum (VBP)	$VBP = \frac{\sum_{i=1}^{n}(S(f)_i - MBP)^2}{n-1}$
Skewness of band power spectrum (SkBP)	$SkBP = \frac{1}{n}\frac{\sum_{i=1}^{n}(S(f)_i - MBP)^3}{VBP^{3/2}}$
Kurtosis of band power spectrum (KuBP)	$KuBP = \frac{1}{n}\frac{\sum_{i=1}^{n}(x_i - \mu)^4}{\sigma^3}$
Relative spectral peak per band (RSPBP)	$RSPBP = \frac{1}{n}\frac{\sum_{i=1}^{n}(x_i - \mu)^3}{\sigma^3}$
Total harmonic band power (THBP)[a] *Where m = ¼ $\mathbf{1}, \mathbf{2}, \ldots, \boldsymbol{N}$ where $\boldsymbol{P}(\boldsymbol{m})$ is the power at the fundamental tooth frequency, body cutter, and their harmonics, and $\boldsymbol{N}$ is the largest integer for which $\boldsymbol{N}$ is the cut-off frequency for the sensor*	$THBP = \sum_{m=1}^{N} P(m)$
Frequency of maximum peak of band power (FPBP)	Highest amplitude frequency
Maximum (peak) of band power (PBP)	The peak of power spectrum in a specific frequency band. Expressed by the energy level (W/Hz).

[a] -This feature is only applied to the three-directional force signals [87]

The cutter tooth frequency with THBP is calculated by using the equation:

$$f_t = \frac{S}{60} n \tag{3.12}$$

Where S=spindle RPM and n= the number of teeth on the cutter. The main frequency of the body can also be found from equation 3.13 [36].

$$f_c = \frac{S}{60} \tag{3.13}$$

Jemielniak et al [86] further identifies only 17 AE features from both the time and frequency domain as useful, after removing similar features. Only six features from AE_{raw} and AE_{RMS} were identified.

3.2.4 Wavelet transform (WT)

Wavelet analysis has attracted much attention in signal processing [41] [88], It has been successfully applied in many applications such as transient signal analysis, image analysis, communications systems, and other signal processing applications.

Wavelets are mathematical functions that segments data into different frequency components, and observe each component with a resolution matched to its scale. Like Fourier analysis, wavelet analysis deals with expansion of functions in terms of a set of basic functions. It expands functions not in terms of trigonometric polynomials but in terms of wavelets, which are generated in the form of translations and dilations of a fixed function called the mother wavelet. The wavelets obtained in this way have special scaling properties. They are localized in time and frequency, permitting a closer connection between the function being represented and their coefficients. Therefore wavelet analysis does provide superior signal assessment and greater numerical stability in reconstruction, and manipulation is ensured [89]. To clearly identify the differences in the time and frequency domain a plot of time and frequency coverage with respect to time is helpful. Figure 3.2 shows a pictorial view of basic function time windows and coverage of the time-frequency plane [41].

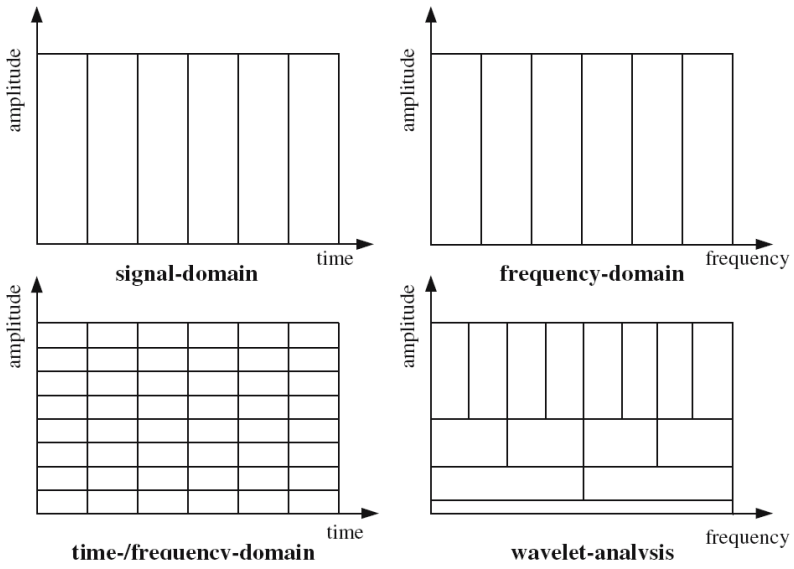

Figure 3.2 Wavelet signal division [41]

Wavelet algorithms process data at different scales and resolutions. The scale factor is proportional to the dimension of the wavelet and inversely proportional to its frequency content. A compressed wavelet is characterized by a smaller scale factor and a high frequency while a stretched wavelet with a larger scaling factor and houses low frequency contents. Based on these distinctions, Chen [41] concluded that wavelet analysis is an appropriate tool for analysing AE data to determine the rate of wear form. They also stated that compared to the wavelet resolution coefficient modulus maxima, wavelet resolution coefficient norm was more stable and useful than other AE character parameters for providing information of cutting in tool condition monitoring.

It is shown that wavelet is competitive to other signal analysis approaches because of its multi resolution ability, sparsity, and localization properties. Zhu [88] stated that WT was effective in analysing non-stationary machining sensor signals. Based on the benefits of WT discussed, applications of wavelet in TCM are reviewed in time–

frequency analysis, denoising, feature extraction, singularity analysis, and density estimation. It has achieved a lot of success in TCM over the years [19] [41] [88].

3.3 Feature selection

Based on the high number of features which can be generated in the various domains during extration, features seletion is employed to optimally reduce feature set. Bensaied et al [36] identifies 138 featues from five sensor signals for wear identification. Jemelniak et al [86] identified 582 signal features from three sensor values. In their research they indicated 133 to be useful in the decision making process and they reduced this number to 40 basic features after removing similar features. Features are selected based on their correlation value to the desired output.

Correlation determines how similar two signals are to each other. Correlation generates a single number known as the correlation coefficient which shows the positive or negative proportionality of one signal to the other. The coefficient correlation approach estimates the dependency of the signal with a specific value. It could be employed in two ways:

- The correlation level of individual features to the predicted output category
- The inter-correlation level amidst the features.

Equation 3.14 gives the correlation of signal features to the desired outputs. This approach indicates the non-linear relationship between these values.

$$\rho = \frac{x_{i\,max}\sum_i(x_i-\overline{x})(y_i-\overline{y})}{x_{i\,min}\sqrt{\sum_i(x_i-\overline{x})^2}\sqrt{\sum_i\,(y_i-\overline{y})^2}}. \tag{3.14}$$

Where $\overline{x}$ and $\overline{y}$ are the mean of x and y, respectively; x_i are features extracted from signals; y_i are tool wear values, ρ is the correlation coefficient. When $|\rho|$ is approaching the value of one, the relation between x and y is approaching linear, and when ρ is close to zero y is independent of x.

Nine distinct features have been selected in this research based on their correlation efficiencies to the target output. From these features two are from the operating parameters of the end milling machining process. These are used to identify their effects in the wear formation. Table 3.2 shows AE parameters utilised. Further review on the selection process is found in chapter five.

Table 3.2 AE paramters used in the framework

Symbols	**Definitions**
AE_{MEAN}	The mean value
AE_{RMS}	The RMS value
AE_{D1}	The D1 wavelet coefficient
AE_{D2}	The D2 wavelet coefficient
AE_{D3}	The D3 wavelet coefficient
AE_{ERG}	The wavelet total energy
$AE_{WAV-SUM}$	The sum of wavelet coefficient

3.4 Decision making

TCM adapts artificial evolutionary techiniques in making its decisions. Some of these techiques range from neural networks using multi layer perceptron to the use of fuzzy logic classifiers. Other methods employed are the use of statistical analysis of features.

Data fusion of mutli-sensor TCM is also mostly practiced at this level. After signal pre-processing, feature extraction, selection and signal conditioning algorithm have been applied, data sets present less challenges in a sensor fusion approach. The choice of decision making process is influenced by complexity of implementation based on the number of parameter to be set, form of desired output and efficiency level.

3.4.1 Artificial neural network (ANN)

An Aritificial neural network (ANN) technology is derived from the emulation of the brain's process in solution solving. It is a mathematical model make-up of neural activities. Neural Networks (NN) use real and processed data to build ideal systems for decision, classification and forecasts. Knowledge is acquired by the ANN through a learning process. Learning is a process by which matching patterns in data are identified and adequately classified and new data patterns are predicted from the update of free parameters (i.e. synaptic weights and bias levels).

There are two types of neural networks, supervised and unsupervised. The type of neural network is differentiated by the mode of parameter change. This may be classified as follows:

- **Supervised learning:** This mode of learning projects towards a known ground-defined set of training data. It is a form of learning with assitance, where the NN has known target output. e.g. backpropagation
- **Unsupervised learning:** In unsupervised learning, the learning process identifies without assistance based on similar pattern of a set of outputs for the network.

The backpropagation algorithm has emerged as the workhorse for the design of a special class of feedforward networks known as multilayered peceptrons (MLP) [90]. Backpropagation networks (BPNN) are hierarchical feedforward networks with highly interconnected neurons, organized in a layered structure as shown in Figure 3.3. Most NN problems are solved using three distinct layers: the input layer for receptions, the hidden layer which captures the non-linearities of the input/output relationship and the output layer. Each layer is interconnected to the other via a set of associated weight. The sum of the weight inputs through an activation function produces the neurons output. With one or two hidden layers, MLP's can virtually approximate any input-output map. They have been shown to approximate the performance of optimal statistical classifiers in difficult problems [91].

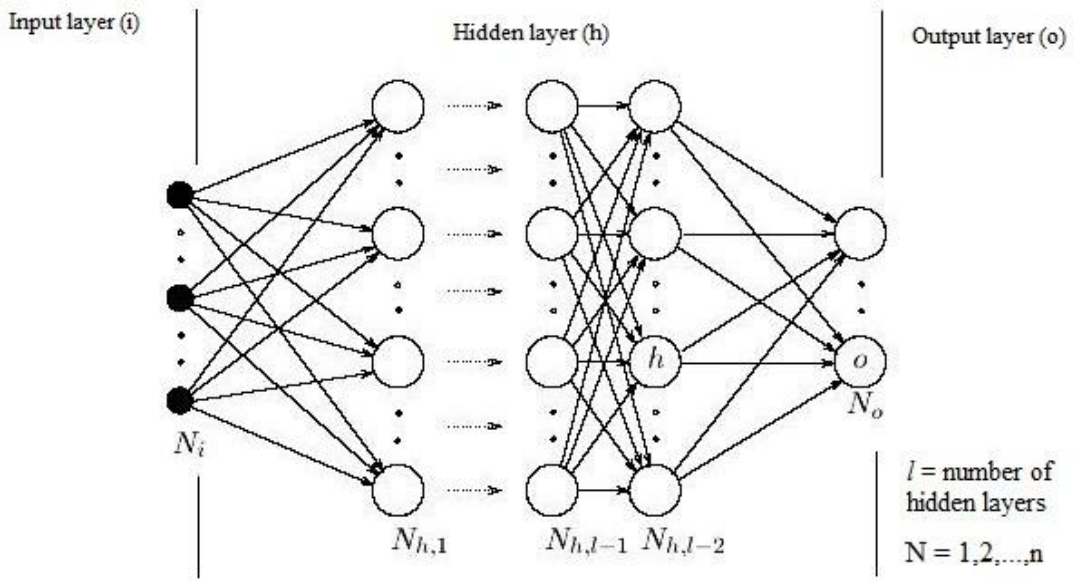

Figure 3.3 Back propagation neural network

BPNN is a popular articial neural network that has been used successfully in most research and in many industrial applications, especially in control applications.This technology is greatly adapted for decision making, diagnosis, prediction and control.

This research employed a feed forward BPNN with one hidden layer based on tests results. A lower mean square error was obtained using this network architecture. BPNN may not need further optimization algorithms such as genetic algorithm and particle swarm optimization due to the reverse process of computation and makes it quick and easy to apply.

ANN presents some advantages over coexisting classification techniques. Some of these advantages can be observed from their ability to classifify data without prioir knowledge. Fuzzy logic models do not posses huge learning capabilities, and draw back in their generalisation. The combination of these models in the neuro-fuzzy approach is challenged with the number of learning parameters employed in the classification. Though there are other techniques such as statisitical and bayesian models. ANN's ability to learn in noisy environments is instrumental in machining.

Chapter 4 Experimental Design

This chapter presents the experimental design setup. The design encompasses the machining process utilised, the choice of equipment and the process parameters chosen for monitoring the tool wear.

4.1 Research equipment

4.1.1 Machine tool

The research project tests were implemented on an industrial five axis Deckel Maho DMU 40CNC machine. (Figure 4.1) The DMU 40 CNC machine belongs to the set of innovative monoBLOCK series of CNC machining centres produced by Deckel Maho. This machine set presents improved performance in terms of dynamics, high precision, higher machined surface, enjoys quality and lower space requirements. The DMU 40 possesses a motor spindle with a speed up to 12000 rpm. Its extensive large range of expansion options, advanced CNC control and numerous software features makes this machine ideal for conducting machining tests.

Figure 4.1 CNC 5-axis Deckel Maho Milling machine

4.1.2 Cutting tool

End milling cutting experiments were performed in this study. The cutting tests were conducted on using a 25 mm diameter indexable end-mill with two cutting edges. Figure 4.2 shows a sample picture of the tool from Kennametal (Table 4.1). KC520M Inserts utilised are composed of carbide grade with a TiAIN coating.

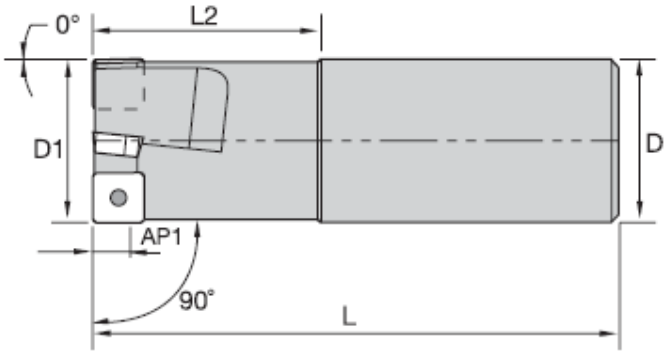

Figure 4.2 Tool from Kennametal

Table 4.1 Kennametal tool manufacturer designation

Tool	*End Mills —Weldon Shank from Kennametal*	
25mm diameter	25A02R039B25SSP10G	*Tool manufacturers designation*

4.1.3 Workpiece

The workpiece, W302 also known as H13 tool steel is a commonly used for hot and cold tooling uses. H13 is an air hardening chromium die steel, utilised for a range of applications. This alloy possesses a hot hardness which preserves the metal during cyclic heating and cooling cycles in hot work application in combination with an excellent resistance to thermal shock. It is composed of chromium, vanadium for increased resistance to heat and molybdenum. They also act as strengthening agents. It is commonly used in hot die work, die casting and extrusion dies. In the experiment the workpiece was machined in its unhardened state. The decomposition of the H13 steel is shown in Table 4.2.

4.1.3.1 Microscopic properties

The H-13 grade tool steel was chosen for this research because of its common use in industries for die casting. H13 tool steel can withstand high temperature fluctuations during machining and possesses very good toughness properties. These qualities made it an ideal choice in experimental trials on high speed milling without coolant. Its commercial value also supported its selection. The machinability of H13 is medium to good.

Table 4.2 Chemical composition of W302 (H13) tool steel

	C	Si	Mn	Cr	Mo	V
COMPOSITION %	0.39	1.10	0.40	5.20	1.40	0.95

4.1.4 Optical microscope with image analyser

The ZEISS stereo Microscope version 20 provides observation with a magnification as high as 150X. It possesses three focal lenses with motorised zoom expansion and resolution adjustment. The panel combines buttons, joystick and touch screen in a compact design, allowing intelligent control of all microscope functions with real time display of main microscope parameters. In order to determine the inserts wear state, the optical microscope and analysis software Figure 4.3 was utilised.

Figure 4.3 ZEISS light microscope with image analyser

4.1.5 Acoustic emission sensing system

The continuous and burst type AE signals are acquired by Kistler 8152B AE-piezotron sensors (Figure 4.4a). The coupler (Figure 4.4b) is used for signal pre-processing and conditioning. Figure 4.6 shows the experimental workflow of the research. An AE sensor basically consists of a sensor case, a piezoelectric measuring element and an integral impedance converter. In AE sensors, the diameter of the piezoelectric element is the main factor which defines the properties

of that sensor. This piezoelectric measuring element is mounted onto a thin film steel diaphragm which is sensitive to elastic stress waves emitted during machining. It is however isolated from the metal case and other AE interference by design. Kistler AE sensors have a high sensitivity to surface and longitudinal waves over a wide frequency range. The type 8152B (Figure 4.4 a) covers the range of 50 KHz to 900 KHz and outputs a low impedance voltage.

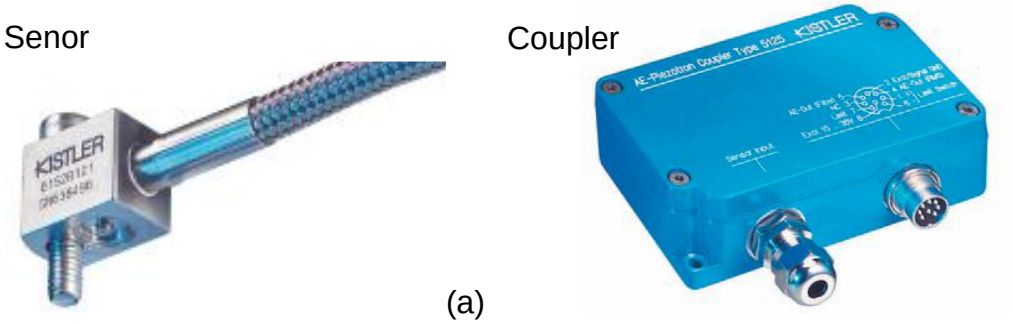

Figure 4.4 (a) AE Sensor (Kistler 8125B) (b) AE coupler (Kistler 5125B)

The acquired signals from the sensors are then relayed for pre-processing to a Kistler piezotron coupler type 5125B for amplification, filtration and RMS conversion. Kistler coupler is equipped with a jumper connection for adjustment of the gain from X10 to X100 indicating a 20dB or 40dB amplification factor. A high pass filter with frequency range from 50 kHz to 700 kHz and low pass filter of frequency range from 100 kHz to 1 MHZ are configurable to remove noise embedded within the signal. The output signal of the filter can then be digitized via an inbuilt RMS compartment over a range of 0.12ms to 120ms time-constant. Figure 4.5 displays the operation workflow of the coupler. The signals are then relayed to a data acquisition card via a NI BNC connection block and custom cable design.

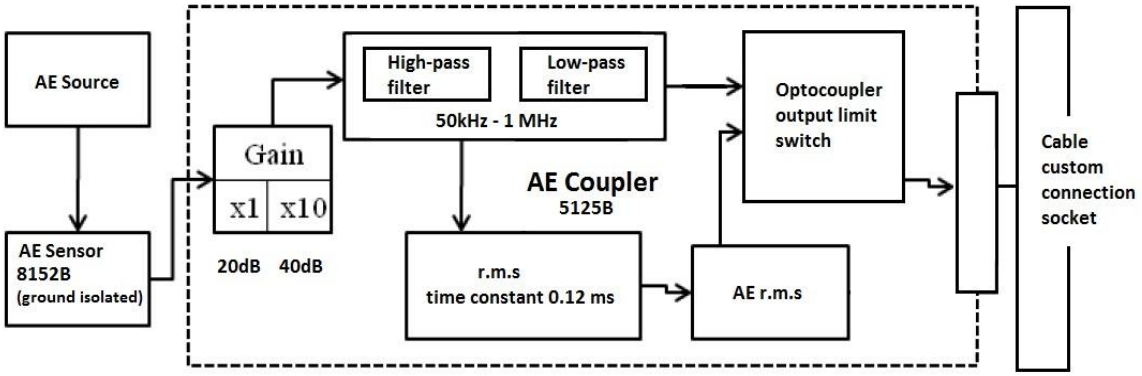

(b)

Figure 4.5 AE coupler circuit framework

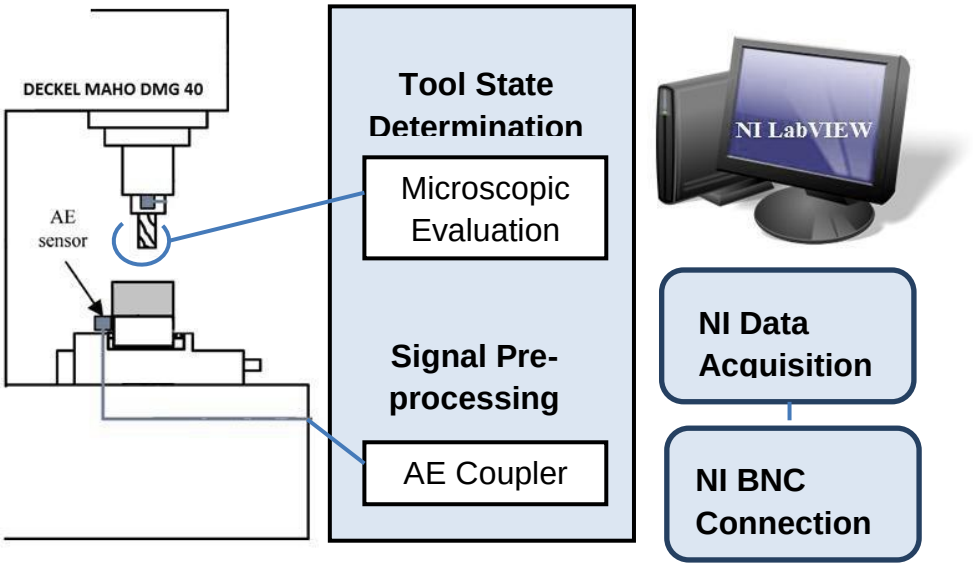

Figure 4.6 Experimental process workflow

4.2 Tool wear measurement and chip analysis

There are numerous methods which could be used to measure the wear formed on a cutting tool. Some of these methods are listed below:

- Microscopic evaluation
- Weight change identification

Tool wear measurements and chip form identification are further explained below. For the purpose of this research microscopic evaluation of the inserts was employed.

4.2.1 Tool wear measurements

The inspection of the tool was conducted on the ZEISS stereo Microscope to identify the wear progression. Magnified tool inserts images were recorded intermittently between the different machining time phases to monitor the progression of the flank wear observed on the tool. Measurements were obtained from the captured pictures using the image analyser the microscope was equipped with. This process was conducted until significant wear damage was formed on the tool.

Figure 4.7 shows some images of flank wear observed on the tool flank during the beginning of a machining test.

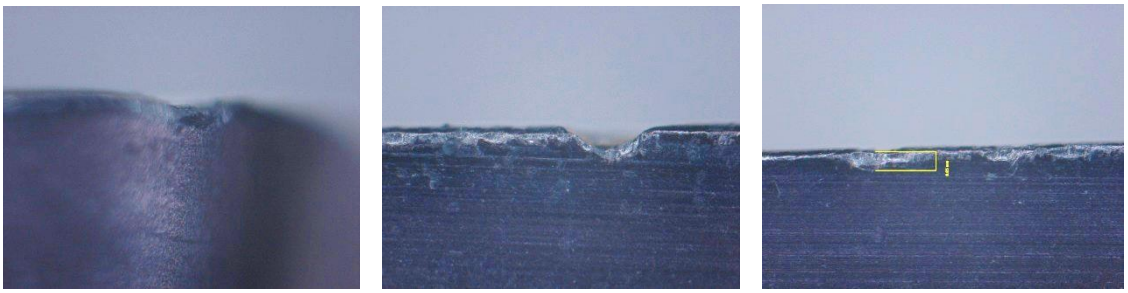

Figure 4.7 Examples of tool wear formed on the tool flank

4.2.2 Microchips characterization

Chips obtained during the cutting process differ in size, shape, and colour based on the parameters chosen for machining. These chips size and geometry formation are influenced by the speed, feed and depth of cut. The chips difference in colour is the result of heat generated due to the friction between the chip and tool face. Therefore, chip colour identification gives an idea of the extent of machining temperatures.

4.3 Experimental setup

Machining tests were conducted in dry machining conditions on the Deckel Maho 5-axis CNC machine. The acoustic sensors were connected at different positions on the workpiece via the use of the magnetic clamp. Figure 4.8 depicts experimental setup used to perform cutting tests on Tool steel H13 and the sensor positions.

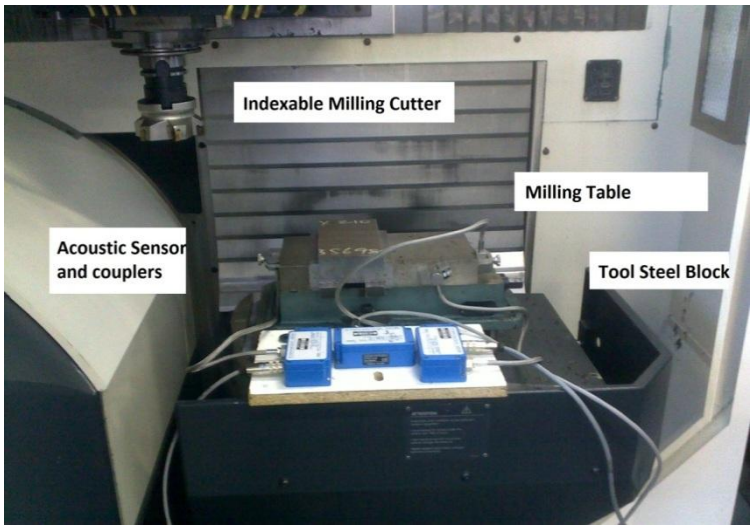

Figure 4.8 Machining setup of H13 tool steel and sensor positions

4.4 Experimental procedure

A usual technique was employed for the acquisition of the data during the different machining phases. Listed below are the steps employed to retain consistency of data.

- For clear results and consistent tests, the workpiece face was first cleaned and squared before conducting the primary tests with rough cutting inserts.
- Before machining tests at each layer depth, a shoulder of at least 25 mm in radial direction was cut to allow the whole tool to be within the workpiece

before experiments commenced in order to prevent the acquisition of high amplitude data from collision entry.

- Machining tests were conducted with vertical and radial depth of 2mm.
- Each experiment was represented with specific cutting inserts which were stopped every certain number of passes to examine the wear progression on the microscope.
- Each machining test cutting pass were conducted along the length of the workpiece and the AE data of each pass was recorded.
- Prior to every cutting phase, the tool wear formed was observed in the laboratory with the microscope.
- Each cutting phase consists of various cutting passes based on the observed wear progression observed from the microscope.
- AE raw data only was recorded over a time frame of 30 seconds over each cutting pass.
- Chips sample were collected for each phase of experiments.

4.5 Machining parameters

A record sheet of the machining parameters used and the experimental report sheet of test parameters are shown in Table 4.3 and Table 4.4, respectively.

Table 4.3 Machining parameters used in experiment

Parameters	1	2	3
Speed (m/min)	170	200	230
Feed (mm/min)	200	250	300
DOC (mm)	2	2	2

4.5.1 Experiments data sheet

Numerous mathematical models and equation are employed in the analysis of features. Time series and frequency models are heavily employed in the TCM.

The realisation of tool wear monitoring in metal cutting requires precise classification and definitions of parameters under study. Metal cutting operations either operate as single-point or multiple cutting point operations. Some correlations exist between the number of cutting points and the wear rate, however the effect of the number of cutting points on the tool wear is still an area under study.

Table 4.4 Experimental report sheet

Description	**Experiments**								
	1	2	3	4	5	6	7	8	9
Machine	DECKEL MAHO DMG-40								
Holder	HSK - 63								
Insert	KC 520 M								
D. O. C. radial (mm)	2								
D. O. C. axial (mm)	2								
Speed (rpm)	2546			2928			2164		
Speed (m/min)	200			230			170		
Feed Rate (mm/min)	200	250	300	300	250	200	300	250	200
Workpiece	H13 tool steel								
Passes	119	134	125	123	106	72	132	135	113
Total time (min)	23.8	26.8	25	24.6	21.2	14.4	26.4	27	22.6
Total Length (m)	23.8	26.8	25	24.6	21.2	14.4	26.4	27	22.6
Diameter (mm)	25 mm end-mill indexable tool								
Pass Length (mm)	200								

4.6 AE signal processing software

The signals relayed are further processed using NI LabVIEW® software and Matlab® for additional processing. Labview® is a development platform for a visual programming language. It is used for the systematic processing and measurement of laboratory data. Figure 4.9 displays the LabVIEW® instruments developed for the acquisition of the AE data.

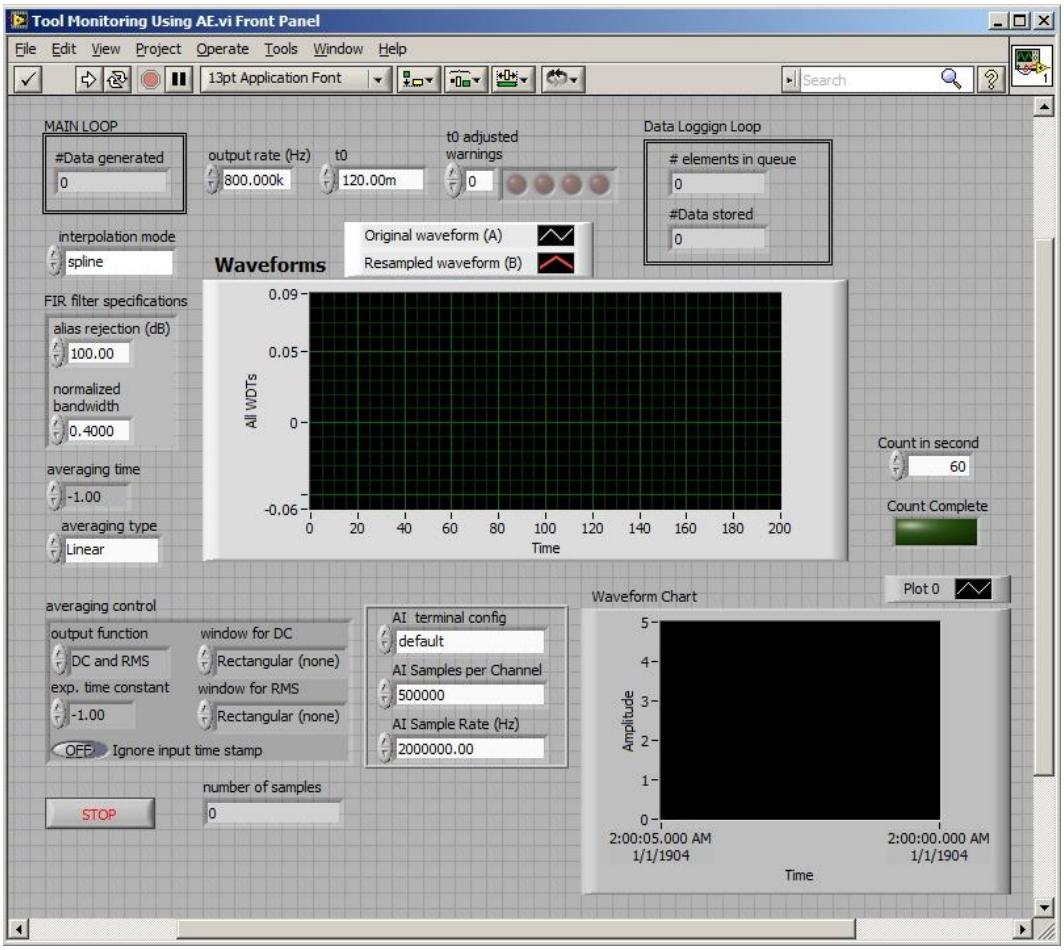

Figure 4.9 LabVIEW® data acquisition instrument for acoustic emission measurement

Chapter 5 Results and discussion

5.1 Introduction

Tool wear classification was categorized into three different levels. Based on the experimental runs and observed wear from the machining parameters selection, a range from 0.01 to 0.3 mm was adapted. A maximum wear of 0.3 was reached in some experiments, but most tools were not machined to reach extreme levels to prevent an avalanche broken tool state. Severely worn tool state was an adequate level for result processing. Table 5.1 indicates the various wear classes.

Table 5.1 Tool wear classification

Class	**Flank Wear (Vb)**	**Tool state**
0	$\mathrm{Vb} < 0.1$	New tool
1	$0.1 < Vb < 0.2$	Moderately Worn
2	$0.3 > Vb > 0.2$	Worn tool

Based on the cutting parameters shown on Table 4.3, the cutting tool performed several passes along the length of the workpiece.

In this chapter, review of results and observations obtained during the research are discussed. Figure 5.1 gives a pictorial representation of the machining experiments and process definitions.

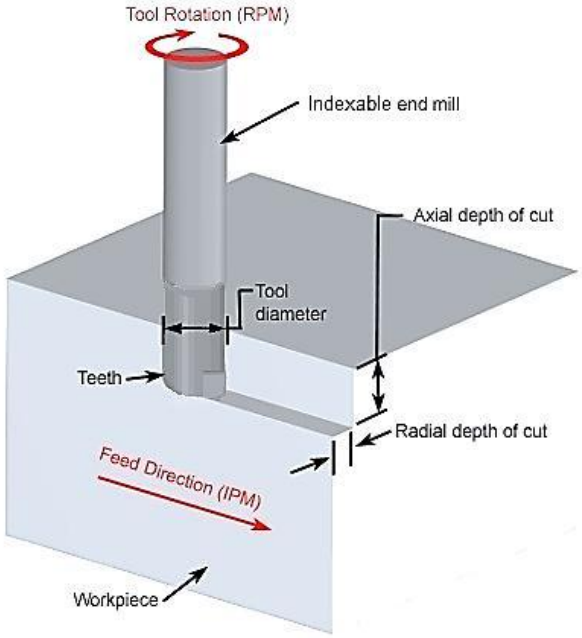

Figure 5.1 Machining process definitions

5.1.1 Segmentation of data

The theoretical frequency of the process indicates the number of tool entry into the workpiece per second. This information helps in the selection of a time segment frame for signal processing. The theoretical cutting frequency of the milling operation was obtained from the equation below:

$$f = T \times {}^{n}/_{60} = \frac{T \times V_c \times 1000}{\pi \times D_c \times 60} \tag{5.1}$$

Where f is the theoretical cutting frequency, T the number of teeth on the tool, n the rotational speed of the cutter in rpm, V_c (m/min) and D_c (mm) are the corresponding cutting speed and cutting tool diameter.

In this experiment, the theoretical cutting frequencies of the process were 72.13 Hz, 84.86 Hz and 97.6 Hz. Table 5.2 shows the segmentation of data values and the

number of tool entry per segments. Based on the 2 MS/s choice of sampling rate, segmentation of the data for processing was implemented. The sampling occurred over a time frame of 30 seconds, yielding to an acquisition throughput of 60 million samples per pass.

The feature extraction process involved the creation of data segments of 64ms over the 30 second acquisition frame. Five distinct segments of the frame were created but only one segment set is necessary for signal processing and feature extraction. This number of segments is to assess the average characteristic of the whole acquisition frame and ensure appropriate segment selection. Each data segment consisted of sets of 128,000 samples.

Table 5.2 Segmentation of data

Parameters	**values**		
Rotational speed (rpm)	2164	2546	2928
Sampling rate (S/s)	2,000,000		
Theoretical cutting frequency (Hz)	72.13	84.86	97.6
Acquisition time frame (s)	30		
Total acquired data	60,000,000		
Number of segments	5		
No. of segments selected for extraction	1		
Segment time frame (ms)	64		
Number of samples per segment	128,000		

At a feed of 200, 250 and 300 mm/min, machining passes ran for 60, 48 and 40 seconds, respectively. The signal acquired was digitally filtered using an FIR equiripple filter of cut-off frequency of 96 kHz.

5.2 Signal analysis

In relation to the process monitoring approach, numerous signal processing techniques have been described in Chapter Three. Techniques such as time series, Fourier transforms are universally used in tool condition monitoring.

As earlier mentioned, AE signal waves are elastic stress waves emitted during machining on the surface of the work piece [79]. These waves are characterised by continuous or transient nature form. A vivid correlation can be observed from the magnitude of the amplified voltage value to the machining state but further processing is necessary based on its non-linear characteristics to the process flow.

An appropriate method is required in TCM to provide information on the non-stationary and stationary signals. Short time Fourier transform (STFT) methods are employed to provide such information but this technique is limited to an appropriate window length size which is used to describe transient response in the applied static time gap. However, wavelet transforms were employed to handle the resolution challenge in STFT. Wavelet transform adapted the time frame to a frequency band of interest to have an entire coverage of the signal.

The analysis of this research was carried out using MATLAB® software for the time and frequency domain feature extraction process. Discrete wavelet transform was performed to decompose the signal into five distinct levels. This section of the results highlights feature characteristics and trends for the successive correlation process. Spectral charts and time charts are used to review these traits.

5.2.1 Result observation set

An observation set is used to display acquired data values utilised in the study. Amidst the overall data set, Table 5.3 presents some sample experimental data collected against few parameters of interest. One exemplary line of the extraction process from each machining experimental test can be identified. Each of these lines portrays characteristic response in time and time-frequency domain and the corresponding wear output. These values constitute a portion of the data used to train the network and design the model. The table below only display an example of data set analysed. Parameters for the experiments can be seen from table 4.4.

Table 5.3 Result observation set

Exp.	$\boldsymbol{Vc}$ *(m/min)*	f *(mm/min)*	AE mean	AE rms	D2	Wavelet energy	wear (x in mm)	Distance covered (m)	Wear stage
1	200	200	0.9320	0.8284	0.3353	0.1154	0.2<x<0.3	23.8	Severe
2	200	250	0.6142	0.6057	0.2226	0.0421	0.2<x<0.3	26.8	Severe
3	200	300	0.0708	0.0715	0.0266	0.0005	x<0.1	0.4	New
4	200	300	0.3452	0.2607	0.0603	0.0075	x<0.1	1	New
5	230	250	0.7480	0.6192	0.2321	0.0804	0.1<x<0.2	8	Moderate
6	230	200	0.6150	0.5450	0.1914	0.0519	0.1<x<0.2	11.6	Moderate
7	170	300	0.5005	0.5604	0.2024	0.0354	0.1<x<0.2	17.4	Moderate
8	170	250	0.5621	0.5447	0.1686	0.0259	0.1<x<0.2	19	Moderate
9	170	200	0.5389	0.4028	0.1049	0.0564	0.2<x<0.3	22.6	Severe

5.2.2 Spectral analysis observations

AE signals were collected at each stages of the study. Some results are shown and the respective AErms, power spectral density and signal wave are displayed in Figure 5.2, Figure 5.3 and Figure 5.4. These figures clearly demonstrate the combined effect of the cutting speed and feed have on generated AE values. All processing calculations were done with MATLAB®.

AE wave figures showcase the five distinct acquisition segments described in Table 5.2, which identify the tool entry and distinctive transient response at different stages during a tool pass. Similarity in amplitude from these five segments connotes identical conditions in the waveform within a tool pass and notifies of no incumbent acquisition fault within that acquisition section.

Figure 5.2 a, b, and c demonstrate the acquisition of experiment number 1 for cutting parameters of v = 200m/min and f = 200mm/min. This figure is used to describe the preliminary stages of each experiment at initial wear conditions of tool life. From Figure 5.2 a, the five distinct tool entries which correlates to a 200 mm/min feed are shown. The tool entries are of low amplitude and noticeably separate from one another due to the new nature of the tool. The transient of each of the two distinct tool entries differ due to the rate of formation of wear at each tooth edge.

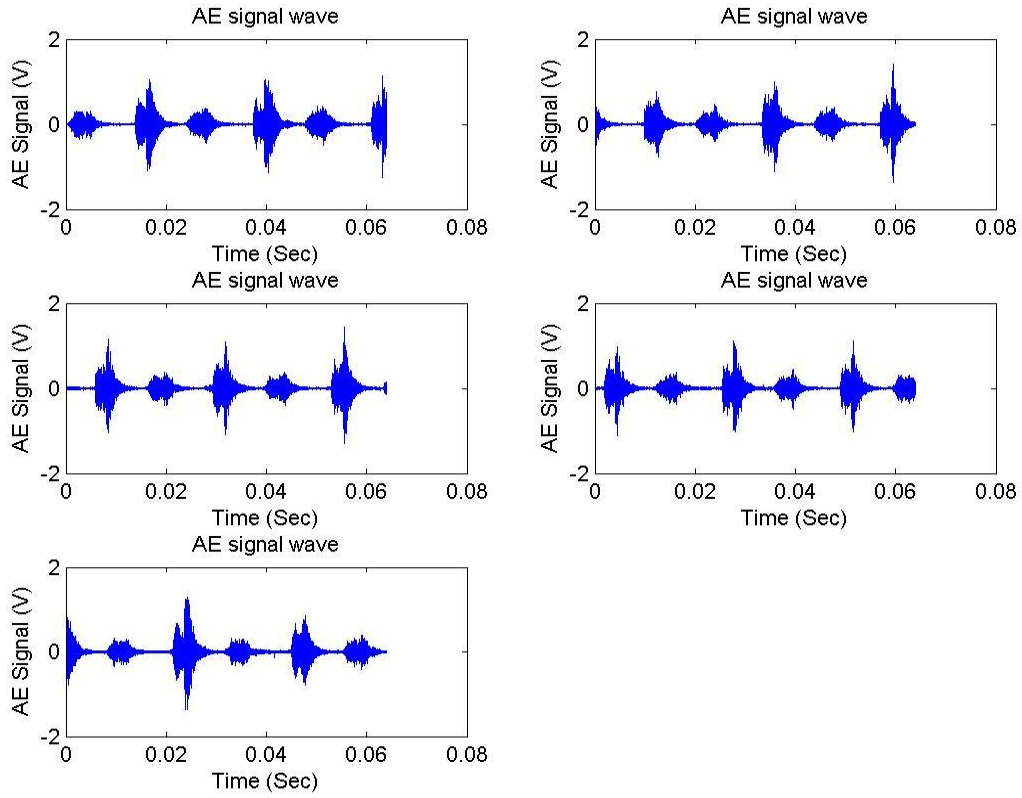

(a)

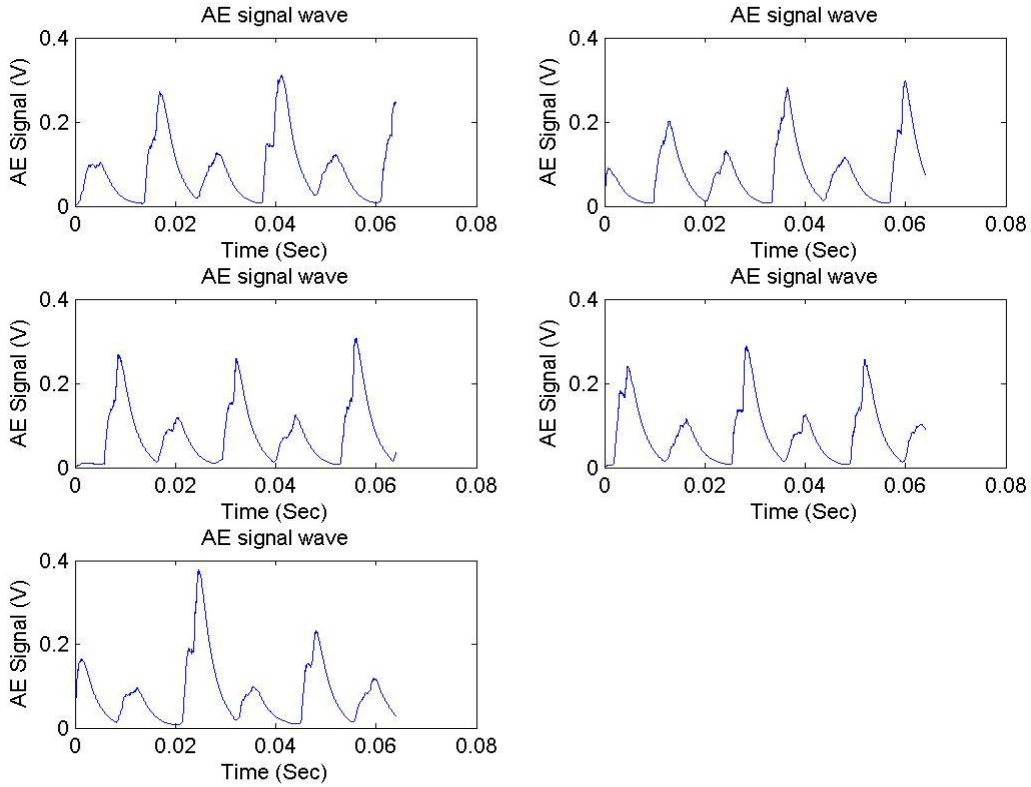

(b)

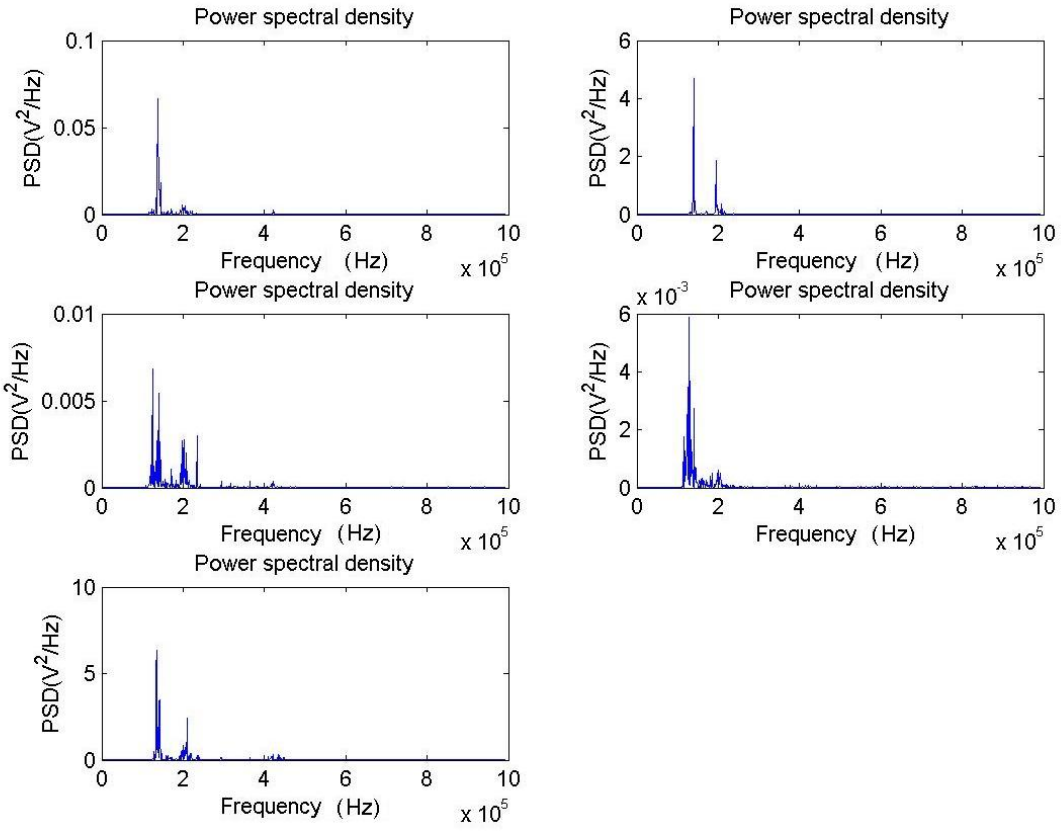

(c)

Figure 5.2. AE signal wave, $AErms$ and PSD diagram of at initial level of tool life (v = 200m/min and f = 200mm/min).

The $AErms$ (Figure 5.2 b) shows the averaged waveform with similar low amplitudes of 0.7 V. Rms values provide an average of the signal over at 1.2 ms time constant, and give a clearer identification of the signal amplitude response with time in the course of this study. From the PSD diagram (Figure 5.2 c) high energy components are mostly concentrated at frequencies of 150 kHz.

Observations identified from Figure 5.3 a, b, and c, for cutting parameters of v = 200m/min and f = 300mm/min demonstrate characterisitic traits of the moderate level of tool life. The figures indicate an increase in the AE wave and AErms amplitude (Figure 5.3 a,b). These waveforms are characterised with double or multiple high peaks which resulted due to cracks and chipping. Wider tool entries also points to the inception of built-up edge (BUE) formation at this moderate wear level in tool life.

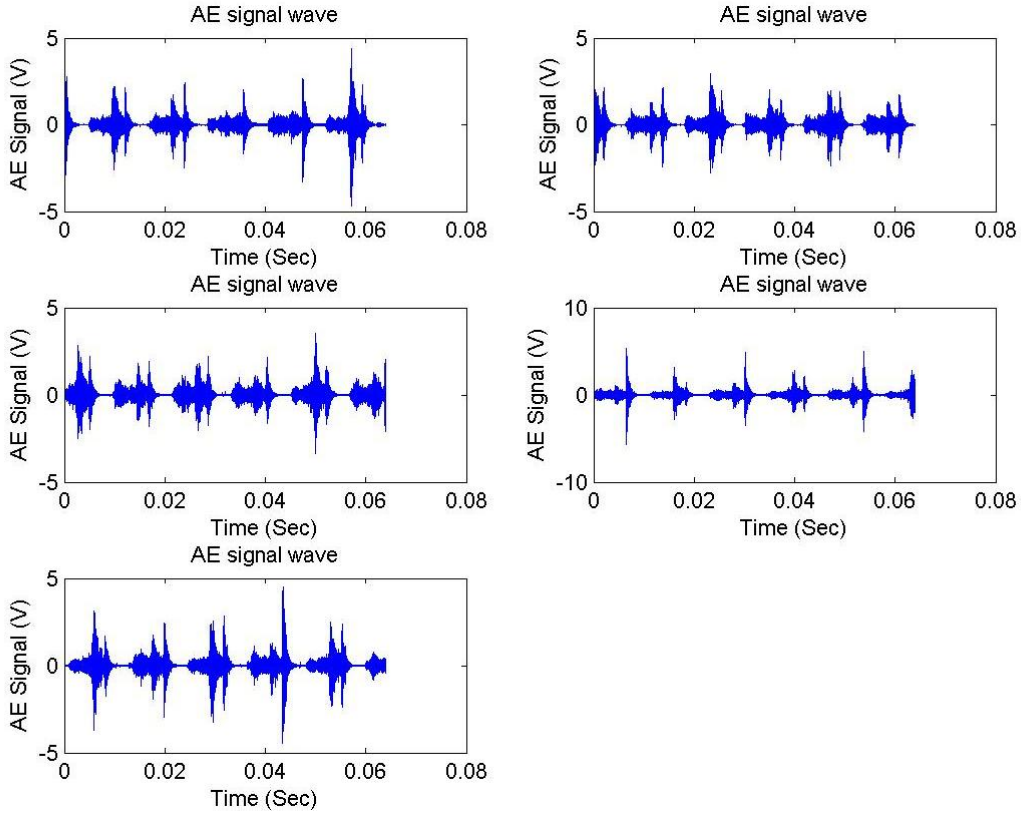

(a)

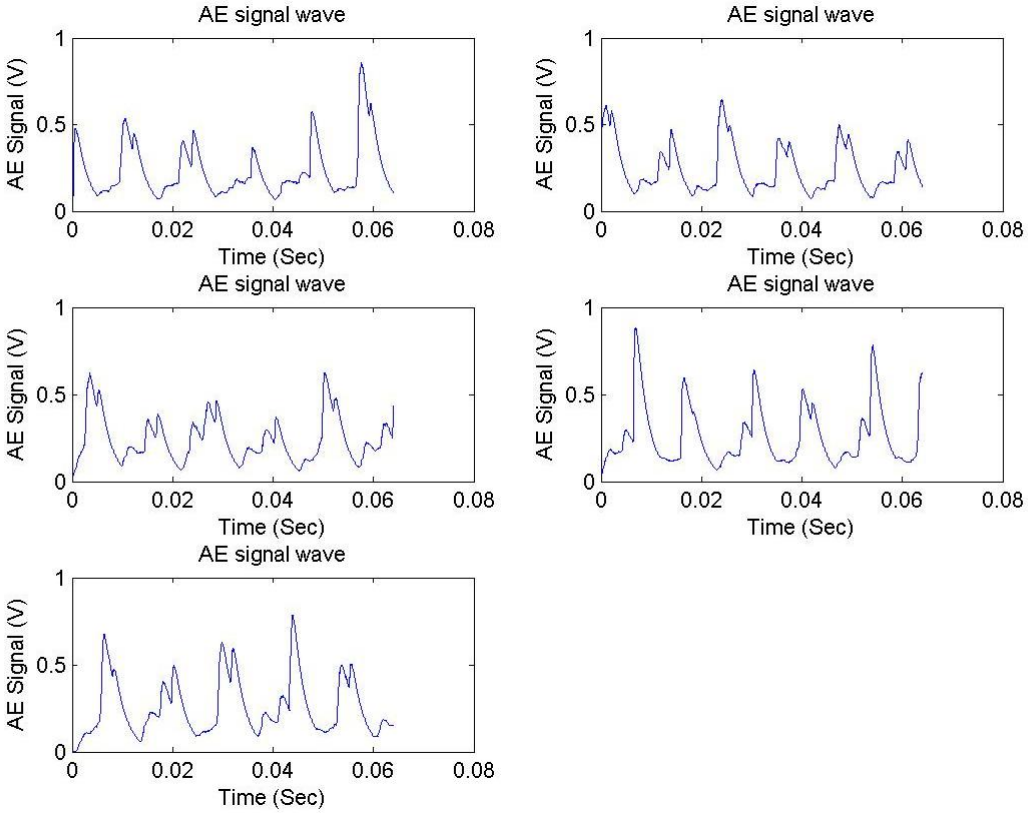

(b)

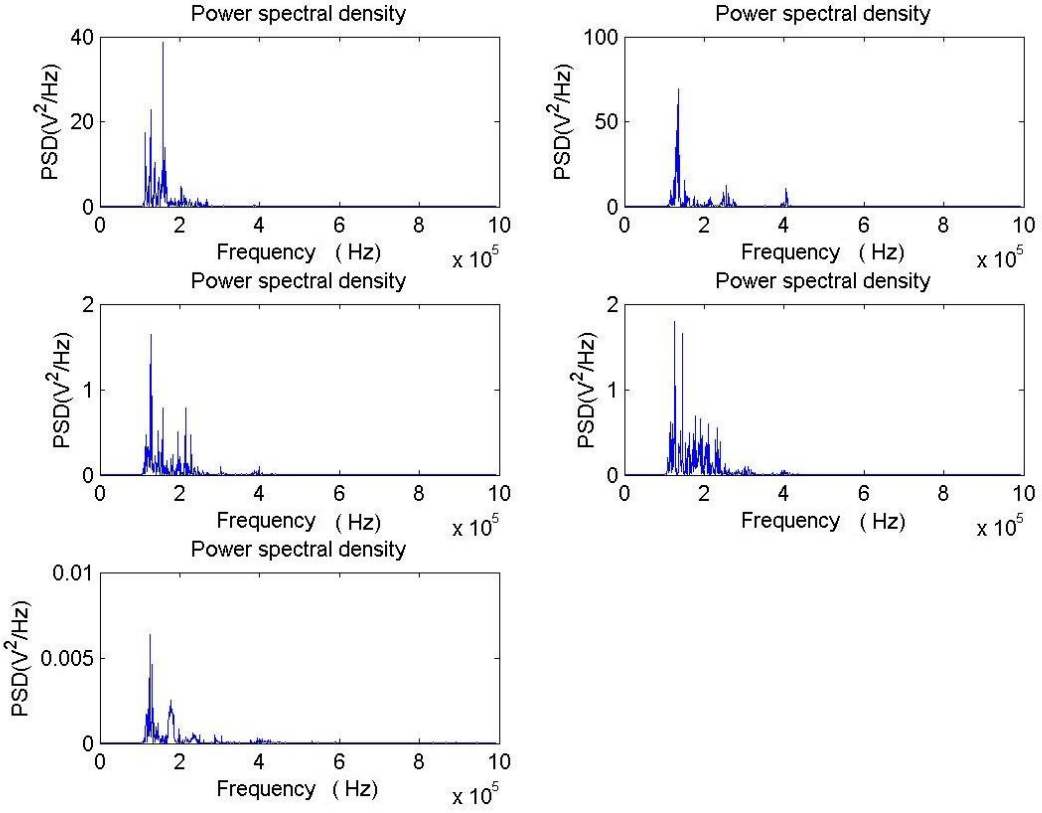

(c)

Figure 5.3 AE signal wave, $AErms$ and PSD diagram at moderate level of tool life (v = 200m/min and f = 300mm/min).

The PSD evaluation examplified for moderate stages (Figure 5.3 c), show an expansion in frequencies of high energy from 150 kHz to 220 kHz. This increase with corresponding increase in energy density, comforms to the wear formation increase found on the tool.

Observations identified from Figure 5.4 a, b, and c, for cutting parameters of v = 230m/min and f = 250mm/min demonstrate characterisitic traits of the worn level of wear stage. Significant increase in the amplitudes of AE wave and $AErms$ indicate a sharp rise in the wear on the tool face. Peaks from chipping and cracks are frequent within the waveform. A widespread of energy density within higher frequency band with a corresponding increase in amplitude highlights the fast deteriorating tool state from the PSD diagram (Figure 5.4 c). The widespread change in power from the 5 PSD diagrams in Figure 5.2 c,5.3 c and 5.4 c is proposed to be due to the different acquisition positions within a tool pass.

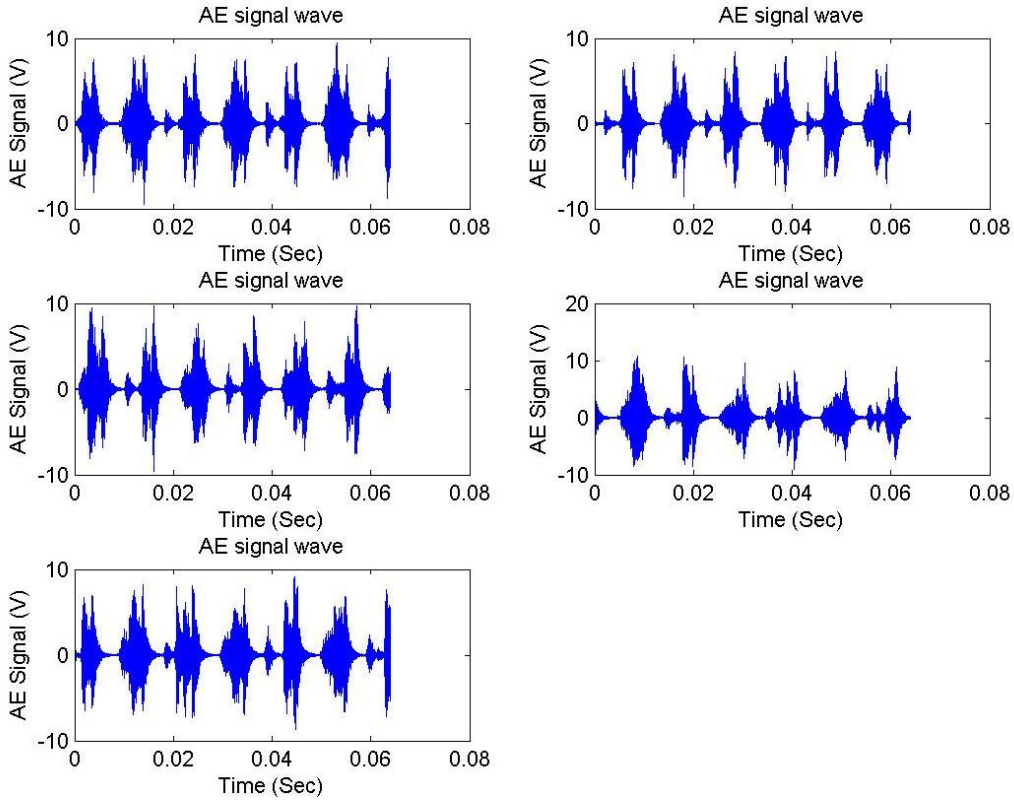

(a)

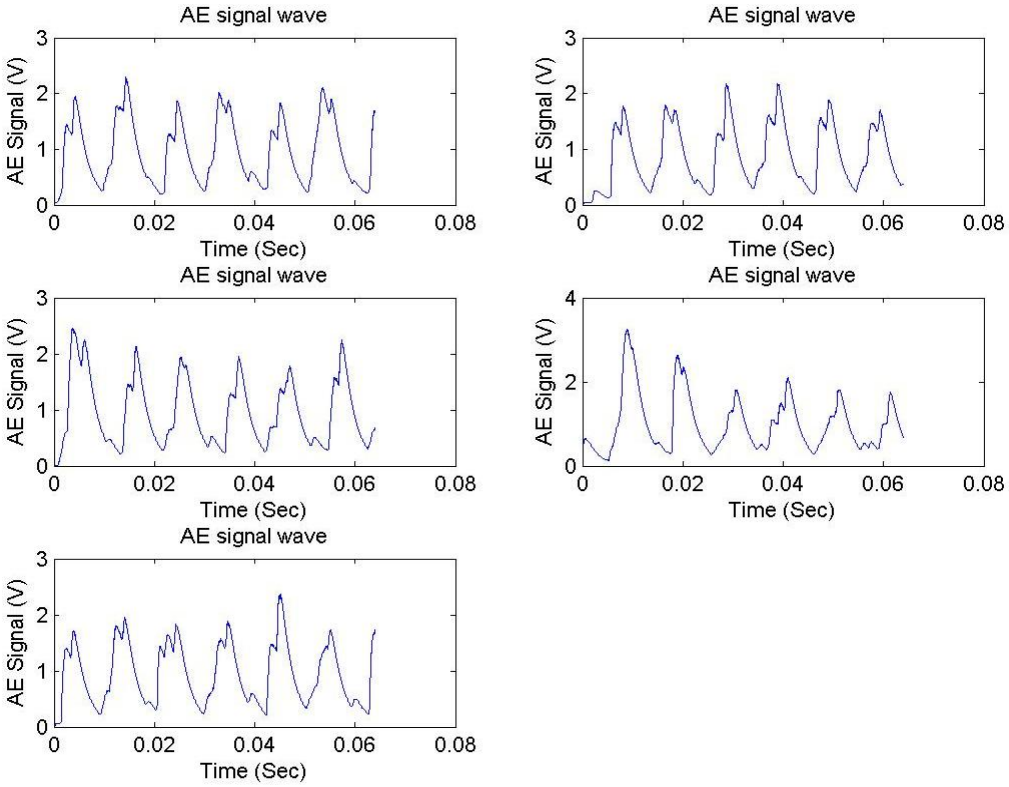

(b)

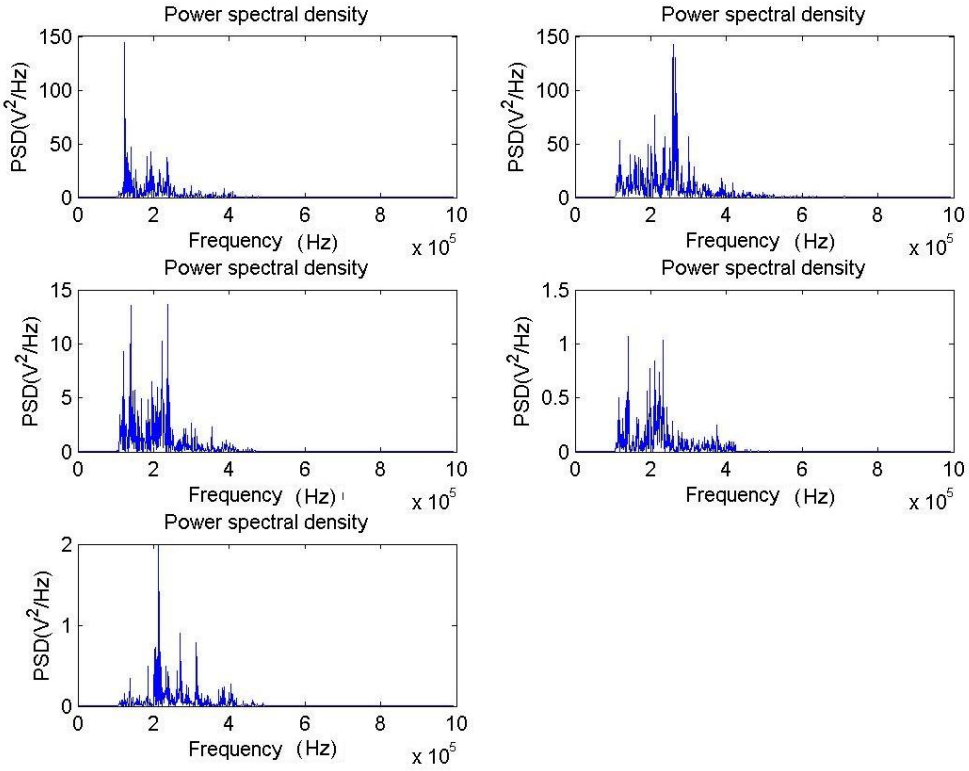

(c)

Figure 5.4 AE signal wave, $AErms$ and PSD diagram at worn level of tool life (v = 230m/min and f = 250mm/min).

Observable increase in trends from AE wave diagrams (Figure 5.2 a, Figure 5.3 a, Figure 5.4 a) amplitude from peak values of 0.7, 4.2 to 9.8 V with the changing parameter values are observed. This trend was also identified from $AErms$ values from amplitude values of 0.28, 0.9 and 3.2 V. The AE signals amplitude showed progressive increase during machining conditions as wear formation increased.

Furthermore, Essential information about the process was obtained from the PSD analysis. The PSD analysis showed information on the concentration of the AE energy within specific frequency bands. This AE spectrum calculated from the Fourier transform based approach resulted in an increased level of activity, within frequencies of 125 kHz to 250 kHz progressively (Figure 5.2 c, Figure 5.3 c, Figure 5.4 c). The energy density at various frequency bands is further studied using more distinct methodlogies such as wavelet and energy analysis charts in the next section.

5.2.3 Wavelet analysis observations

The most commonly identified wavelet family is the Daubechies wavelet discovered by Ingrid Daubechies. This family of wavelet is categorized into order which defines its degrees of smoothness. Daubechies wavelets have orthogonal and biorthorgonal geometry but yet possess a variable analytic form. The lower order daubechies wavelets are not differentiable every-where and comprise of a sharp edge geometrical appearance, whereas the higher order Daubechies wavelets are relatively smooth in form. Figure 5.5 show typical Daubechies wavelet waveform of the third order with five levels.

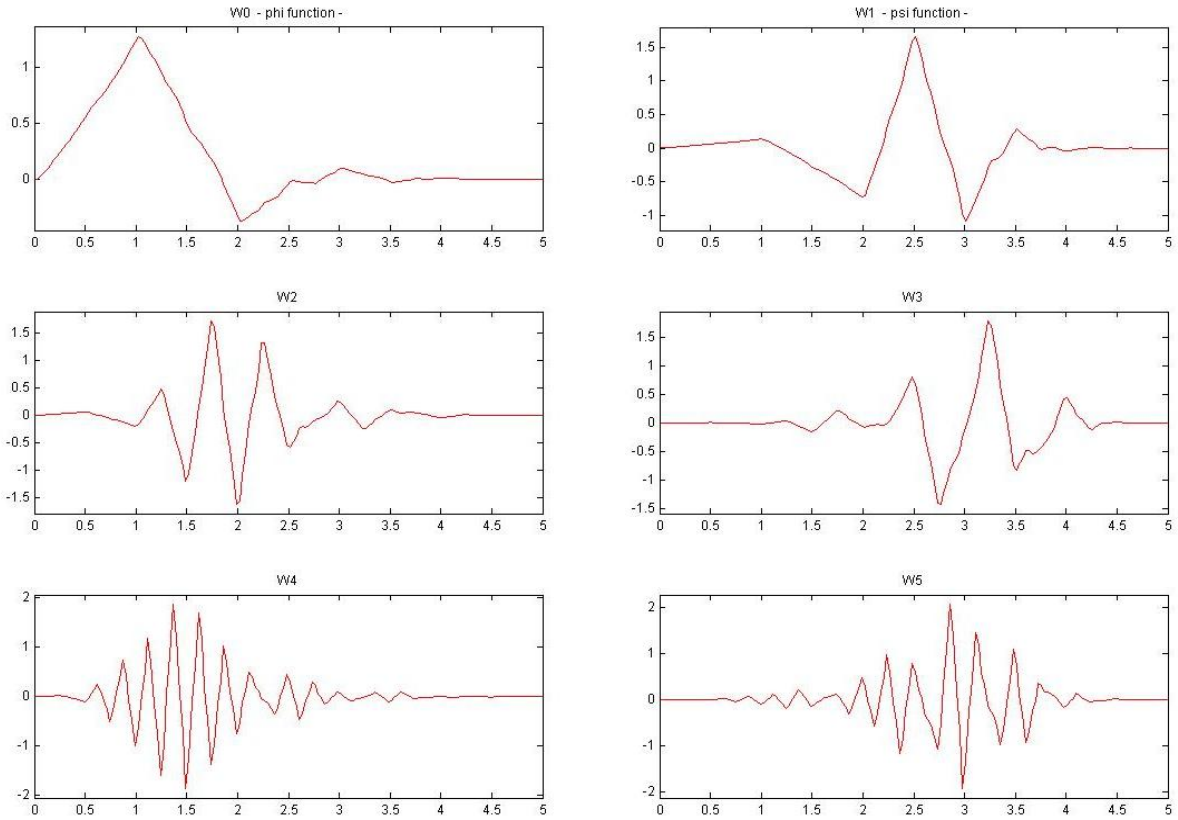

Figure 5.5 Daubechies wavelet waveform of the third order (db3)

The objective of wavelet analysis is to decompose a signal to several frequency bands [92]. The appropriate selection of a waveform and the decomposition level is very important in WT. Wavelet decomposition level is selected based on the dominant frequency components present in the signal. A frequency band which correlates best with the frequencies necessary for classification of the signal are retained in the wavelet coefficient [92].

Each coefficient level is decomposed into a frequency bandwidth of $\left[{}^{\mathrm{f_m}}/_{2} : \mathrm{f_m} \right]$ with the equation shown below.

$$f_m = {}^{f_s}/_{2^{l+1}} \tag{5.2}$$

Where, f_s is the sampling frequency and l is the decomposition level. The obtained decomposition levels of the wavelet in this study are shown in Table 5.4.

Table 5.4 Wavelets decomposition levels frequency band

Decomposed signals	Frequency band (Hz)
D1	500kHz-1MHz
D2	250kHz-500 kHz
D3	125 kHz-250 kHz
D4	62.5 kHz-125 kHz
D5	31.25 kHz-62.5 kHz
A5	0-31.25 kHz

Taking a sample AE signal, a general representation of wavelet traits is shown in Figure 5.6. Figure 5.6 highlights the decomposition level of AE signal by wavelet analysis. AE occurrences were found at higher amplitudes in level D3, with frequency of 125 – 250 kHz. The signal voltage amplitude in D2 and D4 were the subsequent highest amplitude levels observed. Successive random tests within experimental runs produced comparable results. Therefore, the decomposition of the signal wave via wavelet method identified D3 and D4 as prominent frequency band with high energy consolidation.

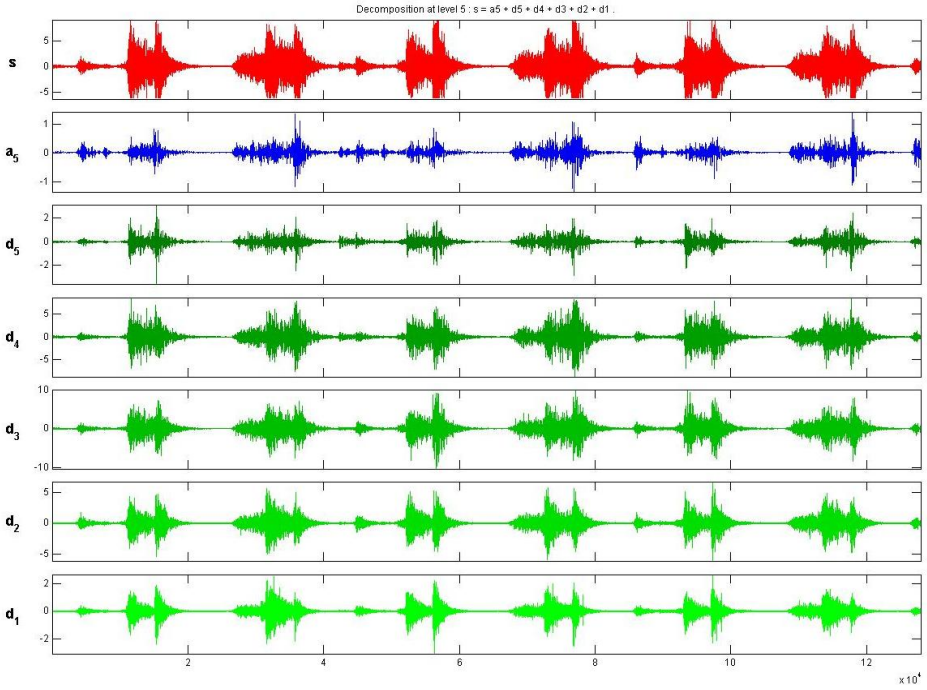

Figure 5.6 Decomposition level of AE signal by wavelet analysis

This section of the analysis study is presented to recognize frequency band of interest. A Daubechies wavelet with an order of 3 “db3” was selected for this research to slightly improve the smoothness of waveform geometry. Energy tests were also used to certify the consistency of these results.

5.2.4 Energy analysis observations

The spectrogram is an efficient method in analysing the energy distribution of source event as a function time. From Figure 5.7, 5.8 and 5.9, sample experimental run at initial, middle and final stages of wear display progressive frequency energy intensity. At the initial stage (Figure 5.7), concise energy signatures occur as a result of distinct entry of the tool. At this preliminary section, all experiments showed prevalence of energy density within the lower ranges of 62 kHz – 250 KHz. This is greatly reflected in features D2 and D3 of the wavelet analysis but the results extended to substantial D2 values within the moderate wear regions (Figure 5.8).

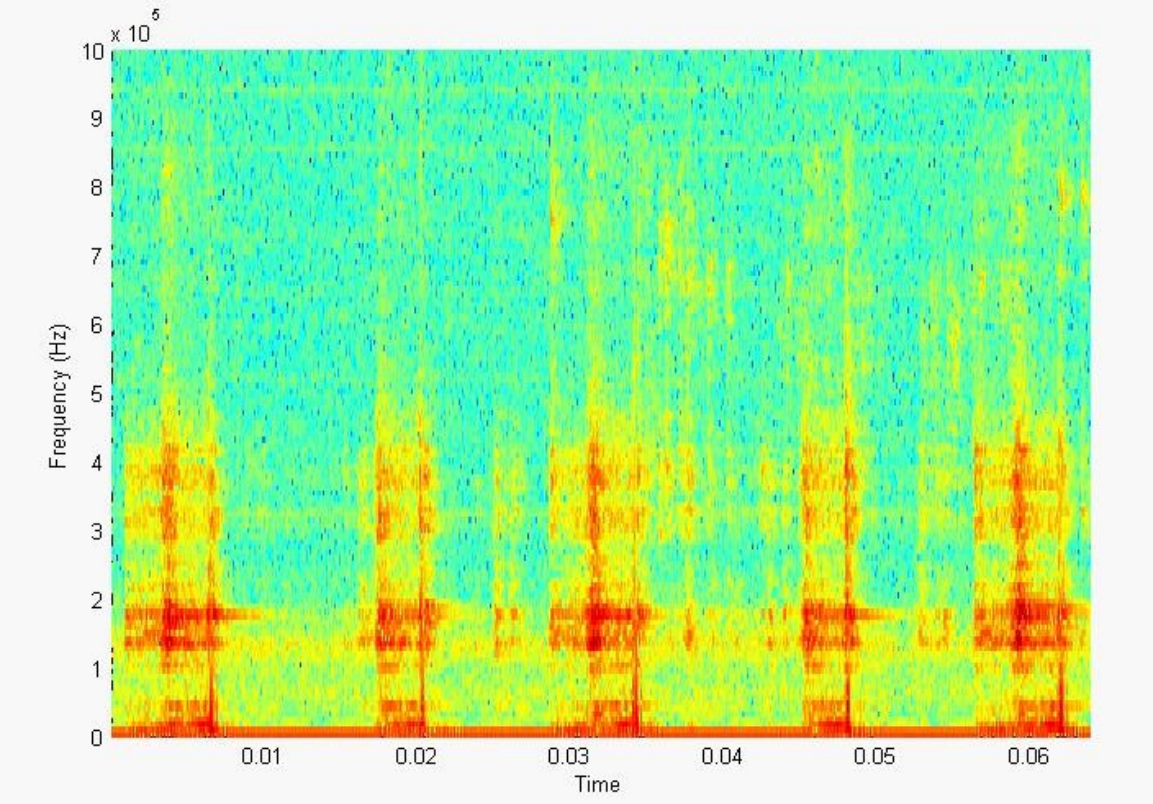

Figure 5.7 Spectrogram of AE signal at initial level of tool life (v = 200m/min and f = 200mm/min).

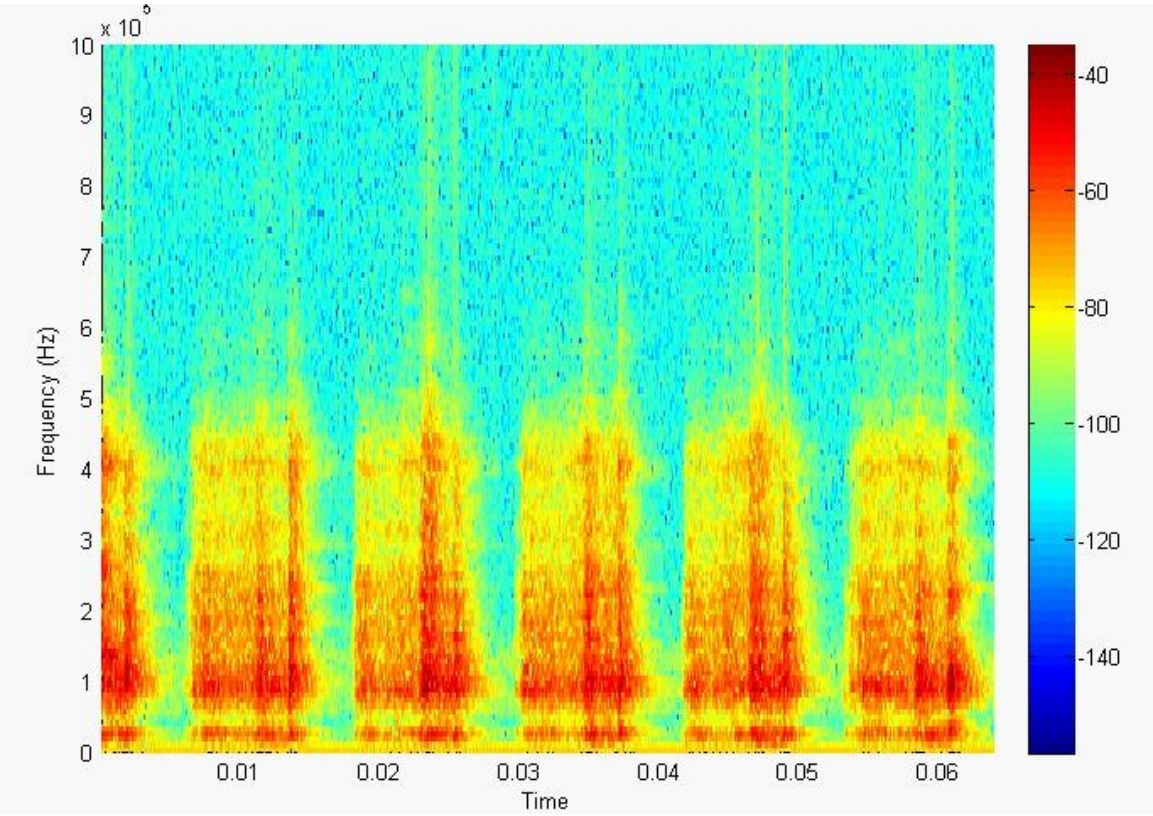

Figure 5.8 Spectrogram of AE signal at moderate level of tool life (v = 200m/min and f = 300mm/min).

From the figure above (Figure 5.8), an extension in the height of high density region showed the move of energy concentration in higher frequency zones (D2). This was a characteristic trait of the moderately worn cutting inserts.

AE waves from rubbing action of the tool and formation of BUE (Figure 5.10) can be seen from the increase of the width of energy density.

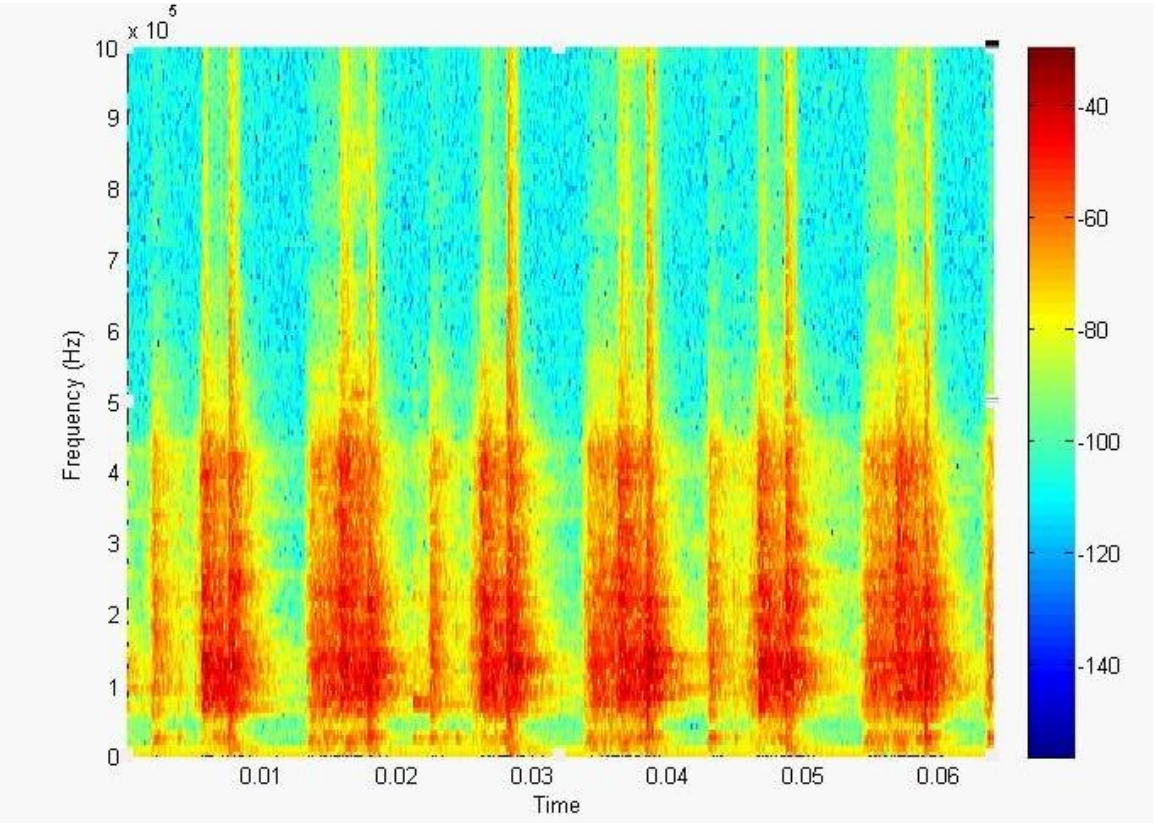

(c)

Figure 5.9 Spectrogram of AE signal at worn level of tool life (v = 230m/min and f = 250mm/min).

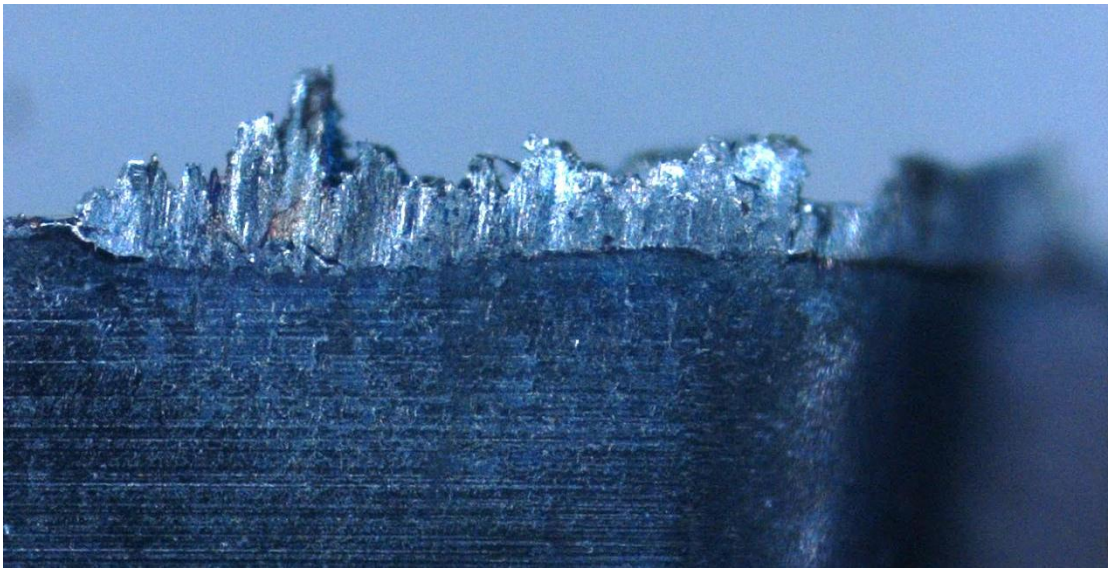

Figure 5.10 Built-up edge formed on the tool flank face

The change in width of energy may also indicate a state of moderate wear or substantial increase of wear formation on the tool. In worn tools, sharp high energy frequency peaks from Figure 5.9 are also utilised to infer wear from cracks and chipping on the tool.

An in-depth analysis of the AE signals via these methods provides clearer connotations for linking features to wear values.

5.3 Modelling and Analysis of tool wear

5.3.1 Data set for ANN

A data set of 160 test samples was selected from the experimental runs for the execution of the neural network. This data set consists of 120 samples which were used for the training of the network and 40 samples were used to test its efficiency. It can be noted that most of the tests samples reflected new and moderately worn tools but a percentage of about ten per cent only reflect severely worn tools.

5.3.2 Evaluation of feature extraction

Features in various domains have been utilised in this research. Time domain and time-frequency domain features were extracted and processed from the digitised data obtained from the coupler. Table below displays various features extracted in the course of the research.

Table 5.5 Extracted time and time-frequency features of AE signal

Time domain		**Time-Frequency domain**	
Features	Definitions	Features	Definitions
$\boldsymbol{AE_{MEAN}}$	The average value	$AE_{WAV-SUM}$	Wavelet sum
$\boldsymbol{AE_{RMS}}$	The RMS value	AE_{D1}	D1
$\boldsymbol{AE_{SD}}$	The standard deviation	AE_{D2}	D2
$\boldsymbol{AE_{VAR}}$	The variance	AE_{D3}	D3
$\boldsymbol{AE_{\mathrm{MX}}}$	The maximum value	AE_{D4}	D4
$\boldsymbol{AE_{MIN}}$	The minimum value	AE_{D5}	D5
$\boldsymbol{AE_{RG}}$	The range (max–min)	AE_{ERG}	Total energy of wavelets
$\boldsymbol{AE_{SK}}$	The skewness		
$\boldsymbol{AE_{KU}}$	The kurtosis		

A total of 16 signal features have been used. From these sixteen features; nine time domain and seven time-frequency domain features. The Time-frequency domain features in Table 5.5 were obtained from the decomposition of the signal via wavelet transform.

5.3.3 Evaluation of feature selection

During selection, some features from the experimental runs on the CNC machine were identified for training. From the total of 16 features extracted, a careful selection process which reviewed the correlation of each of these features to the desired target output was applied through the correlation function (Equation 3.14).

Table 5.6 shows the results of the correlation of each feature to the targeted output wear. The Table indicates higher correlation in time-frequency analysis. Time-frequency features show an average correlation efficiency of 64 % over time domain features with only 48%. The selection is however based on choices of feature from both domains. The strength of the mean and rms signals amidst these features indicates their importance in classification.

As identified from the wavelet graph decomposition in section 5.23, higher energy density band; D3 and D2 obtained sufficiently high correlations. It could be assumed to be due to its time and frequency domain characteristics. These time-frequency features outmatched others in correlation efficiencies. D1 also showed the transference of high energy signals during worn states to higher frequencies.

Table 5.6 Correlation results of AE features to target output

S/N	Feature	Correlation type	correlation coefficient
1	speed	max correlation coefficient:	0.3225
2	feed	min correlation coefficient:	-0.3218
3	rms	max correlation coefficient:	0.7374
4	mean	max correlation coefficient:	0.7579
5	standard deviation	max correlation coefficient:	0.5736
6	variance	max correlation coefficient:	0.5353
7	maximum value	max correlation coefficient:	0.5768
8	minimum value	max correlation coefficient:	0.3087
9	range	max correlation coefficient:	0.5768
10	skewness	max correlation coefficient:	0.3215
11	kurtosis	min correlation coefficient:	-0.2933
12	wavelet sum	max correlation coefficient:	0.6829
13	d1	max correlation coefficient:	0.7753
14	d2	max correlation coefficient:	0.7725
15	d3	max correlation coefficient:	0.7145
16	d4	max correlation coefficient:	0.4152
17	d5	max correlation coefficient:	0.4816
18	wavelet total energy	max correlation coefficient:	0.6231

5.3.4 Feature classification

This section of the study replicates the biological neural system using computational representation to classify wear output. It addresses the usability of evolutionary computing as an adequate tool in machine tool monitoring.

Data set with the selected key features were used to run a neural network. A feed forward BPNN was utilised for classification. Table 5.7 shows the various parameters employed in network training. A learning rate of 0.3 on a gradient descent training function with a momentum of 0.7 was used. An adaptive learning rate method aided in quick generalisation of the error and reduced training time. The training was run for a thousand epochs with no validation queries. The weights of the network were selected at random from a range of -1 to 1. No optimization algorithms were implemented on the BPNN due to its reverse operation mode which provides an adequate optimization structure for the system.

Table 5.7 Neural network parameter section

Parameters of multilayer neural network	**Values**
Epochs	1,000
Performance function	Mean square error
Number of layers	3
Transfer Function at layer 1	Log-sigmoid
Transfer Function at layer 2	Log-sigmoid
Transfer Function at layer 3	Log-sigmoid
Layer 1 size	9
Layer 2 size	20
Layer 3 size	3
Learning rate	0.3
Momentum	0.7
Weights	Random from [-1 1]
Training Function	Gradient Descent with adaptive learning rate and momentum

5.3.5 Network methodology

The system is developed on a MATLAB programming platform. This platform offers easy programming interface. The neural network process is characterised by the adjustment of weights and biases to achieve a desired output response for every input selection introduced into the network. Training of the network mathematically connotes the minimisation of the error in its classification. As earlier mentioned, there are two ways of training; supervised and unsupervised. Back propagation is a supervised training methodology in which the target output is supplied for the network classification. An activation function is used in networks to estimate the error of classification.

In the study, the sigmoid activation function was utilised to determine the net firing output from the artificial neuron. The sigmoid function takes known sample inputs from the data set and classifies them within a range of 0 to 1.

$$\varepsilon = \sum_{P=1}^{P_T} (t_p - o_p)^2 \qquad (5.3)$$

Where ε is the error, t_p the target output, o_p actual output, with input sample $P = 1, 2, \ldots T$.

This activation function (equation 5.3) was used due to the non-linear relationship of the AE sample data and target wear output.

5.3.6 Objective of the neural network

The network was trained to recognise each sample line from the data and output a binary number corresponding to a target wear value. Table 5.8 shows the binary representation of wear values corresponding to target output for the neural network.

Table 5.8 Binary representation of wear values for neural network training

Wear ranges	0.01<x<0.1	0.1<x<0.2	0.2<x<0.3
Binary representation	0 0 1	0 1 0	1 0 0

Momentum, dynamic learning rate and network architecture were used to test training performances and optimal parameter choices were made in this study. Comparison of performances of network architectures is further explained in the next section.

5.3.7 Network architecture

The network architecture was chosen based on the experimental test procedure. Individual networks were tested over the data set to obtain a least mean square error (MSE). Table 5.9 displays the results of the findings.

Table 5.9 Neural Network architectural evaluation

Hidden Layer	**Node**	**RMS error**	**hidden layer**	**Nodes**	**RMS error**
1	4	0.0579	2	4-4	0.0539
	8	0.0176		8-8	0.0194
	12	0.00972		12-12	0.0110
	16	0.0142		16-16	0.0136
	20	0.00523		20-20	0.0164

From the Table 5.9, two series of tests were performed on both single and double hidden layer architecture. A trend was identified with an increase with higher nodes in the hidden layer before a decrease in efficiency. However, a single hidden layer structure with 20 nodes produced the least MSE for a run of a thousand epochs. Generally, both layer structures produced acceptable results but much lower MSE was observed for single hidden layer system. Chen et al [58] identified an rms error below 0.05 as acceptable in network classification. A much lower error performance

of 0.005 was achieved in the study. The network architecture (Figure 5.11) with the best performance was therefore selected for classification.

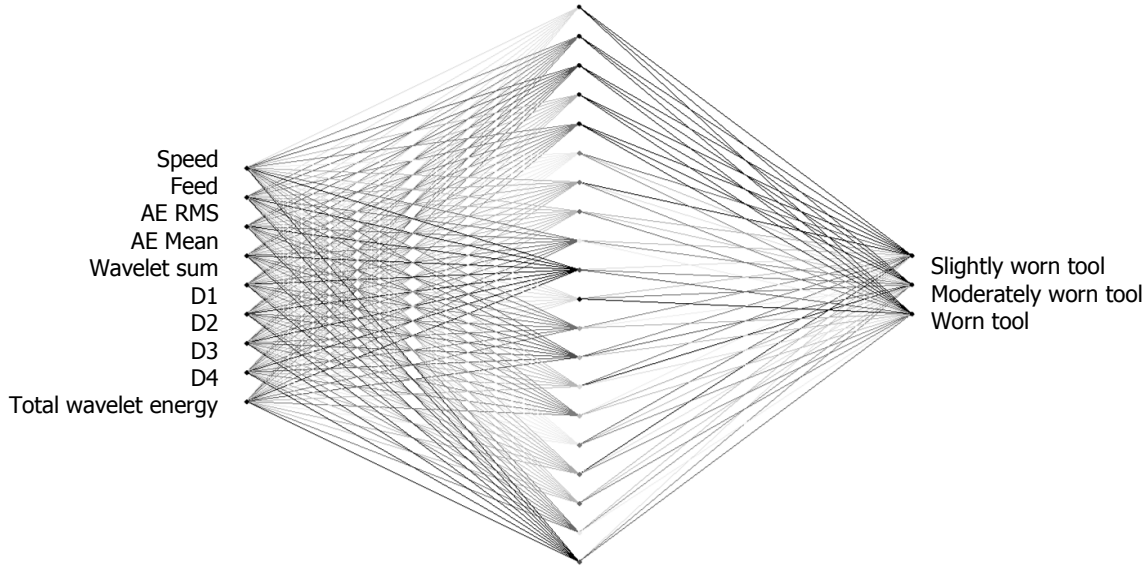

Figure 5.11 Neural network architecture

5.3.8 ANN process evaluation

The process evaluation of the neural network discusses the network performance and performs simulations tests to portray its classification capabilities. Network performance can be seen from the training curves (Figure 5.12). This shows the gradient descent of the sum of squared error versus number of training cycles.

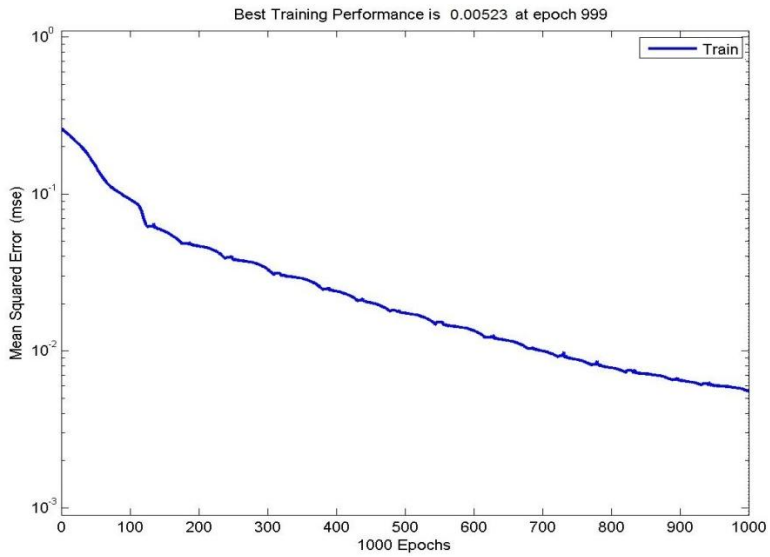

Figure 5.12 Performance function of neural network

A very efficient network with a very low training error state evaluated in mean square value gave a performance of 0.00523. This performance ratio indicates a capability of above 95% classification accuracy for this network.

5.3.9 Network testing

Simulation tests were conducted on the network to assess its efficiency in the wear classification. Sample transposed solutions for experimental run of varying parameters of speed and feed at the initial stage of the study is simulated with the network. The binary output of 0 0 1 as indicated in Table 5.8, which symbolises an initial wear state should be generated. Figure 5.13 displays a bar chart of the actual output. It shows high and low digits for solution classification.

Digital devises have a range where high or low digits are registered, this account for any noise that may exist. Despite the vivid correct classification, residual noise can be found at minimal levels on alternate digit bit indicating correlation to successive classification groups. It is necessary for all output digits to stay in its correct range; this is challenged by errors made by the neural network approximations and noise of the physical system.

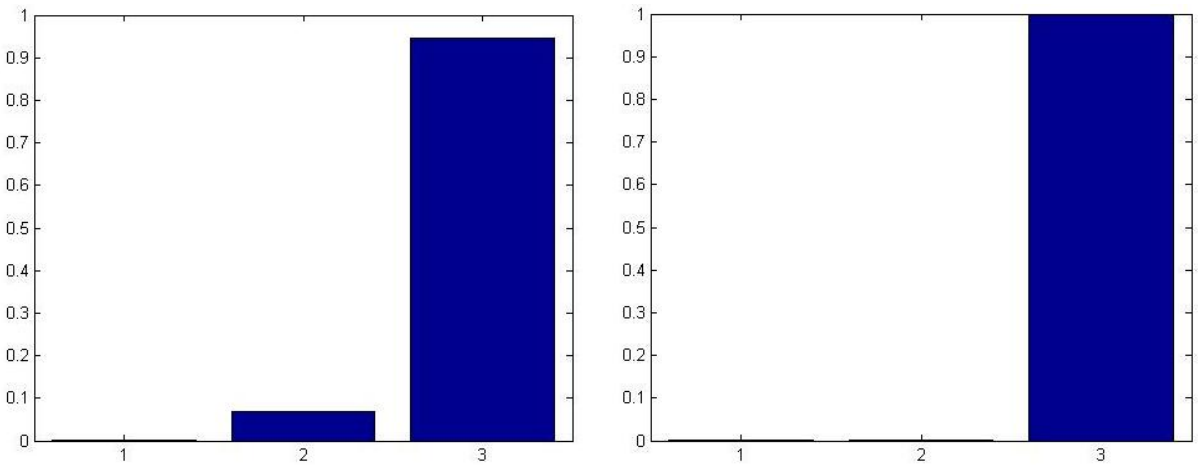

v = 200m/min and f = 200mm/min (a)

v = 200m/min and f = 250mm/min (b)

Figure 5.13 Testing chart of the neural network at the initial stage of wear

Data tests at the moderate stage (Figure 5.14) in wear progression also were adequately classified. Binary output of 0 1 0, which symbolises a moderate wear state was generated. Some residual noise components were observed as well in alternate digits.

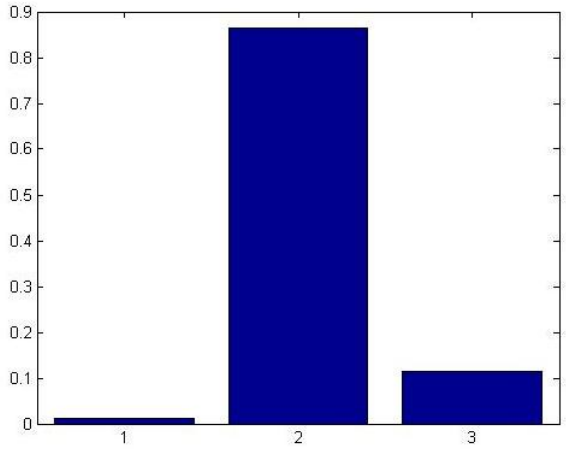

v = 170m/min and f = 250mm/min
(a)

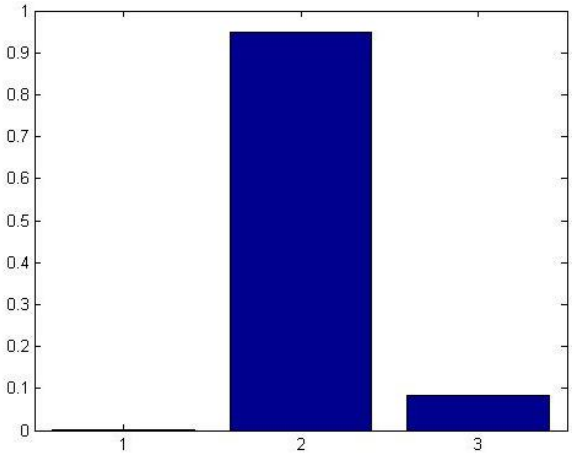

v = 200m/min and f = 300mm/min
(b)

Figure 5.14 Testing chart of the neural network at moderate wear stage

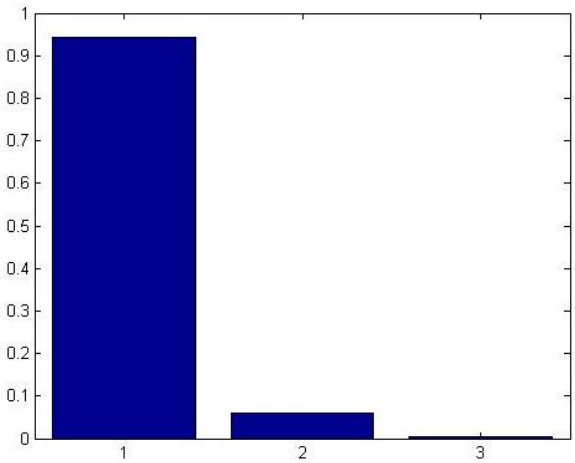

v = 230m/min and f = 300mm/min
(a)

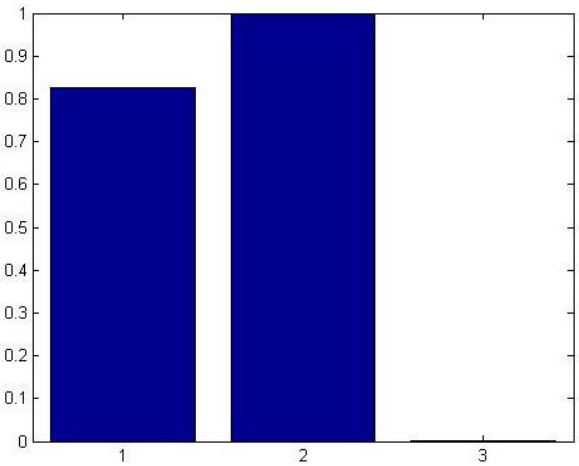

v = 170m/min and f = 200mm/min
(b)

Figure 5.15 Testing bchart of the neural network at worn wear stage

Some experimental test samples for worn states were simulated with the network. A binary output of 1 0 0, which symbolises a worn tool state was generated. A clear classification can be seen from Figure 5.15a, but Figure 5.15b shows some

misclassification anomalies. This occurs due to the generalisation error of the network or inadequacy of sample data size for classification. The network identifies high correlation to both moderate and worn tool states. This may be utilised to represent transitionary characteristics between stages in sample data and classified based on its tendency towards worn tooling.

5.4 Experimental correlations results

Investigative studies of chipping property have been conducted in this thesis. AE features used in this study showed ample response for specified events during machining. The most correlated features are the rms, mean, wavelet sum, energy and some wavelet coefficients. Notable time domain and time-frequency domain features which consistently correlated to tool events are the mean, rms and wavelet sum.

Figure 5.19 shows the correlation for experiment 1. In this figure, two events were observed within the entire machining of the tool. At a distance of 13.2 m, huge notch wear occurred on the tool (Figure 5.16). This event was characterised by rising peaks in rms, mean and wave features of the AE signal. Progressive peaks occurred at a distance of 20 m of machining length, where heavy chipping of the tool flank (Figure 5.17) face was observed. Strong correlation of the mean, rms, variance, standard deviation and some wavelet coefficient were noticed at this stage. The chips coloration between these events changed from a light purple to a bluish violet colour due to the amount of heat generated from the rubbing action of the tool on the workpiece.

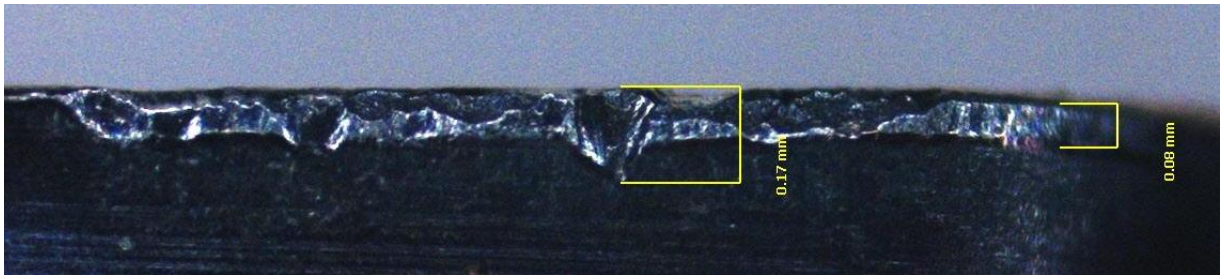

Figure 5.16 Notch wear and edge chipping on the tool flank face

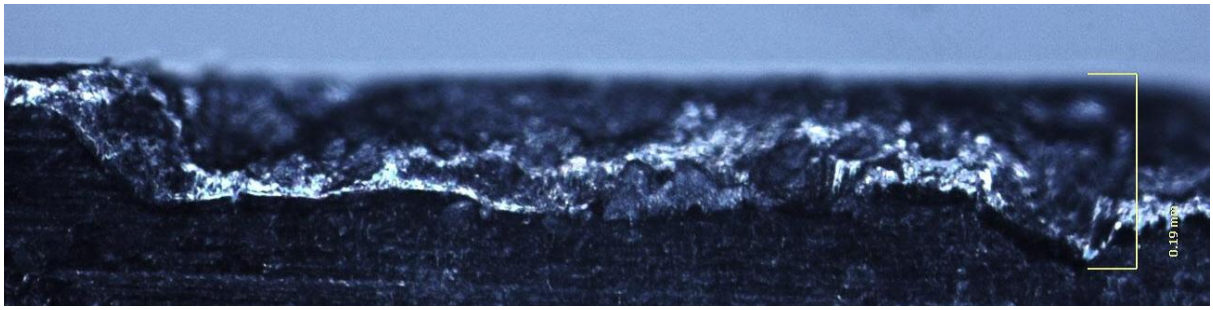

Figure 5.17 Progressive chipping of tool flank face

Experiment 2 (Figure 5.20) was assessed at a distance of approximately 7 m and 18 m of machining length. At 7 m, observable uniform flank wear rose to 0.05 mm due to the abrasive effect at the flank face of the tool. This was captured by the wavelet sum, d3 and d4 wavelet coefficient with a mild peak in the signal amplitude. More AE features were noticed as a result of grooves propagation after 18 m of machining. Time domain and time-frequency domain features responded at various proportions to this wear formation. A progression from a golden brown chip to a purple chip indicated the rise in temperature which led to wear intensification a on the tool.

Figure 5.18 shows some of the various chip colours obtained during the machining of H13 tool steel. A gradual change from golden brown to blue is shown.

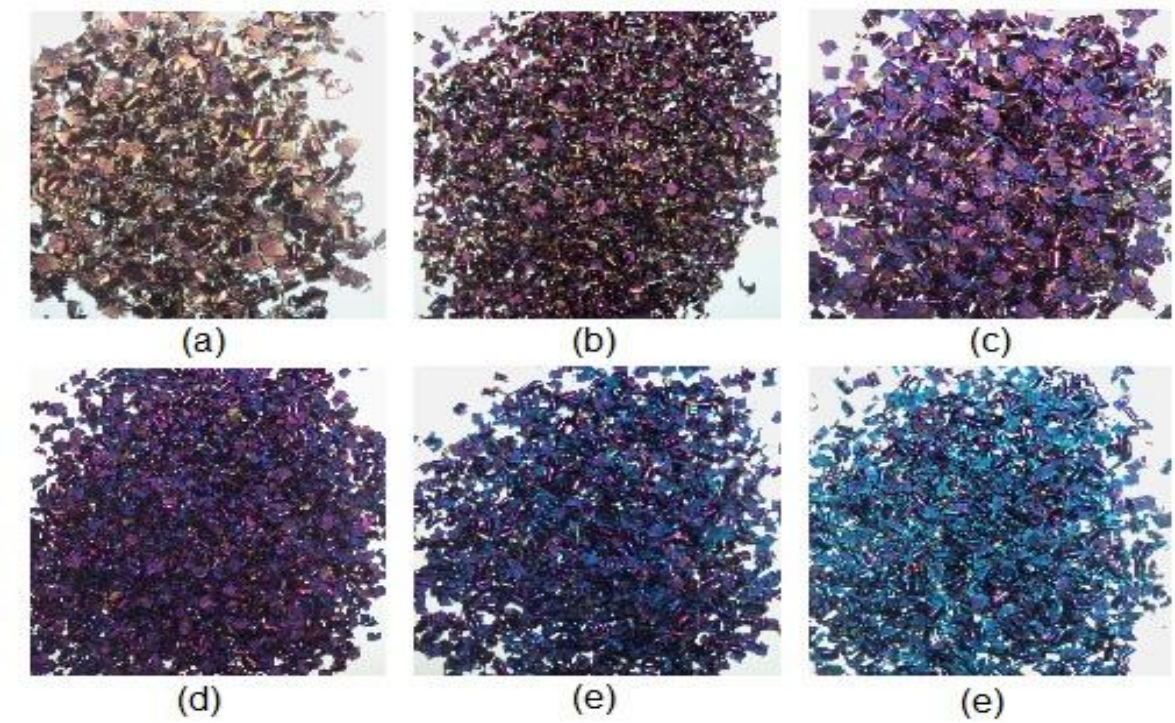

Figure 5.18 Chip coloration progression

At the preliminary stage in experiment number 3 (Figure 5.21), the formation of micro-grooves on the tool flank edge after a machining distance of only 2 m resulted in a major peak rise in skewness. A notch groove of 0.07 mm which formed at the flank face deepened on a worn flank face of length of 1.71 mm. Major expansion by chipping formation was observed within 9 m of machining of the tool. Wear caused by abrasive mechanism can be observed from Figure 5.21. Chips at 1 m of machining were of a combined colour of yellowish brown and light purple. This indicates the gradual rise in heat during cutting. An eventual darker colour which took place at the moderate wear was noticed. A good correlation from all selected AE features were observed but the rms, mean and d4 wavelet coefficient showed a stronger correlation. However the skewness showed a negative correlation with a down peak. This shows that the data distribution is skewed left which is due to long lasting consistent wear value observed on that tool during machining phases.

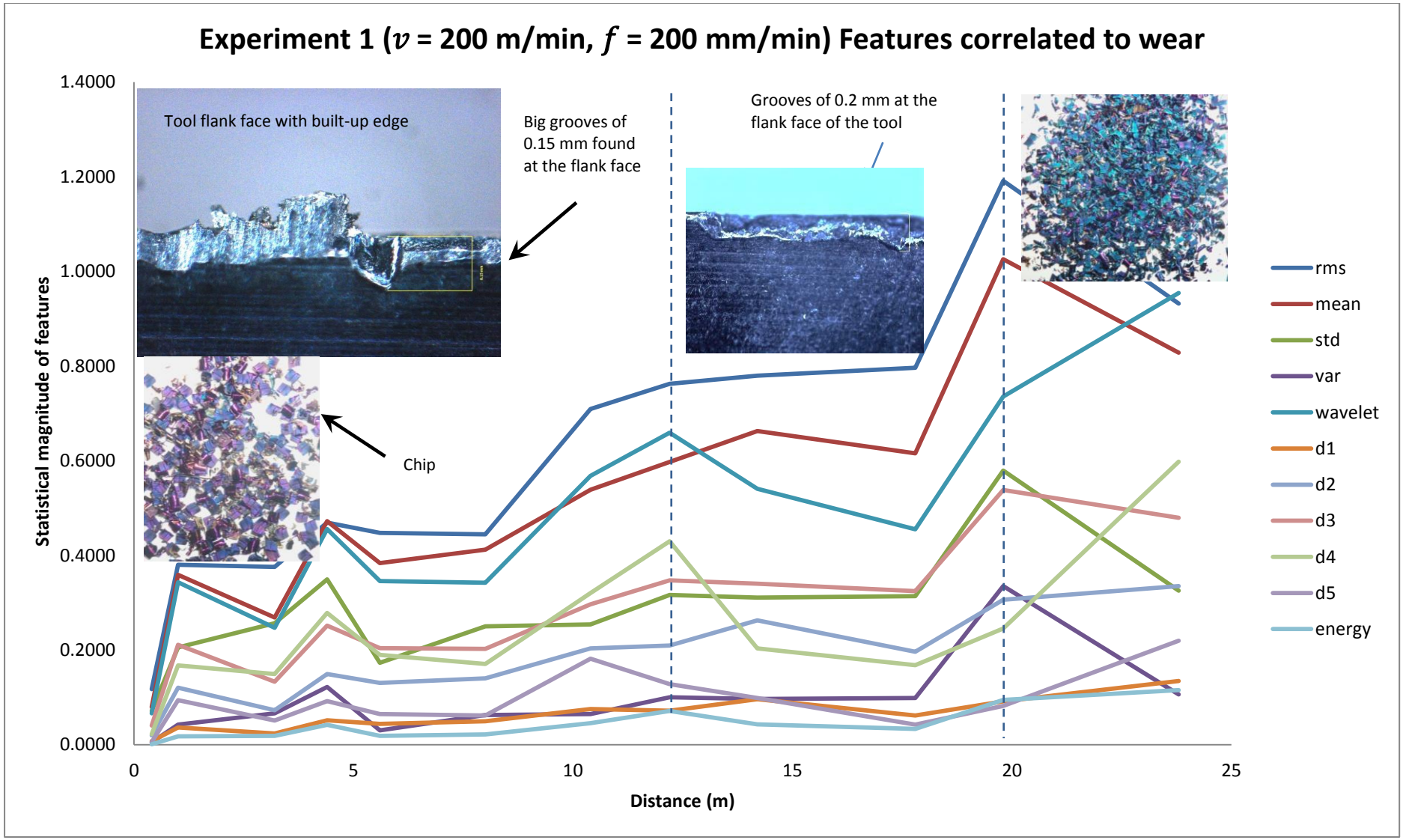

Figure 5.19 Experiment 1 features correlated to wear

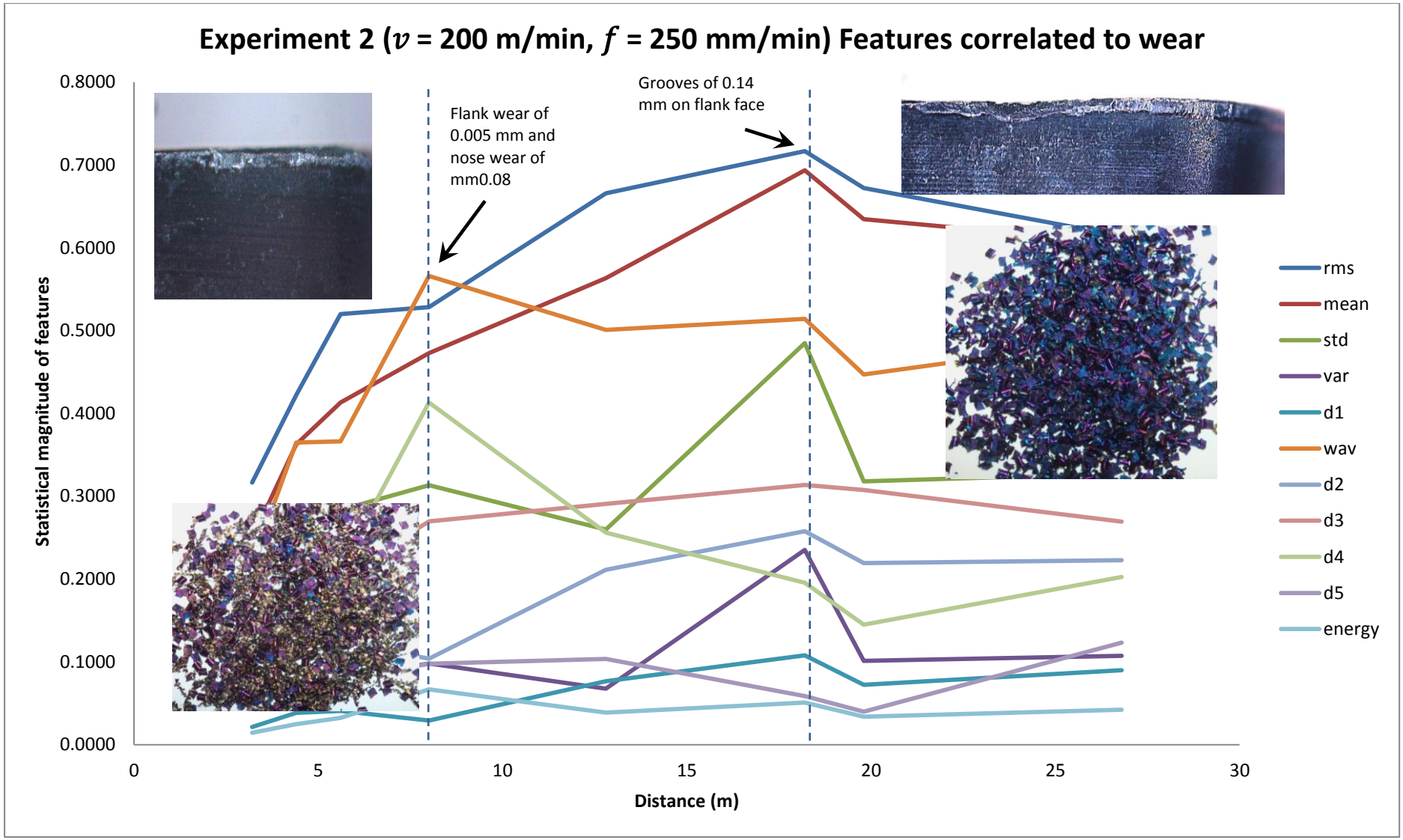

Figure 5.20 Experiment 2 features correlated to wear

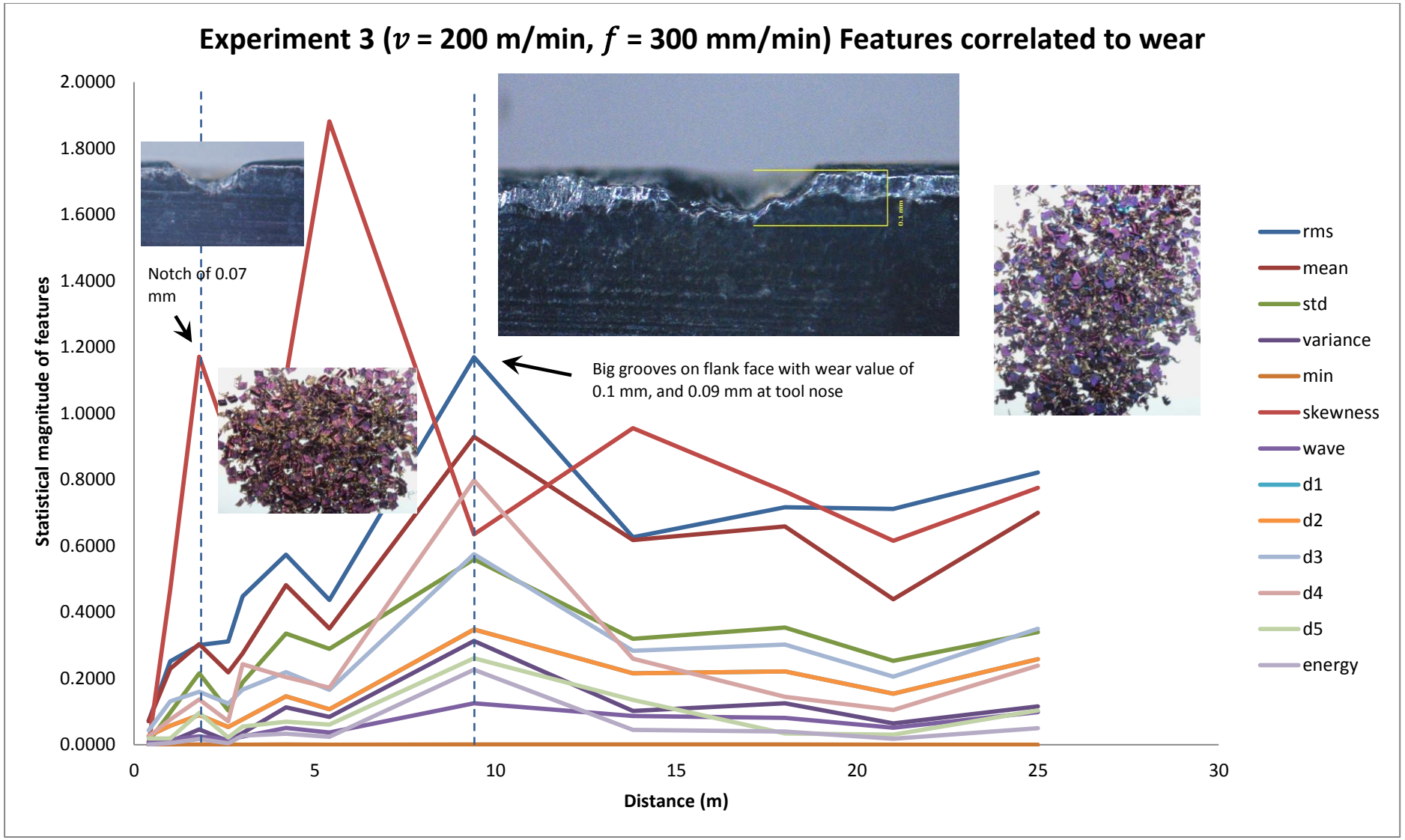

Figure 5.21 Experiment 3 features correlated to wear

Experiment number 4 shows (Figure 5.22) a flank wear progression at a distance of 13 m of machining. Continuous wear formation is observed on the tool flank face and is characterised with dark purple chip coloration. Progressive machining at distances above 21 m shows a generation of deep violet blue chips. High wear formation can be observed at this stage with built-up edge (BUE) formation and a huge groove at the nose of the tool. The wear values at the later stage are above 0.2 mm at the nose. The rms, mean, wavelet sum are still predominant correlated features in this evaluation.

Evaluation of chipping from experiment number 5 (Figure 5.23), shows similar chip colour progression. A colour change from golden brown which is mostly identified within machining distances below 5 m is seen. The AE mean correlated with a sharp peak rise to the minor wear formation at the early machining stage. Gradual metamorphose to purple chip is identified with BUE formation and extended nose wear at a distance of 8 m. Correlation from all displayed AE features can be observed from this experiment as well.

Experiment six evaluates a region of machining and identifies the distinct progressive change in coloration of chips. The flank wear increased to a state with high BUE formation. The chip colour gradually progressed from a brownish purple to a deep purple colour. Abrasive and adhesive wear mechanisms which enhanced the rubbing action of the tool on the workpiece could be the reason for this chip coloration change. An exponential increase in wear due to increase in temperature causes the tool to suddenly reach a worn state after 14.4 m of machining. High correlation of energy, rms, mean, standard deviation, wavelet coefficient sum and d3 coefficient can be observed at individual stages within machining.

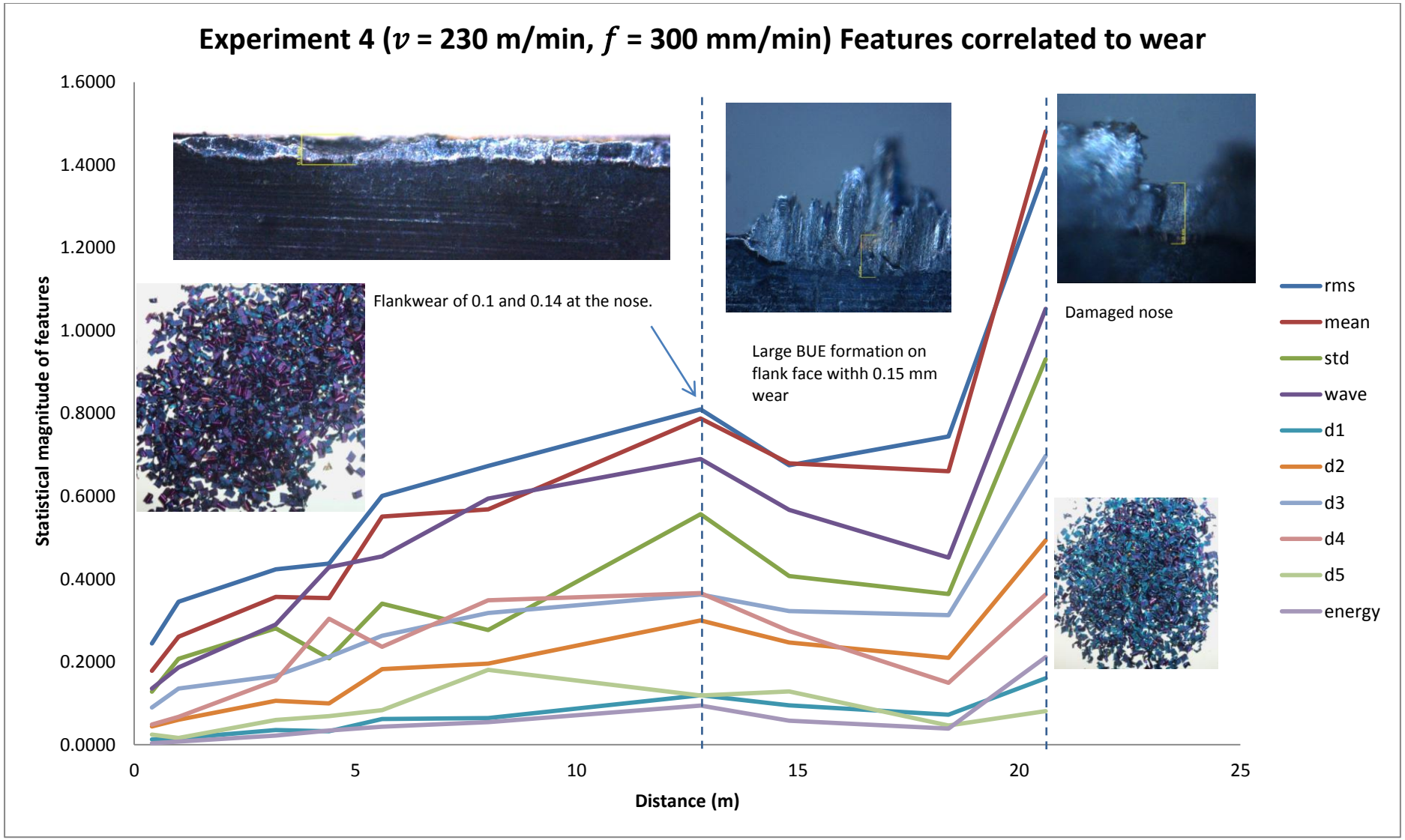

Figure 5.22 Experiment 4 features correlated to wear

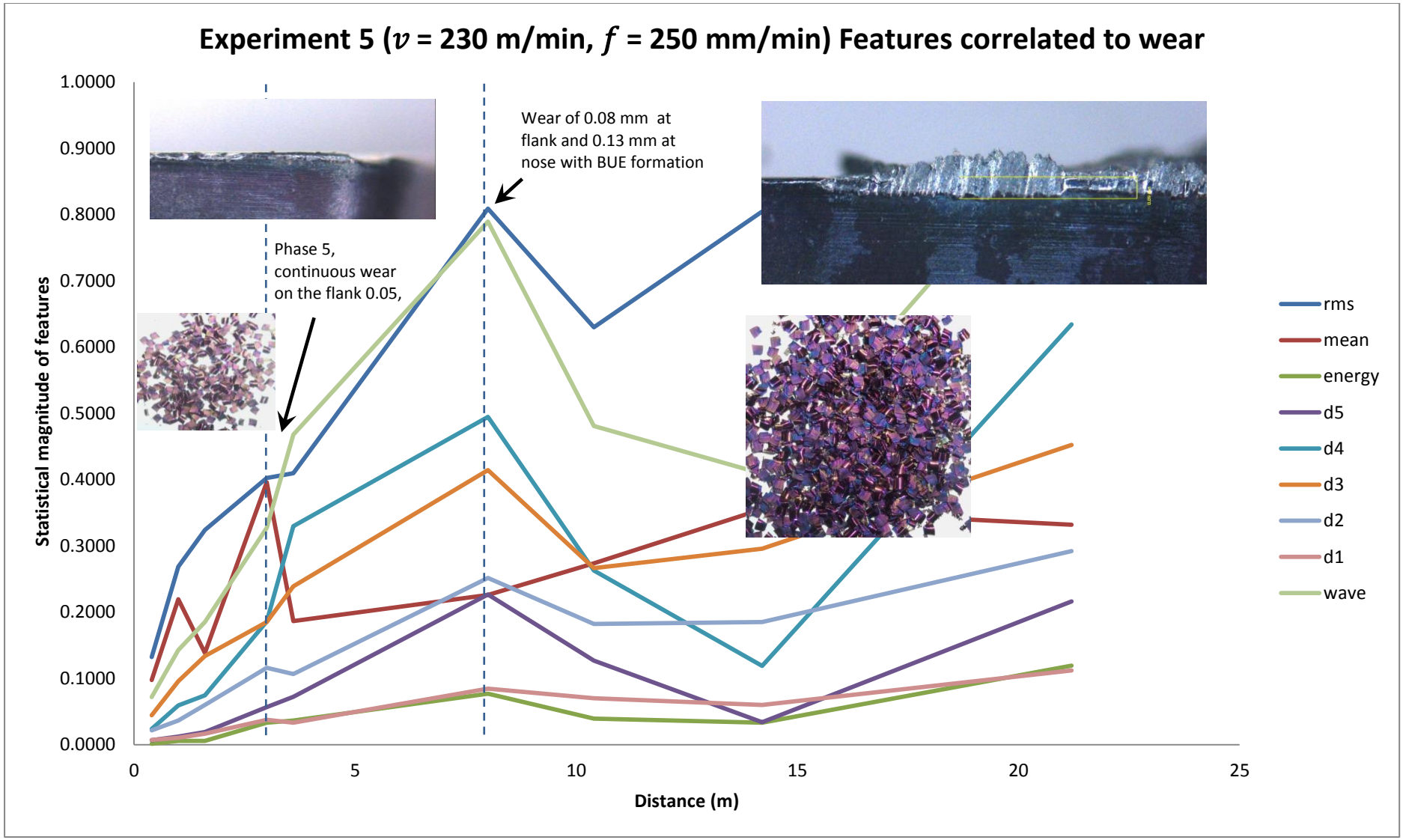

Figure 5.23 Experiment 5 features correlated to wear

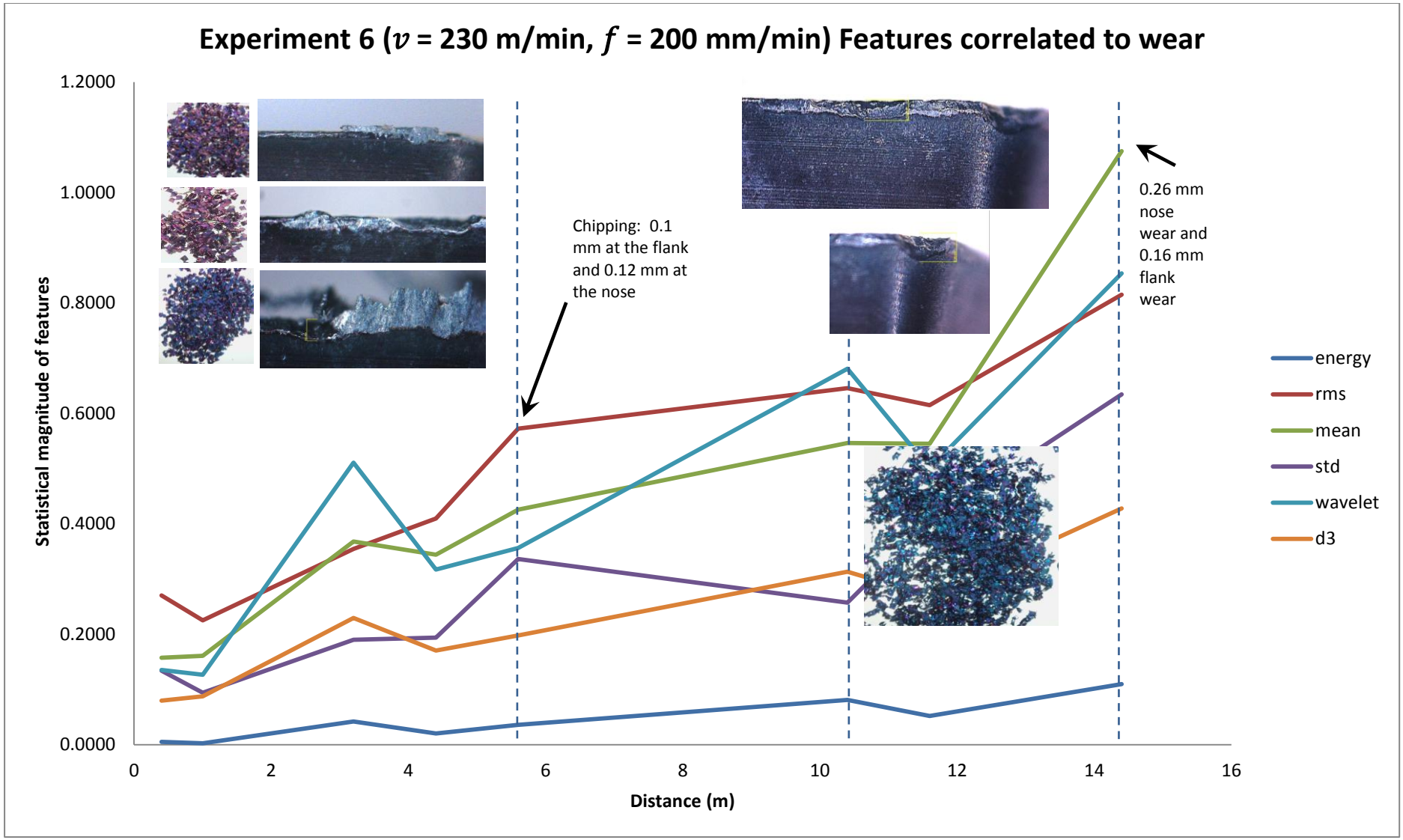

Figure 5.24 Experiment 6 features correlated to wear

In experiment 7, within 5 m of machining (Figure 5.25), a higher correlation from time-frequency features characterised with a golden-brown chip colouration is observed. The high correlation in rms and wavelet sum with a protruding peak rise indicates an increase in wear to a value of 0.07 with a BUE formation on the flank. This stage of machining produced brownish purple chip indicating that the temperatures obtained at this level were not too high.

In experiment number 8 (Figure 5.26) identification of wear did not produce proportional increase in time domain features. At a distance of 13 m, the rms correlated with large grooves formation and a flank wear value of 0.08 mm whereas, the mean reflected a progressive increase in the nose wear at a later distance of 17 m of machining. A deep purple chip colour indicated high temperatures and rising wear formation on the tool.

Experiment number 9 was characterised by the formation of early grooves due to its low feed rate which resulted in strong impacts of the tool edge against the workpiece during tool entries. Distinct chip colours in the experiment at the three identifiable stages of wear were observed. Chips progressed from yellow to reddish brown and deep purple blue. Early cracks were detected adequately from most AE features. At a distance of 13 and 22 m subsequent sudden jump in wear values were observed. These jumps were identified by most of the AE features adequately.

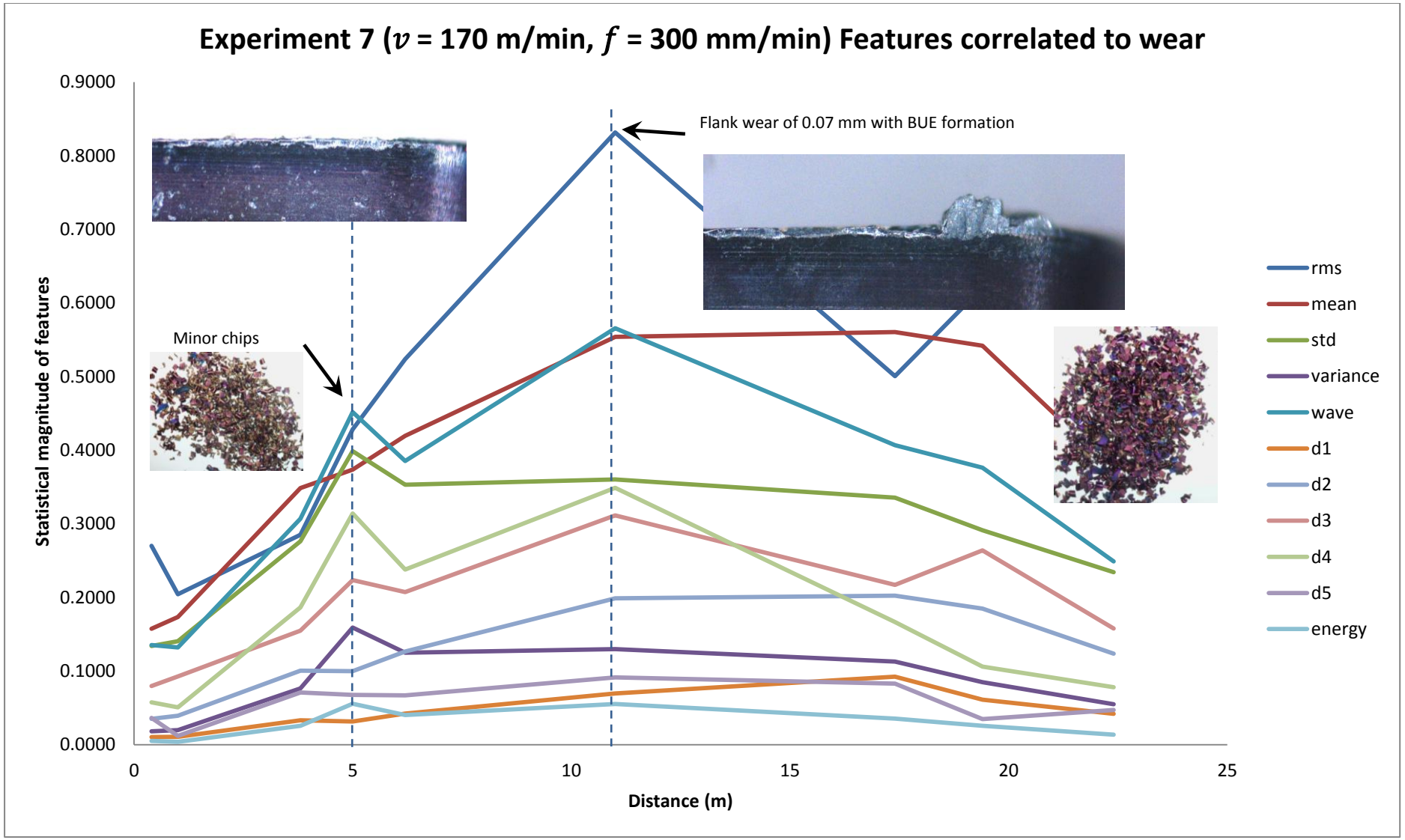

Figure 5.25 Experiment 7 features correlated to wear

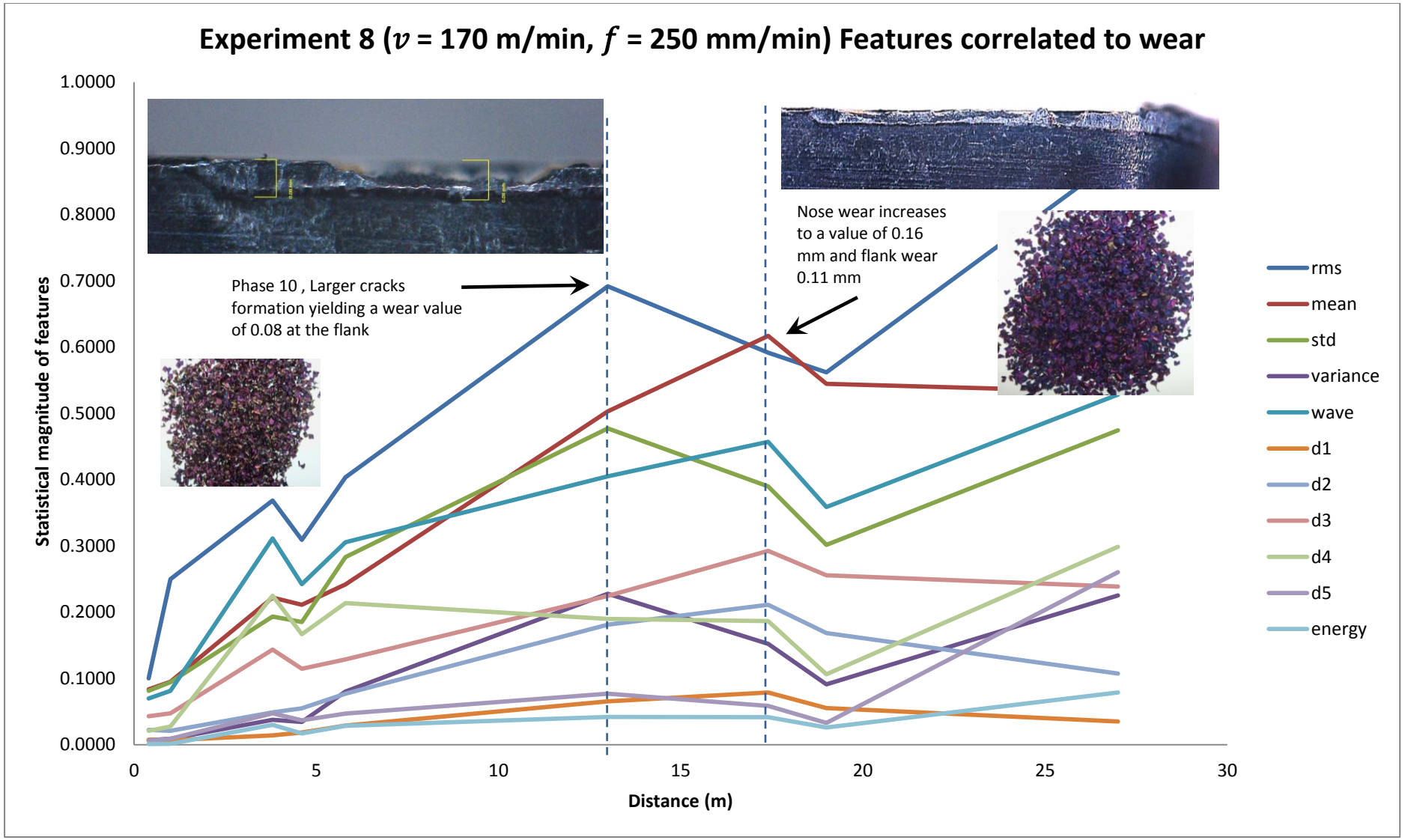

Figure 5.26 Experiment 8 features correlated to wear

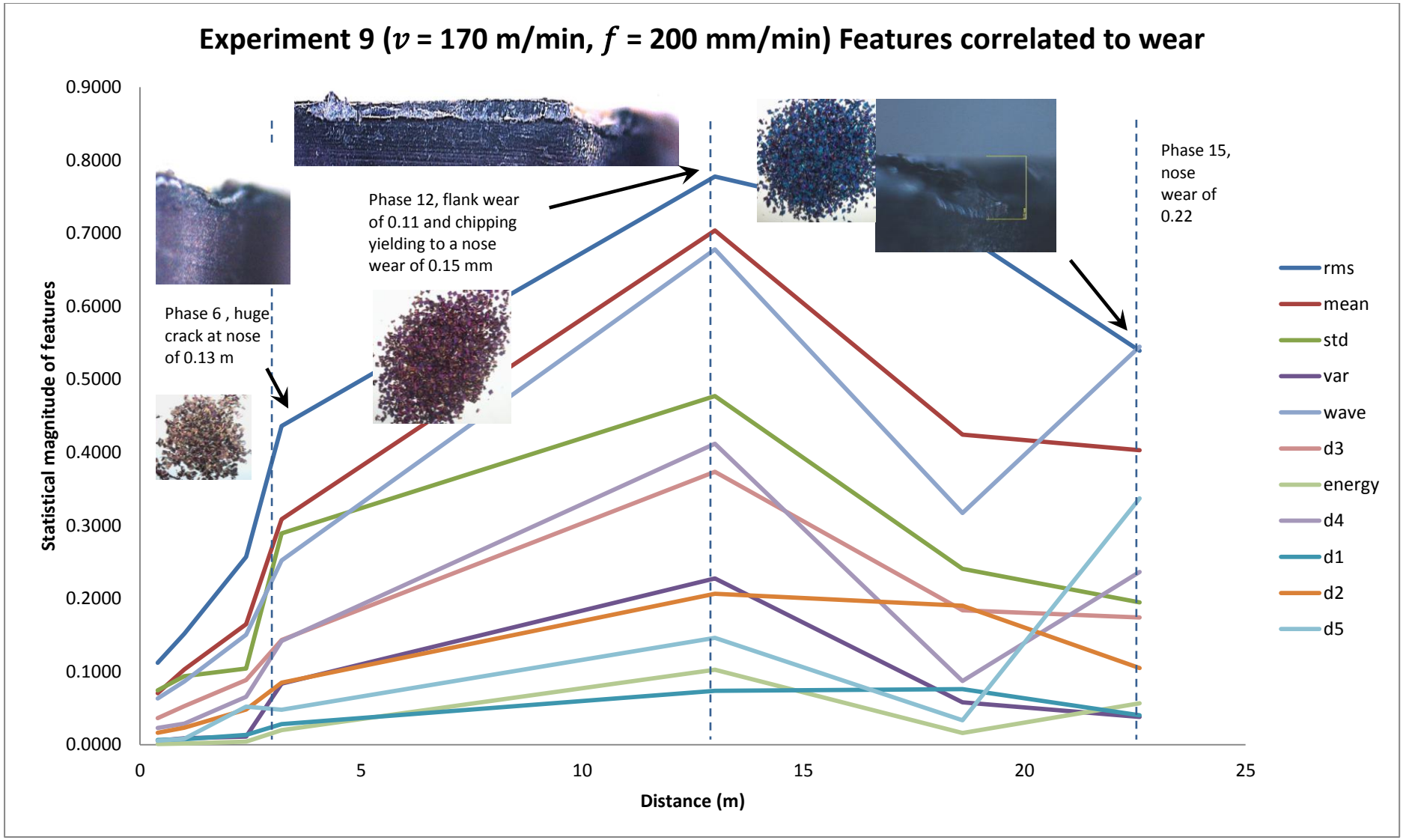

Figure 5.27 Experiment 9 features correlated to wear

AE rms, mean, wavelet sum, energy and some wavelet coefficient provided adequate information about machining conditions. This could be accrued from their correlation throughput to minor and major jumps in wear values during machining.

Chip colour change investigated in this study showed three major variations of chip coloration. Table 5.10 shows the experimental run and the various chip colours observed during this experiment. These chip colours were seen to progressively change to metamorphose during experimentation. Some experiment trials possessed transitionary variations of two distinctive types of colours. This progressive information possessed correlative reference to tool wear.

From observations, during the preliminary stages of the research, chip formed had a golden-brown colour. This phase of chip colouration was observed throughout the main stages of the experimental runs. From this observation, an indication of the low machining temperatures could be inferred. This phase was succeeded with a brown/pink/purple colour of chips. Each experimental runs observed these traits at distinct stages. This phase was briefly overtaken with deep purple/blue chipping at the worn state of the tool.

Table 5.10 Chip colour identification and progression with tool wear

		Number of passes per experiments (from pass 1 to 15)														
		Pass 1	**Pass 2**	**Pass 3**	**Pass 4**	**Pass 5**	**Pass 6**	**Pass 7**	**Pass 8**	**Pass 9**	**Pass 10**	**Pass 11**	**Pass 12**	**Pass 13**	**Pass 14**	**Pass 15**
Experiments	**1**	G	G/P	G/P	G/P	G/P	G/P	G/P	P	P	P	P	P/V	P/V	V	V
	2	G	G	G/P	G/P	G/P	G/P	G/P	G/P	P	P	P	P	P/V	P/V	V
	3	G	G	G	G	G	G/P	G/P	G/P	G/P	P	P	P	P	P/V	P/V
	4	G	G	G	G	G	G	G/P	P	P	P	P	P	P/V	P/V	P/V
	5	G	G	G	G	G	G	G	G/P	P	P	P	P	P/V	P/V	P/V
	6	G	G	G	G	G	G	P	P	P	P	P/V	P/V	V	V	V
	7	G	G	G	G	G	G	G	G/P	G/P	P	P	P	P	P	P
	8	G	G	G	G	G	G	G	G	G	G/P	P	P	P	P	P/V
	9	G	G	G	G	G/P	G	G	G/P	G/P	G/P	G/P	G/P	P	P	P/V

$* \ where, G = \ golden\ brown, \ G/P \ = \ golden\ brown\ with\ purple\ chips, P = \ purple/pink\ chips,$
$P/V \ = \ purple/pink/violet\ chips\ and\ V \ = \ purple/violet\ chips$

The chip coloration could be linked to the machining temperatures produced during cutting operation. Temperature rise during average wear stages was due to the rubbing action of the roughened edge of the tool against the workpiece. The degree of tool degradation as a result of wear had tremendous effects on temperature and therefore chips coloration. Worn tooling which possessed grooves and deeper wear formation produced consistent purple chip coloration. Threaded chips were also formed during these stages from the formation of BUE on the tool face.

5.5 Tool wear progression

Similar progression from the tool life diagram can be seen (Figure 2.4). Figure 5.28 presents graphs of wear progression over machined distance for the nine experiments. Experiments with higher speeds attained high level of wear rate faster at the initial stage and final stage of the chart. The lower feed values have resulted in intensive wear rates. Based on the fact that the number of collisions per machined distance is the same, it could be suggested to be due to smaller area of collisions impact of the tool entry, causing a higher force per area leading to faster tool edge chipping and deep groove formation. An example of this was observed in experiment 9 with a rapid increase in the moderate stage.

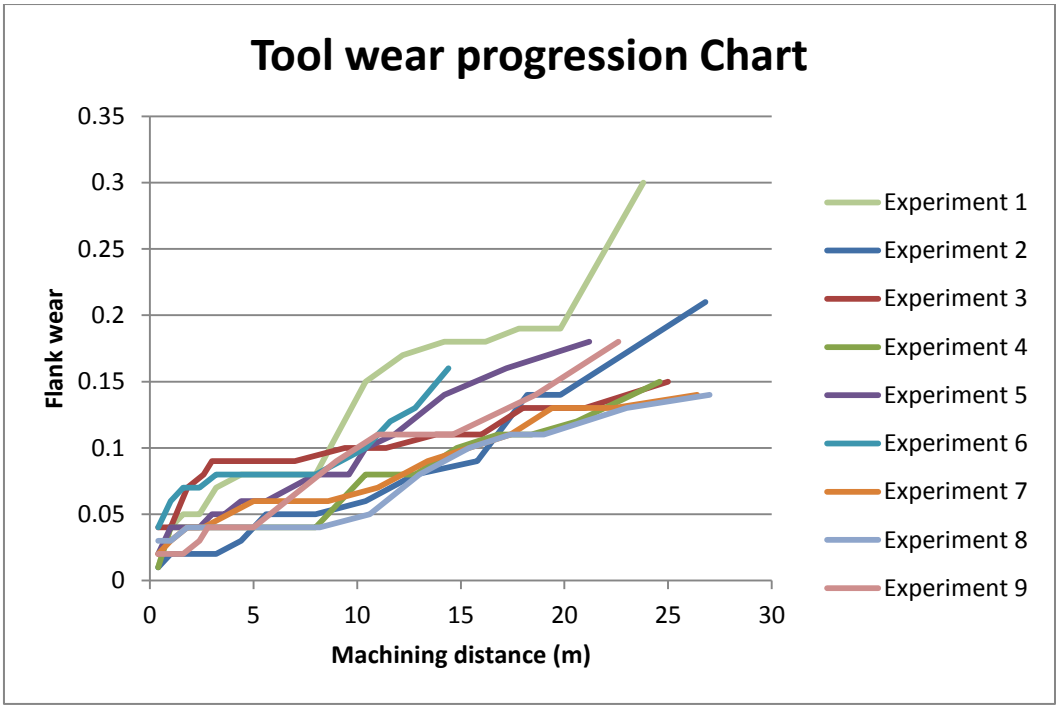

Figure 5.28 Tool wear progression chart

5.6 Proposed wear model

Based on the findings, a higher correlation can be observed from the specific AE features. These features can therefore be utilised in the prediction of the tool state. The rms, mean, wavelet sum, energy and some wavelet coefficient of interest provide adequate information on the machining process.

An artificial neural network model is proposed for the prediction of wear state for machining H13 tool steel at the operating parameters proposed. Figure 5.29 shows the proposed model aimed at adequately identifying of tool state. The number of hidden layers in the ANN model is related to the size of data set and experimentation, but between one or two hidden layers is believed to achieve acceptable results.

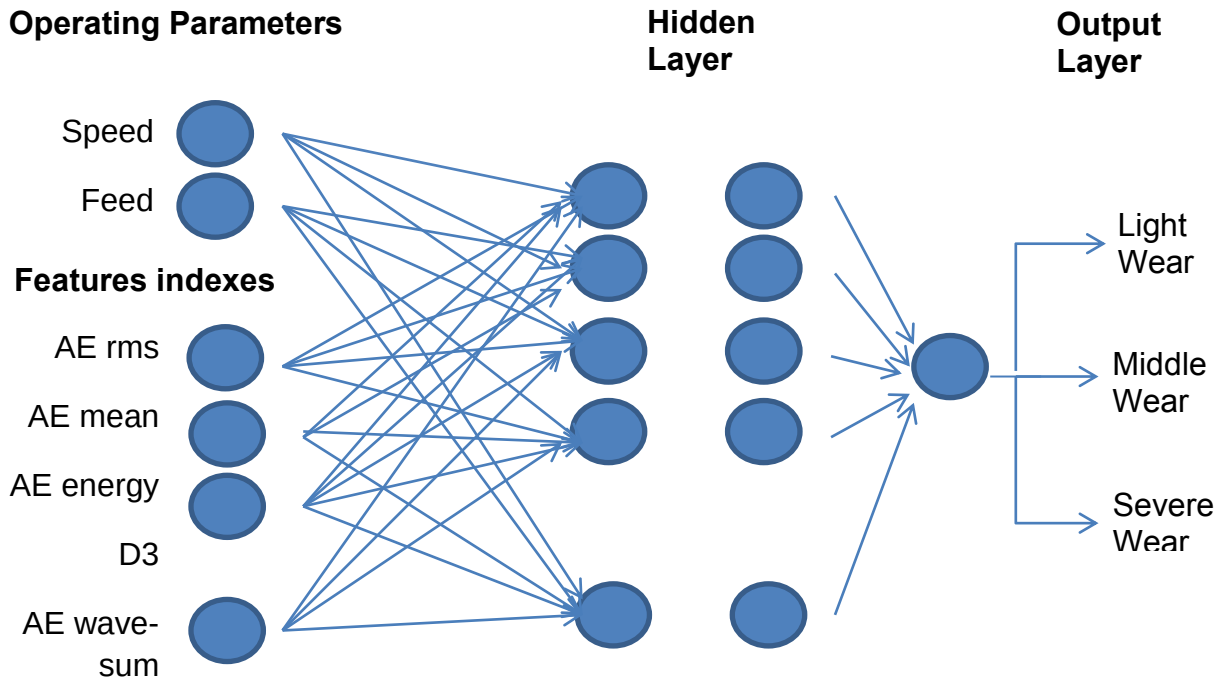

Figure 5.29 Artificial network model

From the study a tool wear coefficient model is also proposed.

$$W = \frac{v\,(\sum_{k=1}^{T}(\frac{D_k}{T}))}{f} + {AE_{ERG}}^2 + AE_{WAV-SUM} \qquad (5.4)$$

Where W is the tool wear coefficient, T the number of wavelet coefficient of interest, D is the wavelet coefficient, v is the cutting speed in m/min and f is the feed rate

The coefficient approach model is based on the correlation assessment during experimentation (Table 5.6). The effect of operating parameters and extracted features of interest is considered within the model. From this model a tool wear coefficient value above 0.7 indicates a moderately worn tool state, while a coefficient above 1.2 indicates a worn tool state.

Conclusions

A fundamental challenge in TCM is the identification of an ideal model for investigating tool wear. In this regard, this research was aimed at analysing AE as a viable means for tool wear identification. The study was performed on H13 tool steel material being machined by end-milling process. To achieve this, a series of experimental trials and signal processing techniques were employed.

In the course of this thesis a comprehensive feasibility study of using the principles of AE sensing technique for TCM was done. A monitoring process framework was used to monitor the end milling operation at different machining parameters utilising three industrial AE sensors. . This thesis proposed a signal processing framework which identifies a feature selection, extraction and conditioning process, and thereby creates a model linking them to wear formation.

Within the processing framework, results certified the importance of both time domain and frequency domain information in wear estimation. AE Sensing provides viable information on wear formation but not all features appropriately describe machining state. The use of a model which uses both time and frequency domain is essential.

A direct link was identified between some AE features and the rate of wear generated on the tool. A model using AE_{RMS}, AE_{MEAN}, $AE_{WAV\text{-}SUM}$, and high energy wavelet coefficient features is adequate to predict deplorable tool state wear. The model identifies the high correlation and influence of these features to tool life.

This study exposed some important results of AE sensing technique in the field of TCM. These include:

- From operating parameters employed, the study confirms that cutting speed more adversely influences wear states than other parameters such as the feed of operation.
- From the results, a negative correlation of the feed rate to the wear was observed. At low feeds sudden chipping took place because of the tool edge impact over the workpiece during tool entry. Results show that low machining feed rates are hazardous to machine tool.
- From result observation, AE_{rms} and AE_{MEAN} are viable time domain AE features in the identification of tool state.
- From the milling of H13 tool steel, colour identification of the chips provides direct correlations to the temperature of machining and tool condition.

Recommendations

Some recommendations have been observed during the time of this study. These include:

- An extension of the process to exploit monitoring of the machine operation is needed.
- The use of wider time-windows in signal processing would further enhance efficiency of the process but requires huge data manipulation.
- Additional AE features from different extraction techniques could be tested on the framework to update the model.

Future works should seek to exploit the proposed model using various machining operation, workpiece selection, operating parameters and processing techniques. More precise wear estimation could be attained from this model.

References

1. Prickett PW, Johns C. An overview of approaches to end milling tool monitoring. International Journal of Machine Tools & Manufacture. 1999; 39: p. 105–122.

2. Rehorn AG, Jiang J, Orban PE. State-of-the-art methods and results in tool condition monitoring: a review. Int J Adv Manuf Technol. 2005;: p. 26: 693–710.

3. Axinte DA, Belluco W, Chiffre LD. Reliable tool life measurements in turning — an application to cutting fluid efficiency evaluation. International Journal of Machine Tools & Manufacture. 2001; 41: p. 1003–1014.

4. Ashar J. Intelligent Drill Wear Condition Monitoring using Self-Organising Feature Maps. 2009. A thesis submitted to Auckland University of Technology.

5. Arsecularatne JA, Zhang LC, Montross C. Wear and tool life of tungsten carbide, PCBN and PCD cutting tools. International Journal of Machine Tools & Manufacture. 2006; 46: p. 482–491.

6. Adesta EYT, Hazza MA, Riza M, Agusman D, Rosehan. Tool life estimation model based on simulated flank wear during high speed hard turning. European Journal of Scientific Research. 2010; 39(2): p. 265-278.

7. Galante G, Lombardo A, Passannanti A. Tool-life modelling as a stochastic process. International Journal of Machine Tools & Manufacture. 1998; 38: p. 1361–1369.

8. Krar SF, Gill AR, Smid P. Techonology of Machine Tools. 6th ed. New york: Mc Graw Hill; 2005.

9. Lim CYH, Lau PPT, Lim SC. The effects of work material on tool wear. Wear. 2001; 250: p. 344–348.

10. Dimla DE. Sensor signals for tool-wear monitoring in metal cutting operations—a review of methods. International Journal of Machine Tools & Manufacture. 2000; 40: p. 1073–1098.

11. Kumar AS, Durai AR, Sornakumar T. The effect of tool wear on tool life of alumina-based ceramic cutting tools while machining hardened martensitic stainless steel. Journal of Materials Processing Technology. 2006; 173: p. 151–156.

12. Astakhov VP. The assessment of cutting tool wear. International Journal of Machine Tools & Manufacture. 2004; 44: p. 637–647.

13. Ertunc HM, Loparo KA, Ocak H. Tool wear condition monitoring in drilling operations using hidden Markov models (HMMs). International Journal of Machine Tools & Manufacture. 2001; 41: p. 1363–1384.

14. Dimla DE, Lister PM. On-line metal cutting tool condition monitoring. I: force and vibration analyses. International Journal of Machine Tools & Manufacture. 2000; 40: p. 739–768.

15. Scheffer C. Thesis: Monitoring of tool wear in turning operations using vibration measurements. 1999. A thesis submitted to the University of Pretoria.

16. Li X. A brief review: acoustic emission method for tool wear monitoring during turning. International Journal of Machine Tools & Manufacture. 2002; 42: p. 157–165.

17. Sick B. On-line and indirect tool wear monitoring in turning with artificial neural networks: A review of more than a decade of research. Mechanical Systems and Signal Processing. 2002; 16(4): p. 487–546.

18. Zhou J, Pang CK, Z. Zhong FLL. Tool wear monitoring using acoustic emissions by dominant-feature identification. IEEE Transaction on instrumentation and measurement. 2010; DOI 10.1109/TIM.2010.2050974.

19. Velayudham A, Krishnamurthy R, Soundarapandian T. Acoustic emission based drill condition monitoring during drilling of glass/phenolic polymeric composite using wavelet packet transform. Materials Science and Engineering A. 2005; 412: p. 141–145.

20. Arul S, Vijayaraghavan L, Malhotra SK. Online monitoring of acoustic emission for quality control in drilling of polymeric composites. Journal of Materials Processing Technology. 2007; 185: p. 184–190.

21. Everson CE, Cheraghi SH. The application of acoustic emission for precision drilling process monitoring. International Journal of Machine Tools & Manufacture. 1999; 39: p. 371–387.

22. Kong LX, Nahavandi S. On-line tool condition monitoring and control system in forging processes. Journal of Materials processing Technology. 2002; 125-125: p. 464-470.

23. Kim JS, Kang MC, Ryu BJ, Ji YK. Development of an on-line tool-life monitoring system using acoustic emission signals in gear shaping. International Journal of Machine Tools & Manufacture. 1999; 39: p. 1761–1777.

24. Jayakumar T, Mukhopadhyay CK, Venugopal S, Mannan SL, Raj B. A review of

the application of acoustic emission techniques for monitoring forming and grinding processes. Journal of Materials Processing Technology. 2005; 159: p. 48–61.

25. Susic E, Grabec I. Characterization of the grinding process by acoustic emission. International Journal of Machine Tools & Manufacture. 2000; 40: p. 225–238.

26. Kwak JS, Ha MK. Neural network approach for diagnosis of grinding operation by acoustic emission and power signals. Journal of Materials Processing Technology. 2004; 147: p. 65–71.

27. Kim HY, Kim SR, Ahn JH, Kim SH. Process monitoring of centerless grinding using acoustic emission. Journal of Materilas Processing Technology. 2001; 111: p. 273-278.

28. Kwak JS, Song JB. Trouble diagnosis of the grinding process by using acoustic emission signals. International Journal of Machine Tools & Manufacture. 2001; 41: p. 899–913.

29. Prateepasen A,.H.J.Au Y, Jones BE. Acoustic emission and vibration for tool wear monitoring in single-point machining using belief network. In IEEE Instrumentation and Measurement Technology Conference; May 21-23,2001; Budapest, Hungary. p. 1541-1546.

30. Kang MC, Kim JS, Kim JH. A monitoring technique using a multi-sensor in high speed machining. Journal of Material Processing Technology. 2001; 113: p. 331-336.

31. Marinescu I, Axinte D. A time–frequency acoustic emission-based monitoring technique to identify work piece surface malfunctions in milling with multiple teeth cutting simultaneously. International Journal of Machine Tools & Manufacture. 2009;: p. 53–65.

32. Qun Ren LB, Marek B, Jemielniak K. Acoustic emission signal feature analysis using type-2 fuzzy logic system. IEEE. 2010;(DOI 978-1-4244-7858-3).

33. Haber RE, Jiménez JE, Peres CR, Alique JR. An investigation of tool-wear monitoring in a high-speed machining process. Sensors and Actuators A. 2004; 116: p. 539–545.

34. Jemielniak K, Arrazola PJ. Application of AE and cutting force signals in tool condition monitoring. CIRP Journal of Manufacturing Science and Technology. 2008;: p. 97–102.

35. Ertekin YM, Kwon Y, Tseng TLB. Identification of common sensory features for

the control of CNC milling operations under varying cutting conditions. International Journal of Machine Tools & Manufacture. 2003; 43: p. 897–904.

36. Binsaeid S, Asfour S, Cho S, Onar A. Machine ensemble approach for simultaneous detection of transient and gradual abnormalities in end milling using multisensor fusion. Journal of Materials Processing Technology. 2009; 209: p. 4728–4738.

37. Pai PS, Nagabhushana TN, Rao PKR. Tool wear estimation using resource allocation network. International Journal of Machine Tools & Manufacture. 2001; 41: p. 673–685.

38. xiqing M, chuangwen X. Tool wear monitoring of acoustic emission signals from milling processes. IEEE, 2009 First International Workshop on Education Technology and Computer Science. 2009;(DOI 10.1109/ETCS.2009.105).

39. Mathews PG, Shunmugam MS. Condition monitoring in reaming through acoustic emission signals. Journal of Materials Processing Technology. 1999; 86: p. 81–86.

40. Pontuale G, Farrelly FA, Petri A, Pitolli L. A statistical analysis of acoustic emission signals for tool condition monitoring (TCM). Acoustics Research Letters Online. Published Online 2002 November 14;(DOI 10.1121/1.1532370).

41. Chen X, Li B. Acoustic emission method for tool condition monitoring based on wavelet analysis. International Journal Of Advanced tool and Manufacture. 2007; 33: p. 968–976.

42. Dolinsek S, Kopac J. Acoustic emission signals for tool wear identification. Wear. 1999; 225–229: p. 295–303.

43. Chiou RY, Liang SY. Analysis of acoustic emission in chatter vibration with tool wear effect in turning. International Journal of Machine Tools & Manufacture. 2000; 40: p. 927–941.

44. Deiab I, Assaleh K, Hammad F. Application of sensor fusion and polynomial classifier to tool wear monitoring. In Proceeding of the 5th International Symposium on Mechatronics and its Applications (ISMA08); May 27-29, 2008; Amman, Jordan.

45. Qun Ren LB, Balazinski M. Application of type-2 fuzzy estimation on uncertainty in machining: An approach on acoustic emission during turning process. In The 28th North American Fuzzy Information Processing Society Annual Conference (NAFIPS2009); June 14 - 17, 2009; Cincinnati, Ohio, USA.

46. Jemielniak K, Otman O. Catastrophic Tool Failure Detection Based on Acoustic Emission Signal Analysis. Annals of the ClRP. 1997 January; 47.

47. Saravanan S, Yadava GS, Rao PV. Condition monitoring studies on spindle bearing of a lathe. International Journal of Advanced Manufacture Technology. 2006; 28: p. 993–1005.

48. Chiou RY, Liang SY. Dynamic modeling of cutting acoustic emission via piezoelectric actuator wave control. International Journal of Machine Tools & Manufacture. 2000; 40: p. 641–659.

49. Sun Jie WYS, Soon HG, Rahman M, Zhigang W. Identification of feature set for effective tool condition monitoring – A case study in titanium machining. In 4th IEEE Conference on Automation Science and Engineering; August 23-26, 2008; Key Bridge Marriott, Washington DC, USA.

50. Lee DE, Hwang I, Valente CMO, Oliveira JFG, Dornfeld DA. Precision manufacturing process monitoring with acoustic emission. International Journal of Machine Tools & Manufacture 46. 2006 June;: p. 176–188.

51. Farrelly FA, Petri A, Pitoll L, Pontuale G, Tagliani A, Inverardi PLN. Statistical properties of acoustic emission signals from metal cutting processes. Journal of Acoustic Society. 2004; 116: p. 981–986.

52. Gao H, Xu M, Shi X, Huang H. Tool Wear Monitoring Based on Localized Fuzzy Neural Networks for Turning Operation. In 2009 Sixth International Conference on Fuzzy Systems and Knowledge Discovery; 2009. p. 417-420.

53. Al-Sulaiman FA, Baseer MA, Sheikh AK. Use of electrical power for online monitoring of tool condition. Journal of Materials Processing Technology. 2005; 166: p. 364–371.

54. Bhattacharyya P, Sengupta D, Mukhopadhyay S, Chattopadhyay AB. Current signal based continuous on-line tool condition estimation in face milling. IEEE. 2006;(1-4244-0726-5/06).

55. Silva RG, Baker KJ, Wolcox SJ. The adaptability of a tool wear monitoring system under changing cutting conditions. Mechanical Systems and Signal Processing. 2000; 14(2): p. 287-298.

56. Aliustaoglu C, Ertunc HM, Ocak H. Tool wear condition monitoring using a sensor fusion model based on fuzzy inference system. Mechanical Systems and Signal Processing. 2009; 23: p. 539–546.

57. Marinescu I, Axinte DA. A critical analysis of effectiveness of acoustic emission

signals to detect tool and workpiece malfunctions in milling operations. International Journal of Machine Tools & Manufacture. 2008; 48: p. 1148–1160.

58. Chen JC, Chen JC. An artificial-neural-networks-based in-process tool wear prediction system in milling operations. International Journal of Advanced Manufacturing Technology. 2005; 25: p. 427–434.

59. Huang S, Tan KK, Hong GS, Wong YS. Cutting force control of milling machine. Mechatronics. 2007; 17: p. 533–541.

60. Chen SL, Jen YW. Data fusion neural network for tool condition monitoring in CNC milling machining. International Journal of Machine Tools & Manufacture. 2000; 40: p. 381–400.

61. Abou-El-Hossein KA, Kadirgama K, Hamdi M, Benyounis KY. Prediction of cutting force in end-milling operation of modified AISI P20 tool steel. Journal of Materials Processing Technology. 2007; 182: p. 241–247.

62. Huang SN, Tan KK, Wong YS, Silva CWd, Goh HL, Tan WW. Tool wear detection and fault diagnosis based on cutting force monitoring. International Journal of Machine Tools & Manufacture. 2007; 47: p. 444–451.

63. Rivero A, Lacalle LNLd, Penalva ML. Tool wear detection in dry high-speed milling based upon the analysis of machine internal signals. Mechatronics. 2008; 18: p. 627–633.

64. Tansel IN, Arkan TT, Bao WY, Mahendrakar N, Shisler B, Smith D, et al. Tool wear estimation in micro-machining part I: tool usage–cutting force relationship. International Journal of Machine Tools & Manufacture. 2000; 40: p. 599–608.

65. Scheffer C, Heyns PS. An industrial tool wear monitoring system for interrupted turning. Mechanical Systems and Signal Processing. 2004; 18: p. 1219–1242.

66. Chiou RY, Liang SY. Dynamic modeling of cutting acoustic emission via piezoelectric. International Journal of Machine Tools & Manufacture. 2000; 40: p. 641–659.

67. Dimla DES, Lister PM. On-line metal cutting tool condition monitoring II: tool-state classification using multi-layer perceptron neural networks. International Journal of Machine Tools & Manufacture. 2000; 40: p. 769–781.

68. Astakhov VP. The assessment of cutting tool wear. International Journal of Machine Tools & Manufacture. 2004; 44: p. 637–647.

69. Mannan MA, Kassim AA, Jing M. Application of image and sound analysis

techniques to monitor the condition of cutting tools. Pattern Recognition Letters. 2000; 21: p. 969-979.

70. Castejon M, Alegre E, Barreiro J, ndez LKH. On-line tool wear monitoring using geometric descriptors from digital images. International Journal of Machine Tools & Manufacture. 2007; 47: p. 1847–1853.

71. Orhan S, Er AO, Camus-cu N, Aslan E. Tool wear evaluation by vibration analysis during end milling of AISI D3 cold work tool steel with 35 HRC hardness. NDT & E International. 2007; 40: p. 121–126.

72. Inasaki I. Application of acoustic emission sensor for monitoring machining processes. Ultrasonics. 1998; 36: p. 273-281.

73. Sun J, Hong GS, Rahman M, Wong YS. Identification of feature set for effective tool condition monitoring by acoustic emission sensing. int. j. prod. res.. 2004; 42(5): p. 901–918.

74. Baifeng J, Weilian Q. The research of acoustic emission techniques for non destructive testing and health monitoring on civil engineering structures. In 2008 International Conference on Condition Monitoring and Diagnosis; April 21-24, 2008; Beijing, China.

75. Jemielniak K, Arrazola PJ. Application of AE and cutting force signals in tool condition monitoring in micro-milling. CIRP Journal of Manufacturing Science and Technology 1. 2008;: p. 97–102.

76. Ghosh, N.; Ravi, Y.B.; Patra, A.; Mukhopadhyay, S.; Paul, S.; Mohanty, A.R.; Chattopadhyay, A.B. Estimation of tool wear during CNC milling using neural network-based sensor fusion. Mechanical Systems and Signal Processing. 2007; 21: p. 466–479.

77. Ertekin YM, Kwon Y, Tseng TLB. Identification of common sensory features for the control of CNC milling operations under varying cutting conditions. International Journal of Machine Tools & Manufacture. 2003; 43: p. 897–904.

78. Aliustaoglu C, Ertunc HM, Ocak H. Tool wear condition monitoring using a sensor fusion model based on fuzzy inference system. Mechanical Systems and Signal Processing. 2009; 23: p. 539–546.

79. Guo YB, Ammula SC. Real-time acoustic emission monitoring for surface damage in hard machining. International Journal of Machine Tools & Manufacture. 2005 March; 45: p. 1622–1627.

80. Teti R, Jemielniak K, O'Donnell G, Dornfeld D. Advanced monitoring of

machining operations. CIRP Annals - Manufacturing Technology. 2010; 59: p. 717–739.

81. Mix PE. Introduction to Nondestructive Testing : a Training Guide. 2nd ed. Hoboken, New Jersey: John Wiley & Sons, Inc.; 2005.

82. Hao S, Ramalingam S, Klamecki BE. Acoustic emission monitoring of sheet metal forming: characterization of the transducer, the work material and the process. Journal of Materials Processing Technology. 2000; 101: p. 124-136.

83. Li X, Yao X. Multi-scale statistical process monitoring in machining. IEEE Transactions on Industrial Electronics. 2005 June; 52(3).

84. Bloomfield P. Fourier Analysis of Time Series: An Introduction. 2nd ed.: John Wiley and Sons; 2000.

85. Ravindra HV, Srinivasa YG, Krishnamurthy R. Acoustic emission for tool condition monitoring in metal cutting. WEAR. 1997 June; 212: p. 78-84.

86. Jemielniak K, Urbański T, Kossakowska J, Bombiński S. Tool condition monitoring based on numerous signal features. Int J Adv Manuf Technol. 2011 June; DOI 10.1007/s00170-011-3504-2.

87. Cho S, Binsaeid S, Asfour S. Design of multisensor fusion-based tool condition monitoring system in end milling. Int J Adv Manuf Technol. 2010 May; 46: p. 681–694.

88. Kunpeng Z, San WY, Soon HG. Wavelet analysis of sensor signals for tool condition monitoring: A review and some new results. International Journal of Machine Tools & Manufacture. 2009; 49: p. 537–553.

89. Lee DTL, Yamamoto A. Wavelet Analysis: Theory and Applications. hewlett packard journal. 1994 December; 45(6).

90. Sandberg IW, Lo JT, Fancourt CL, Principe JC, Katagiri S, Haykin S. Nonlinear Dynamical Systems: Feedforward Neural Network Perspectives: John Wiley & Sons; 2001.

91. Panchal G, Ganatra A, Kosta YP, Panchal D. Behavioral analysis of multilayer peceptrons with multiple hidden neurons and hidden layers. International Journal of Computer Theory and Engineering. 2011 April; 3(2).

92. Omerhodzic I, Avdakovic S, Nuhanovic A, Dizdarevic K. Energy distribution of EEG signals: EEG signal wavelet-neural network classifier. International Journal of Biological and life Sciences. 2010; 6(4).

93. Abellan-Nebot JV, Subirón FR. A review of machining monitoring systems based on artificial intelligence process models. International Journal of Advanced Manufacturing Technolnology. 2010 July; 47: p. 237–257.

Appendix: publications

Online Tool Wear Monitoring

Tool Wear Monitoring Using Acoustic Emission

O.A. Olufayo, K. Abou-El-Hossein, T. van Niekerk
Mechatronics Engineering Department
Nelson Mandela Metropolitan University
6001 Port Elizabeth, South Africa
oluwole.olufayo@nmmu.ac.za

***Abstract*—This research work highlights the effects of acoustic emission (AE) signals emitted during the milling of H13 tool steel as an important parameter in the identification of tool wear. These generated AE signals provide information on the chip formation, wear, fracture and general deformation. Furthermore, it is aimed at implementing an online monitoring system for machine tools, using a sensor fusion approach to adequately determine process parameters necessary for creating an adequate tool change timing schedule for machining operations.**

Keywords-Tool Wear Monitoring, acoustic emission, milling

I. INTRODUCTION

Due to the rapid growth in cutting edge technology the need for a sustainable manufacturing sector is essential to meet the market demand. Machining is an important process to consider in large scale industrial production. Numerous cutting operations are employed in a machining environment. These operations are aimed at the removal of material by power-driven machine tools to mechanically cut the material to generate required geometry. Modern day machining is controlled by the use of computers. Computer Numerical Control (CNC) machines are driven by abstractly programmed commands which automate machining to facilitate the cutting process.

The influence of CNC machining on the automation of the manufacturing process is substantial but this innovation fails to monitor the quality of its operations. The challenge of wear formation on the edges of the tools, which causes defects on the workpiece, poses a threat to total automation. Thus, the introduction of an adequate tool condition monitoring system is vital.

The research is conducted on a Deckel Maho DMU 40 CNC machine. The 5 axis CNC machine is used for machining simple or complex workpieces used for medical technology, aerospace, automobile as well as tool and mould making.

II. TOOL CONDITION MONITORING

A. Tool Condition Monitoring in industries

The industrial revolution of today's manufacturing industry is anchored around various cutting operations. Such processes range from milling, cutting, drilling, turning and grinding operations. These operations which form a potent underlying factor in the production of engineering products are constrained by low efficiency and high cost. Due to these challenges an adequate monitoring system is essential to ensure optimal yield.

Tool Condition Monitoring (TCM) is a modern monitoring approach used in the industrial sector for machining operations. This monitoring process oversees the state of the workpiece during cutting operations to pre-empt deplorable machining state.

TCM in machining operations of today's manufacturing is also paramount for high productivity. This system of monitoring machining operation is used to determine the Overall System Effectiveness (OOE) of the production line. Prickett [1] defines OOE as a factor determined by the system availability rate, performance rate and quality rate. The performance rate relates the on-time and downtime ratios.

In monitoring on-line downtime conditions, two problem sources are identified. One problem is caused by the transfer of work piece between machines and the other by excessive wear and breakage generated on tools during machining [2]. The downtime generated from transfer of work pieces is unfortunately unavoidable during operation, but tool wear can be monitored and controlled.

TCM is performed on various cutting operations to determine the wear rates. Operations such as cutting,

grinding, milling and drilling are common industrial machining operations being monitored today. Numerous research efforts have been conducted in this field but there has been significant interest in the monitoring and study of face-milling and turning operations. The specifics why these researches are delineated towards these conventional cutting operations are based on the ease of monitoring, expenses involved and quality of obtained signals.

Other segregations of research are based on the sensing technology and analysis methodologies employed. Sensors such as sound, acoustic, force and vibration sensors are utilized.

Sensors are positioned at various stages of the machine process to:

- Ascertain the performance of the machines
- Observe the process evolution
- Evaluate the quality of the output
- Supervise and control process parameters utilized.

Research proves that sensor positioning affects data quality [3]. Sensors are most often found placed on the machine, tool or the workpiece.

Numerous articles enumerate various merits of Acoustic Emission (AE) based monitoring methodology. These were based on its frequency range which prevents the intrusion of environmental noises, ease of placement of sensors, low cost involvement and its sampling speed which does not interfere with the cutting operations. [4]. From the literature, AE is termed one of the most efficient TCM sensing methods which can be applied to machining processes [5].

III. Review` of TCM

The design of TCM as a precautionary tool in machining can be viewed as a categorization model. The classification of states of the tool forms its objective. The TCM framework in figure 1 shows the various stages employed in the acquisition and classifications of features from the machine tool.

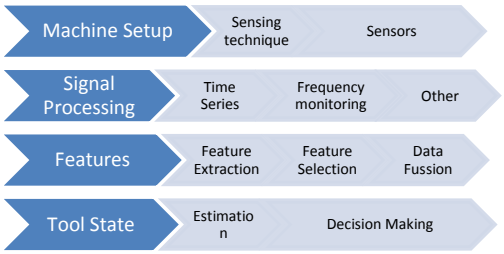

Figure 1. Framework of TCM

B. Sensor Fusion Process

Sensor fusion or multisensory fusion techniques are greatly used in TCM. Dimla [6] describes the utilization of more than one sensor signal from different sources to detect the same parameter as sensor fusion. Noise from the process infiltrates signals and influences the correlation efficiencies of signals. Thus, signal to noise ratio forms a decisive parameter to estimate whether the measurement provides significant correlation to the anticipated quantity. In multisensory fusion techniques, signal features from different sensors determine the output state of the tool. This technique however, executes the fusion process at the decision level of the TCM framework.

The integration of the many sensory correlated features with a single or different process parameters gives a more sensitive and reliable prediction than a single sensory feature. This led Sick [7] to conclude that only a sensor fusion approach provides sufficient information in a monitoring system. However practice has shown that in some cases a multisensory fusion with neural networks may produce worse results than a single sensor approach. This scenario may occur due to over-generalization of the output by an excessive pattern learning [7].In general, research conversely shows a higher efficiency from multisensory fusion techniques.

C. Tool life

Tool life is defined as the time elapsed to produce acceptable workpiece before tool failure [8]. The time of usability of the tool is influenced by the rate of wear formation on its surface. This wear weakens the tool yielding to an eventual tool failure. The life of a cutting tool can thus be determined by the amount of wear that has occurred on the tool profile. This state which reduces the efficiency of cutting until an intolerable level or eventual tool failure occurs.

Several definitions have been postulated for tool life. These definitions are founded on the time criterion of usability, output production of the tool or even wear rate standards. Tool life model have been designed to determine the rate of wear formation on the tool. One of the most common tool life models are Taylor's equation.

Equation 1Taylor's equation

$$T = \frac{A_t}{V_{b_t}} \quad (1)$$

Where T is tool life, V is cutting speed; and At,and bt are
constants.

Equation 2 Extended Taylor's equation

$$TL = f(a_{p,}, f, v, VB) = G \cdot a_p^a \cdot f^b \cdot vc \cdot VB^d \quad (2)$$

Where TL is the tool life, f is the feed, v the speed of cutting, a the depth of cut and VB is the flank wear width. G, a, b, c, d are extended Taylor's equation coefficients. Taylor's extended equation is based on the determination of tool life using all cutting parameters and the amount of wear formed whereas

its predecessor emphasises only on significant parameters i.e. the cutting speed. Although Taylor's equation provides information on the relationship of tool life with the cutting parameters, it also possesses an easy implementation process; it is limited only to the information about tool life. The use of empirical equations to calculate tool life based on cutting parameters such as the depth of cut, feed rate and speed of cutting has been greatly common in research works [8]. Other empirical relations have related the tool life to tool temperature and also modelled tool life as a stochastic process.

D. Mechanism of Wear

Wear formed on the tool edge could occur based on some certain mechanisms. Some common wear mechanisms normally found in the machining environment are as follows:

Abrasion wear: Abrasive wear occurs as a result of the interaction between the face of the tool and the workpiece. This is characterized by a loss of relief on the flank of the tool. Abrasive wear occurs due to the dissimilarity of the hardness of the two mating materials.

Adhesive wear: Adhesive wear occurs in metal when the force elements of the material are not as strong as the interactive forces with the workpiece. This yields to the transference of material between the metals.

Attrition wear: Attrition is a form of erosive wear effect, occurring on cutting tools. It is caused by the impact of particles (liquid, gaseous, solid) on metal surface. This effect gradually erodes fragments of the surface due to its momentum effect.

Fatigue wear: Fatigue wear is the weakening of the material surface by the cyclic loading and unloading during machining. Generally, cracks announce the presence of fatigue wear on the tool surface, which eventually leads to total fracture.

Diffusion wear: Diffusion wear, also known as dissolution wear is an outcome of the gradual dissemination of solid element from one material to the other due to extreme heat and machining conditions. It involves the decomposition of part of the surface of one material and its integration into its opposing mating surface. This normally occurs at a slow sliding velocity. Diffusion wear is greatly dependent on the material composition of the machined surface. The affinity of some elements in the material, towards opposing elements could enhance the rate of diffusion wear experienced in machining. This wear mechanism is mostly experienced in the machining of ceramic materials with diamond tools.

Corrosive wear: Corrosive wear also known as chemical wear is brought about as a result of chemical attack on the surface of the tool. Continuous friction on the tool depletes the protective oxidation films on that surface. This oxidation may accelerate the wear formation on the tool. The effect of high temperature and frictional forces over a long term would eventually alter material composition.

Fracture wear: Fracture wear is commonly experienced in machining. Fracture wear occurs as the gradual chipping and cracking of solid surface due to the sudden loading and collision of both materials. These operations are evident during run time operations.

These wear mechanisms could be found in various combinations during machining. Dominant wear mechanisms found in wear modes are influenced by various factors, such as the cutting parameters, the geometry of the tool, the temperature, and the speed of cutting operations.

E. Forms of Wear on Tool Edge

Tool wear generally occurs in a combination of wear modes. Dominant wear modes depend on cutting conditions and process specifications. These dominant features are mainly responsible for wear formation. Some common identified wear modes are:

- Flank wear
- Crater wear
- Chipping
- Breakage
- Nose wear
- Plastic deformation
- Cracking
- Notch wear.

Wear modes are also dependent on a dominant wear mechanism [9]. Four of the above listed modes are generally more rampant in cutting operations. These are flank wear, crater wear, nose wear and notch wear. Figures 2 and 3 show the various wear zones, region of wear and measurement parameters.

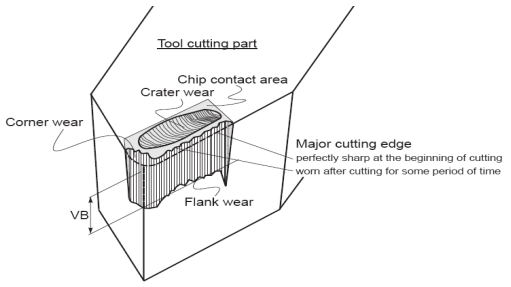

Figure 2. Cutting tool part with wear zones [9]

Flank Wear: Flank wear is dominated by abrasion. It arises due to both abrasive and adhesive wear mechanism from the intensive rubbing action of the two surfaces in contact i.e. the clearance face of the cutting tool and the newly formed surface of the workpiece. This action leads to increase in surface

contact area and heat generation which in turns impair the surface quality. The rate of flank wear generated during machining operations varies along the cutting process [6].

Nose Wear: Nose wear is found on the nose point of the cutting tool. It occurs predominantly due to abrasive effects on the edges of the tool yielding to an increase in the negative rake angle. At high cutting speed, the wear deforms plastically and may result in the loss of the entire nose. Wear formed on the nose affects the quality of the surface finish [10].

Crater Wear: Crater wear arises due to the combination of wear mechanisms: adhesion, abrasion, diffusion, thermal softening and plastic deformation. This mode of wear is generally formed on the rake face some distance away from the tool edge as a crater. The crater wear is quantified by depth and cross-sectional area of the crater for measurement. The most important factors influencing crater wear are temperature at the tool–chip interface and the chemical affinity between tool and work piece materials [11].

Notch Wear: Abrasion and adhesion are the main mechanisms involved in notch wear. Notch wear is formed at the boundary of the machined surface with no chip contact during cutting. This mode of wear also known as groove wear, is predominant in ceramic cutting tools with low toughness value. [11]

Amidst the group, flank wear is often selected as the tool life criterion because it determines the diametric accuracy of machining, its stability and reliability [12].

IV. TOOL WEAR EVOLUTION

Research has shown that tool wear evolves at different rates in cutting operations. The rate of wear formation on the tool is largely dependent on the wear mechanisms occurring in the process. In flank wear, abrasion and adhesion cause a rapid rise on the tool flank face at the initial stage followed by a relatively slowly increase wear rate and ends with another rapid formation of wear before fracture. This curve form is generally accepted by numerous researches as the categorical identification of the three basic stages of wear: the initial stage, the regular stage and the fast stage. Ertunc [13] classifies wear into five major stages from the tool life progression curve shown in figure 3. These stages of wear are:

1. Initial wear;
2. Slight wear (regular stage of wear);
3. Moderate wear (micro breakage stage of wear);
4. Severe wear (fast wear stage); and
5. Worn-out (or tool breakage).

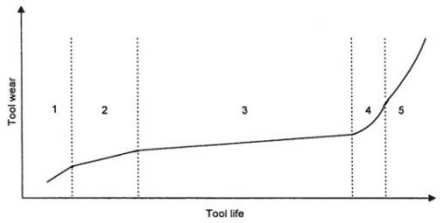

Figure 3. Tool life progression curve [13]

A. Factors influencing tool life

Tool wear formation is subjective to some machining parameters. The parameters, which affect the rate of tool wear, are

- Cutting conditions (cutting speed, feed , depth of cut)
- Cutting tool geometry (tool orthogonal rake angle)
- Properties of work and tool material.

It is generally known that the tool life is directly related to its rate of wear. Therefore the parameters influencing tool wear would as well adversely affect its tool life. The tool life of a cutting tool is not only dependent on the wear but can be influenced by numerous other factors relating to the microstructural properties of the material.

The following factors affect the life of a cutting tool:

- type of material being cut
- microstructure of the material
- hardness of the material
- type of surface on the metal (smooth or scaly)
- material of the cutting tool
- profile of the cutting tool
- type of machining operation being performed
- speed, feed and depth of cut [10]

In their research, Dimla concludes that the cutting speed has the strongest influence amidst these. They postulates that "Regardless of the differences in the values and trends of the normal and shear stresses at the contact interfaces, minimum tool wear occurs and apparent friction coefficient reaches its lowest value at the optimum cutting speed [14]".

V. TOOL MONITORING TECHNIQUES

In the past, various methods of tool wear monitoring methods have been proposed but due to the complex machining process an ideal model has not yet been found. Scheffer [15] classifies the various techniques based on the type of sensor used, the parameter monitored and the state of machine process. Amidst all sensor type ranging from sound, temperature, forces and current, methods sensing parameters have been classified into direct and

indirect sensing methods according to the sensors used [16].

Direct sensing method directly monitors actual quantity of wear variable during operation [7]. It is less utilized in the industrial sector due to its cost implication and intricacy of implementation. Direct sensing is greatly affected by environmental machining factors such as illumination, the use of cutting fluid, chips formation and temperature of material. Some examples of sensing technologies employing this method are the optical sensing, radioactive, laser beams and electrical resistance amidst others.

Indirect sensing has been greatly utilized in the industry despite its lower accuracy due to its ease of implementation and cost-effectiveness [15]. Unlike direct sensing, this method monitors the process parameters correlated with tool wear. Indirect method employs the heavy usage of statistical and analytical models on the tool wear correlations to draw its conclusions. Some of the sensing methods used in the indirect method are acoustic emission, spindle motor current, cutting force, vibration, cutting temperature etc…

The monitoring techniques could be executed during real-time or off-line conditions. Continuous monitoring permits the instant recognition of wear formation and provides a corrective methodology of wear identification. Despite these advantages, on-line tool wear monitoring has been a challenging area of research and industrial implementation due to the various influences from the machining environment and technical set-up.

AE technologies are one of the most effective sensing technologies in monitoring tool wear [16]. AE signals are very effective in indirect method due to its non-intrusiveness, ease of operation and fast dynamic response [17].

VI. ACOUSTIC MISSION

A Comprehensive survey on the use of AE in TCM was conducted by Li [16]. In their survey Li iterates the efficiency and reliability of AE as a viable TCM sensing technique. The impressive amount of research in the last decade also indicates the present day interest in AE [18] [19] [3]. AE originates from the strain energy released as the rubbing process of cutting takes place. This is caused by the considerable amount of plastic deformation which occurs in metal cutting. AE signal refer to transient elastic waves due to the rapid energy release from a localised source within a material [19]. Li [16] reiterates the basic sources of AE during tool monitoring as the following:

- Plastic deformation during cutting in the work piece;
- Plastic deformation in the chip;
- Frictional contact between the tool flank face and the work piece resulting in flank wear;
- Frictional contact between the tool rank face and the chip resulting in crater wear;
- Collisions between chip and tool;
- Chip breakage;
- Tool fracture.

Figure 4 shows the various AE wear zones generated during the cutting operation and how they relate to the various faces of the tool. The interaction of these various AE sources is responsible for the noisy signal generation of AE waves.

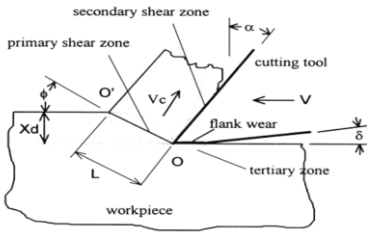

Figure 4. Zones of AE generation during metal cutting [18]

Piezoelectric devices are suitable in the measurement of AE stress waves on the workpiece. Piezoelectric devices convert mechanical stress waves into electrical AE signals. They are resilient to process a higher sensitivity ratio to most other sensors i.e. capacitive, electrodynamics and laser optical [20]. Piezoelectric possess sensitivities as high 1000 V/µm which exceed environmental noise. The AE transducer operates with a flexible range of 20kHz to 1Mhz [5] which can be used to detect most significant machining conditions, but most research were conducted in the range 100kHz – 800kHz. Most recent articles use piezoelectric sensors to establish the wear rate on flank face of the tool [5] [16].

F. Types of AE signals

There are numerous types of AE signals produced in the course of machining, continuous and burst type. Continuous AE signal are associated with plastic deformation in ductile materials [3]. This form of AE signal represents the gradual wear which is generated on the tool. Burst AE signal have been observed to determine brusque coalitions and fractures in metal working. These burst can be generated owed to the engagement and disengagement with the work piece [21]. It is generally acknowledged that AE signals generated are due to plastic deformation and crack growth in the material. Burst AE signal are thus termed to more efficient in identifying fractures than monitoring machining processes AE processes are more successful in continuous machining operations. Due to the frequent nature of entry and exist, AE sensing faces challenges in adequately monitoring intermittent machining process such as milling. These collisions during cutting generate confusing data

values about the present tool state. Numerous research works also identify a link between the magnitudes of the high peak AE parameters with catastrophic tool failure detection [21].

G. Advantages of AE monitoring system

AE signals are easily identified in machining due to their higher frequency rate to machine vibrations and environmental noise which enhances the analysis of the signals. The application of non-destructive sensors therefore plays a major role in the monitoring process. These sensors are of different types and are sensitive to the property of the material involved such as the gauge thickness [22]. The sensors utilized are coupled with the sample to provide uninterrupted elastic energy signal based on the operation performed besides information about the dynamic changes observed on the sample. In the positioning of the sensor, further research on the properties of the transducers confirms a dominant relationship between the choice location and the quality of the observed signals. Inasaki [3] proves the effect of sensor positioning in machining by affixing an AE sensor on the cutting fluid supply nozzle, using the fluid as a medium for the generated signals. This system was conceived to avoid to fluctuations in signal magnitude caused by the variation of the distance connecting the spindle head and the cutting point. They concluded by stating the need to enhance the reliability of a monitoring process due to the high sensitivity of the AE sensing technology.

AE sensing technology can be based on numerous principles for data acquisition. Capacitance based AE sensors possess a high accuracy and are used to calibrate other AE sensors. Unfortunately, capacitance type displacement sensors are very sensitive to sensor position and surface mounting and thus not suitable for machining process monitoring [23].

The basic advantages in using acoustic signals in determining tool wear originate from its high frequency and sensitivity as well as its ease of placement and affordability.

H. AE Signal Parameters

Some feature parameters are used in AE analysis and empirical models to determine tool state. Features such as skew, kurtosis, ring-down count, rise time, event duration; frequency and RMS value are identified. Jemielniak [21] in his article statistically analysed the AE signal from the sensor to determine catastrophic Tool failure. The skew measures the symmetry of the distribution about its mean value but the kurtosis is a measure of the sharpness of its peak. These features have shown to respond to changes in flank wear during machining.

VII. Proposed Designed model

This research is aimed at implementing an online monitoring system using a multi-sensor approach to adequately determine process parameters necessary for creating and adequate tool change timing schedule for machining operations in an automated environment.

In the research we will monitor milling machining operation at high speed when cutting tool steel to link the rate of wear generated on the tools to the AE data. Three AE sensors from Kistler with a band pass frequency from 50 KHz to 1 MHz would be connected to piezotron couplers for signal processing and successively to the BNC 2110 block of the National Instrument (NI)for data acquisition. The data acquisition unit consists of a NI PCI 6110 simultaneous sampling card integrated on a computer and relayed to the sensor via a custom built connection (Figure. 5).

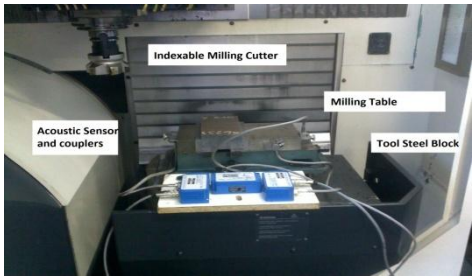

Figure 5. Machine Setup on DMU 40 CNC Machine

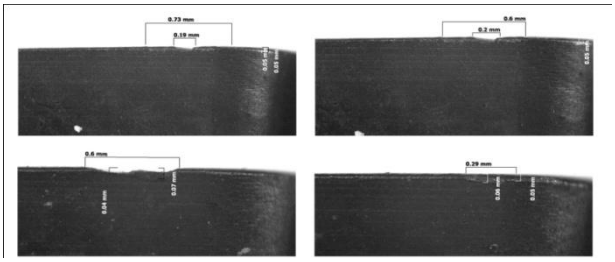

Figure 6. Wear observed on the inserts at different feeds

Figure 6 above shows the first results (after one pass of machining) of the wear observed on the inserts while machining tool steel at various feeds and speed. Numerous experiments are performed following a combination of these parameters to link the parameters to the wear formed. Figure 7 shows the machining setup diagram.

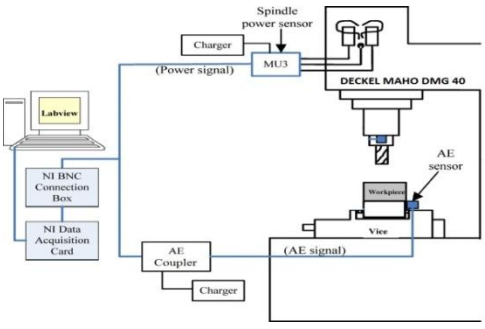

Figure 7. Tool Wear monitoring diagram

The data values will be sampled at 2 M/s and processed using a time-based statistical method to

obtain relevant features parameters. Concurrently, the acquired features will be utilized to train a neural network. Artificial intelligence would be used to create a solution for the classification of wear and establish a model which describes the effects of cutting parameters on tool life. In this research only three categories of wear would be under consideration; light, middle and severe wear.

Based on its high sampling rate and multisensory approach, this model is anticipated to further optimize TCM. Future areas of research geared towards determining an optimal choice number of sensors.

I. Conclusion

In conclusion, the proposed model presents more information on the cutting process and would provide a more efficient method in AE monitoring.

J. Acknowledgement

We would like to thank DST/TIA and eNtsa for the technical and financial support associated with the work presented in this paper.

K. References

[1] Prickett PW, Johns C. An overview of approaches to end milling tool monitoring. International Journal of Machine Tools & Manufacture. 1999;(39): p. 105–122.

[2] Rehorn AG, Jiang J, Orban PE. State-of-the-art methods and results in tool condition monitoring: a review. Int J Adv Manuf Technol. 2005;: p. 26: 693–710.

[3] Inasaki I. Application of acoustic emission sensor for monitoring machining processes. Ultrasonics. 1998; 36 (273-281).

[4] SUN J, HONG GS, RAHMAN M, WONG YS. Identification of feature set for effective tool condition monitoring by acoustic emission sensing. int. j. prod. res.. 2004; vol. 42(no. 5, 901–918).

[5] xiqing M, chuangwen X. Tool wear monitoring of acoustic emission signals from milling processes. IEEE, 2009 First International Workshop on Education Technology and Computer Science. 2009;(DOI 10.1109/ETCS.2009.105).

[6] Dimla DE. Sensor signals for tool-wear monitoring in metal cutting operations—a review of methods. International Journal of Machine Tools & Manufacture. 2000; 40(1073–1098).

[7] Sick B. ON-LINE AND INDIRECT TOOL WEAR MONITORING IN TURNING WITH ARTIFICIAL NEURAL NETWORKS A REVIEW OF MORE THAN A DECADE OF RESEARCH. Mechanical Systems and Signal Processing. 2002;(16(4), 487–546).

[8] Axinte DA, Belluco W, Chiffre LD. Reliable tool life measurements in turning — an application to cutting fluid efficiency evaluation. International Journal of Machine Tools & Manufacture. 2001; 41(1003–1014).

[9] Ashar J. Intelligent Drill Wear Condition Monitoring. 2009. A Thesis submitted to the the Auckland University of Technology.

[10] Krar SF, Gill AR, Smid P. Techonology of machine tools. 6th ed. New york: Mc Graw Hill; 2005.

[11] Kumar AS, Durai AR, Sornakumar T. The effect of tool wear on tool life of alumina-based ceramic cutting tools while machining hardened martensitic stainless steel. Journal of Materials Processing Technology. 2006; 173(151–156).

[12] Astakhov VP. The assessment of cutting tool wear. International Journal of Machine Tools & Manufacture. 2004; 44 (637–647).

[13] Ertunc HM, Loparo KA, Ocak H. Tool wear condition monitoring in drilling operations using hidden Markov models (HMMs). International Journal of Machine Tools & Manufacture. 2001; 41(1363–1384).

[14] Dimla DE, Lister PM. On-line metal cutting tool condition monitoring. I: force and vibration analyses. International Journal of Machine Tools & Manufacture. 2000; 40(739–768).

[15] Scheffer C. Thesis: Monitoring of tool wear in turning operations using vibration measurements. 1999. Thesis.

[16] Li X. A brief review: acoustic emission method for tool wear monitoring during turning. International Journal of Machine Tools & Manufacture 42. 2002;: p. 157–165.

[17] Zhou J, Pang CK, Z. Zhong FLL. Tool Wear Monitoring Using Acoustic Emissions by Dominant-Feature Identification. IEEE TRANSACTIONS ON INSTRUMENTATION AND MEASUREMENT. 2010; DOI 10.1109/TIM.2010.2050974.

[18] Chiou RY, Liang SY. Analysis of acoustic emission in chatter vibration with tool wear effect in turning. International Journal of Machine Tools & Manufacture. 2000; 40(927–941).

[19] Guo YB, Ammula SC. Real-time acoustic emission monitoring for surface damage in hard machining. International Journal of Machine Tools & Manufacture. 2005 March; 45(1622–1627).

[20] Mix PE. Introduction to nondestructive testing : a training guide. 2nd ed. Hoboken, New Jersey: John Wiley & Sons, Inc.; 2005.

[21] Jemielniak K, Otman O. Catastrophic Tool Failure Detection Based on Acoustic Emission Signal Analysis. Annals of the ClRP. 1997 January; Vol. 47.

[22] Jayakumar T, Mukhopadhyay CK, Venugopal S, Mannan SL, Raj B. A review of the application of acoustic emission techniques for monitoring forming and grinding processes. Journal of Materials Processing Technology. 2005; 159(48–61).

[23] Teti R, Jemielniak K, O'Donnell G, Dornfeld D. Advanced monitoring of machining operations. CIRP Annals - Manufacturing Technology. 2010; 59 (717–739).

Appendix: Wear Picture

Exp 1, Phase 15

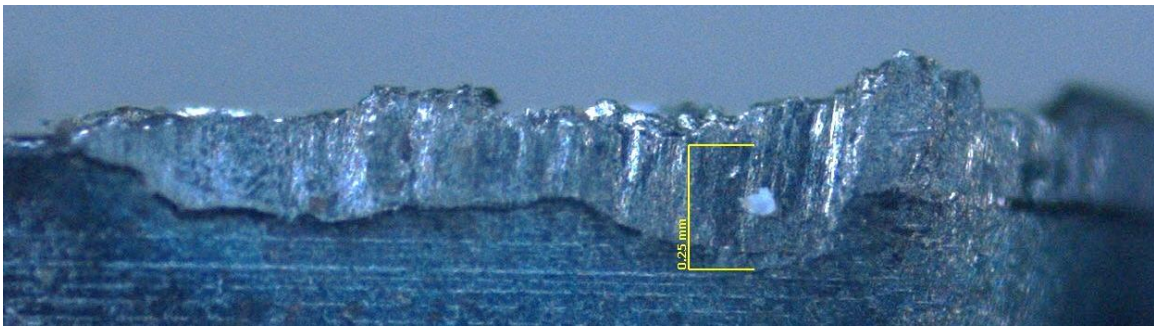

Exp 1, Phase 15

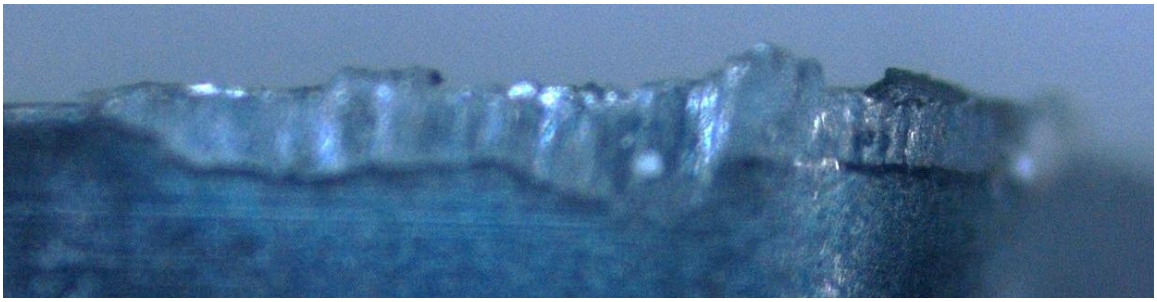

Exp 2, Phase 15

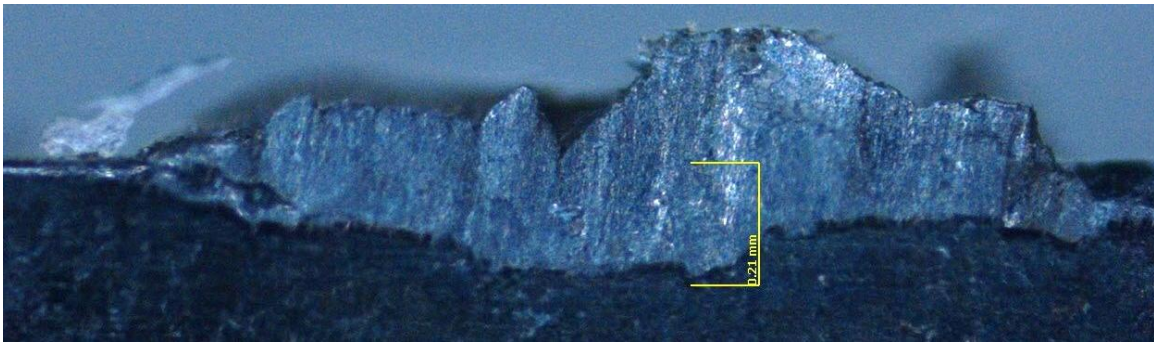

Exp 5, Phase 15

Exp 1, Phase 14

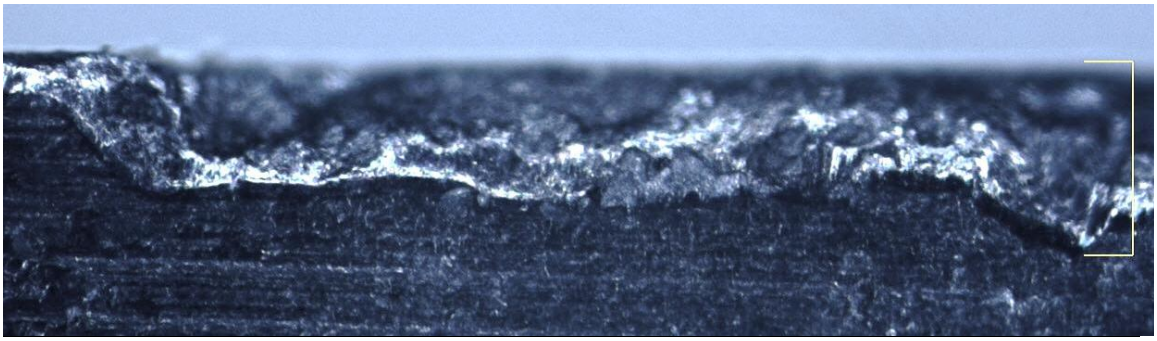

Exp 5, Ph 12

Exp 3, Ph 12

Exp 9, Phase 13

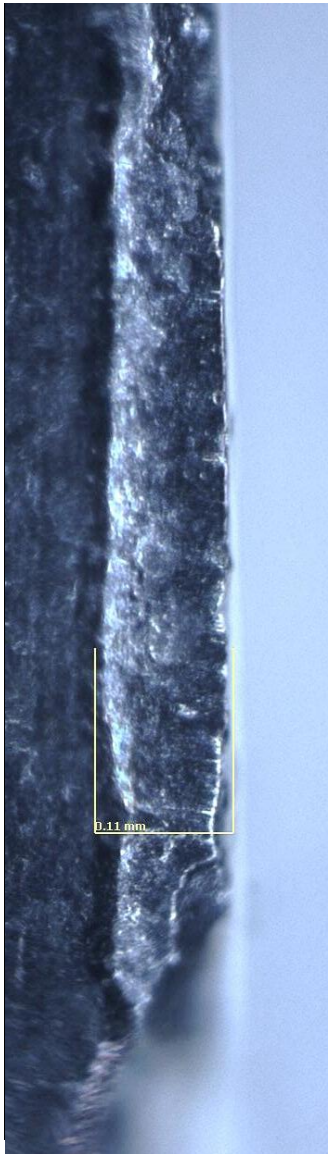

Exp 9, Phase 14

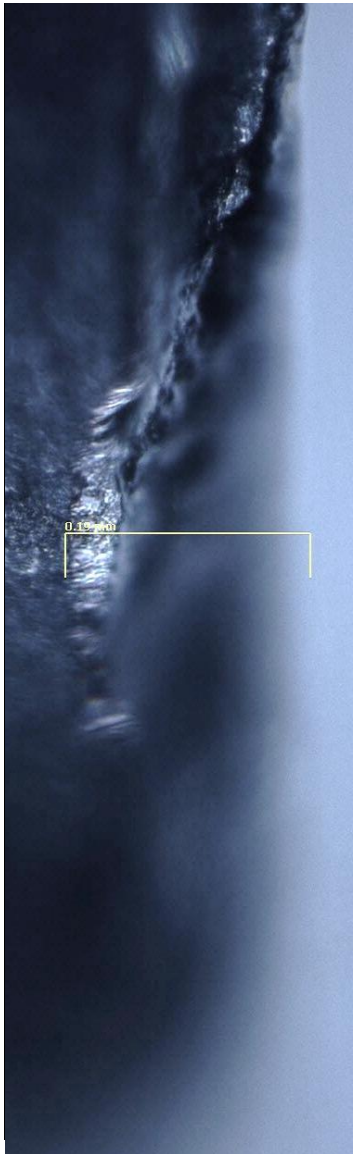

Exp 3, Phase 14

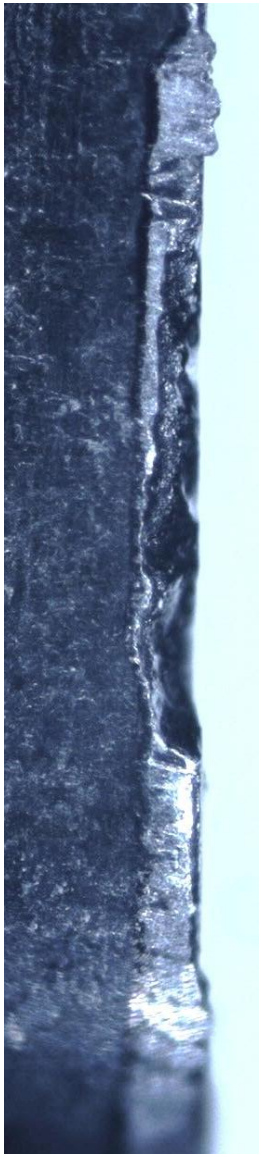

Exp 2, Phase 14

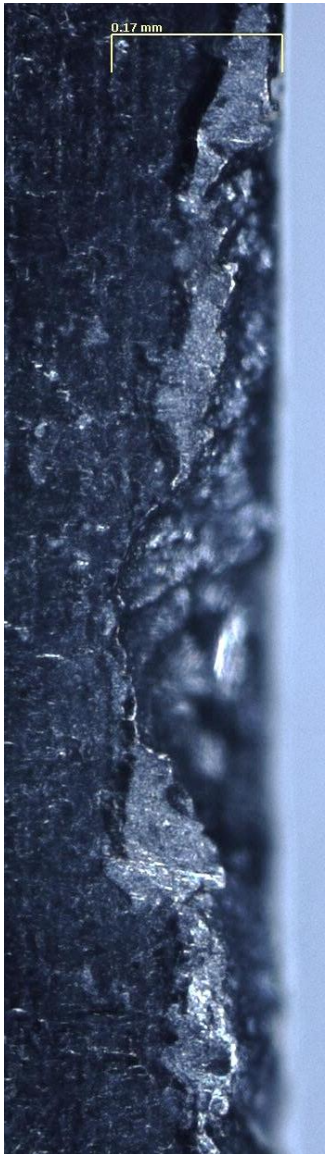

Exp 3, Ph 9

Exp 2, Ph 9

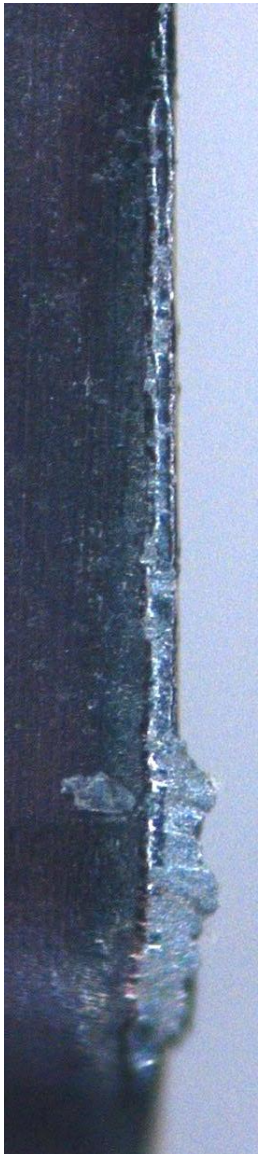

Exp 4, Ph 10

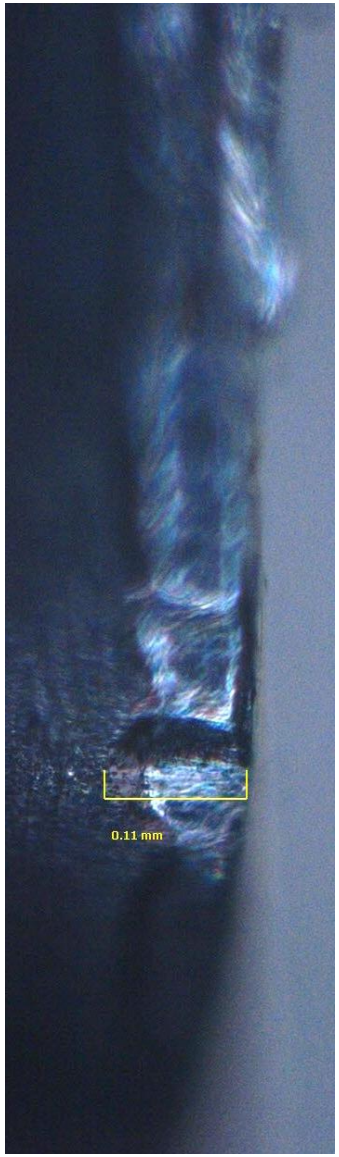

Exp 1, Ph 10

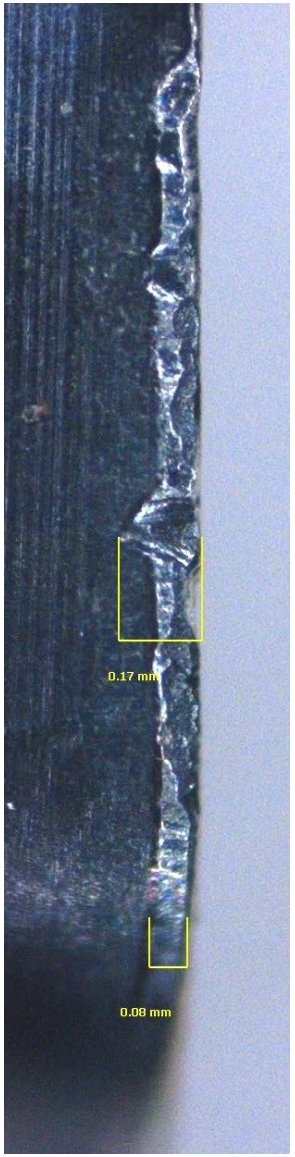

Exp 4, Ph 11

Exp 1, Ph 11

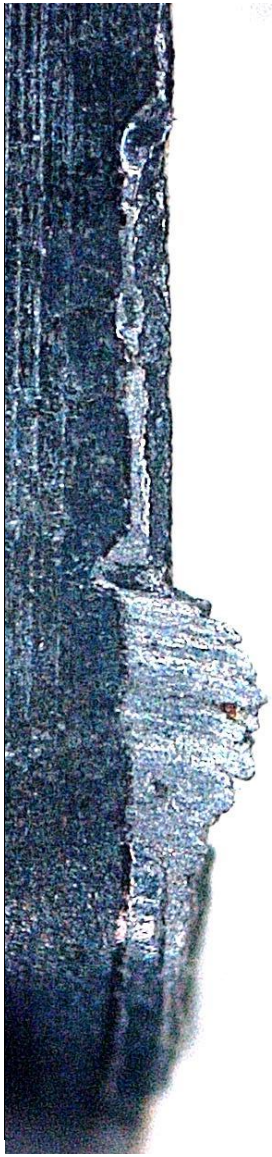

Exp 1, Ph 8

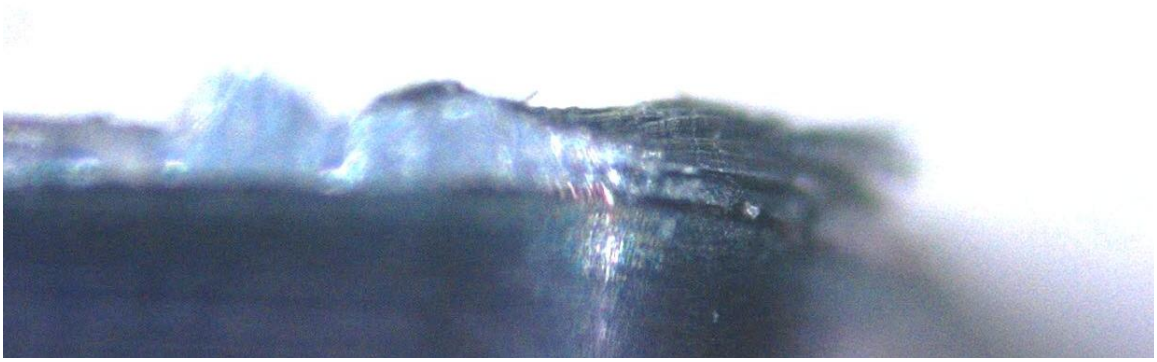

Exp 1, Ph 7

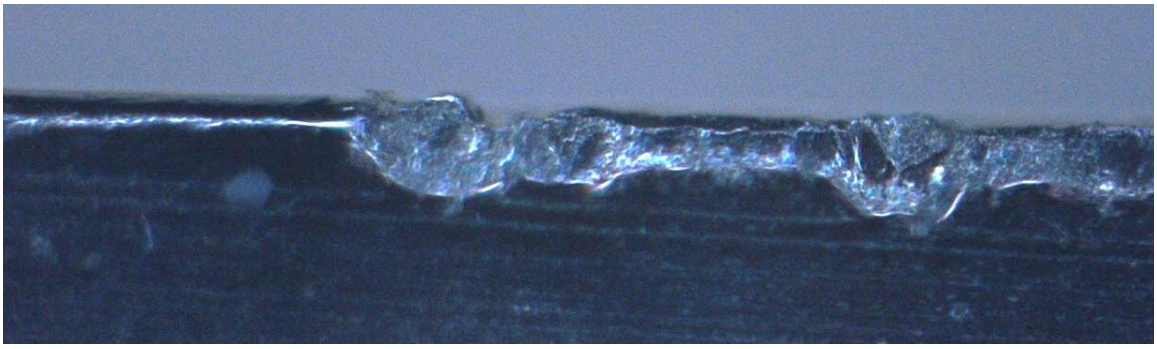

Exp 3, Ph 7

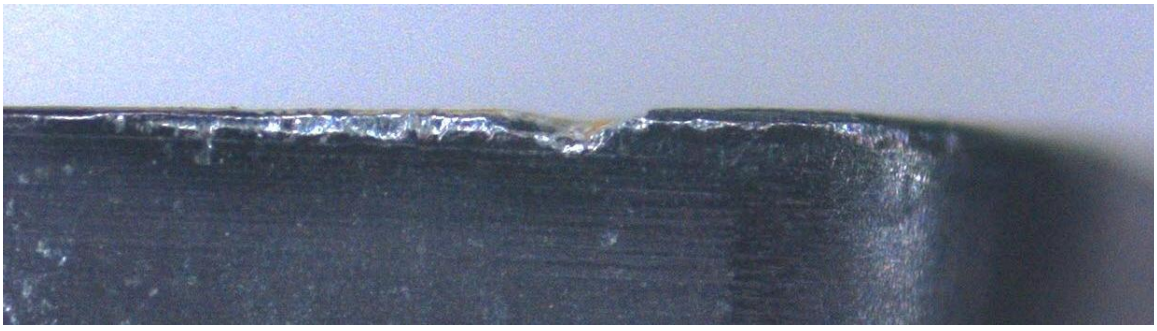

Exp 3, Ph 6

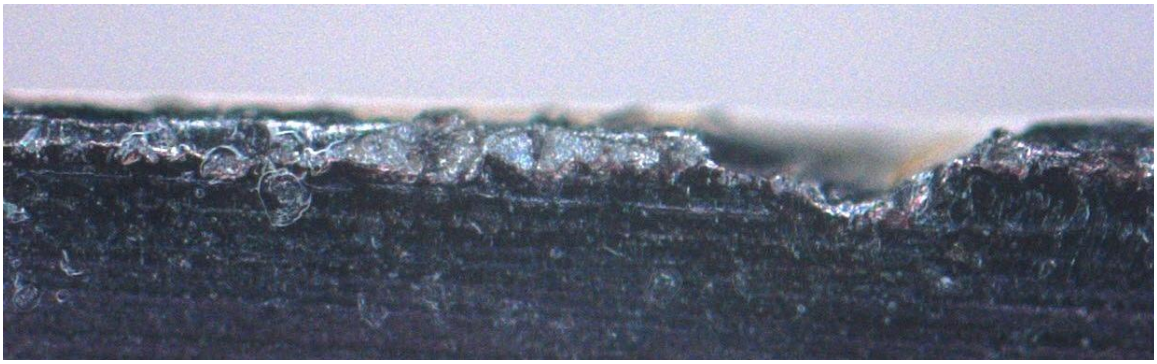

Exp 1, Ph 5

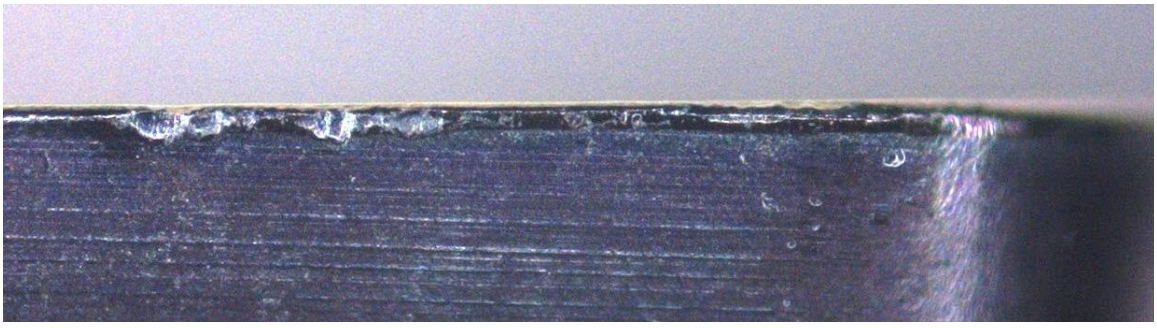

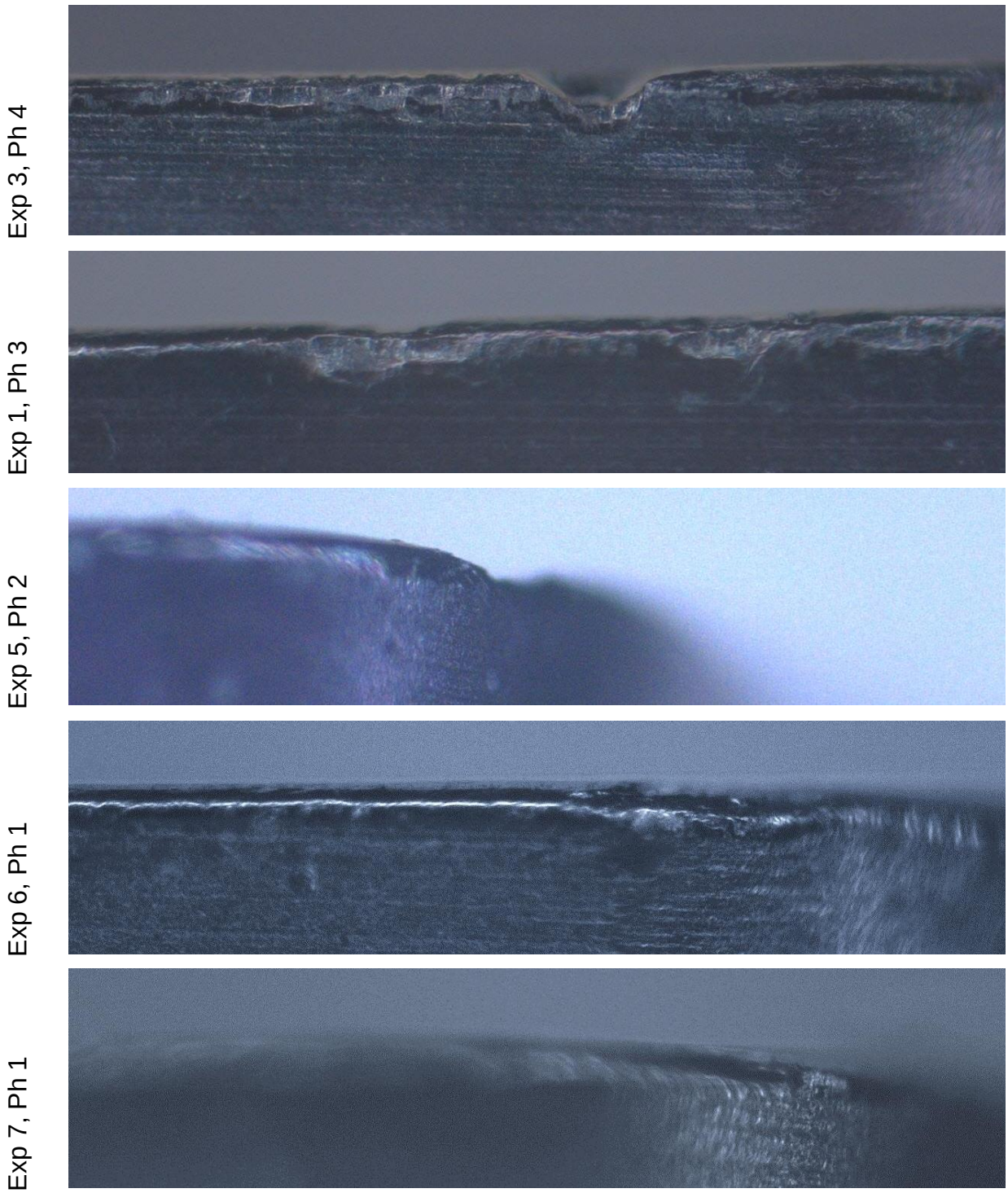
Exp 3, Ph 4
Exp 1, Ph 3
Exp 5, Ph 2
Exp 6, Ph 1
Exp 7, Ph 1

Appendix: Software design

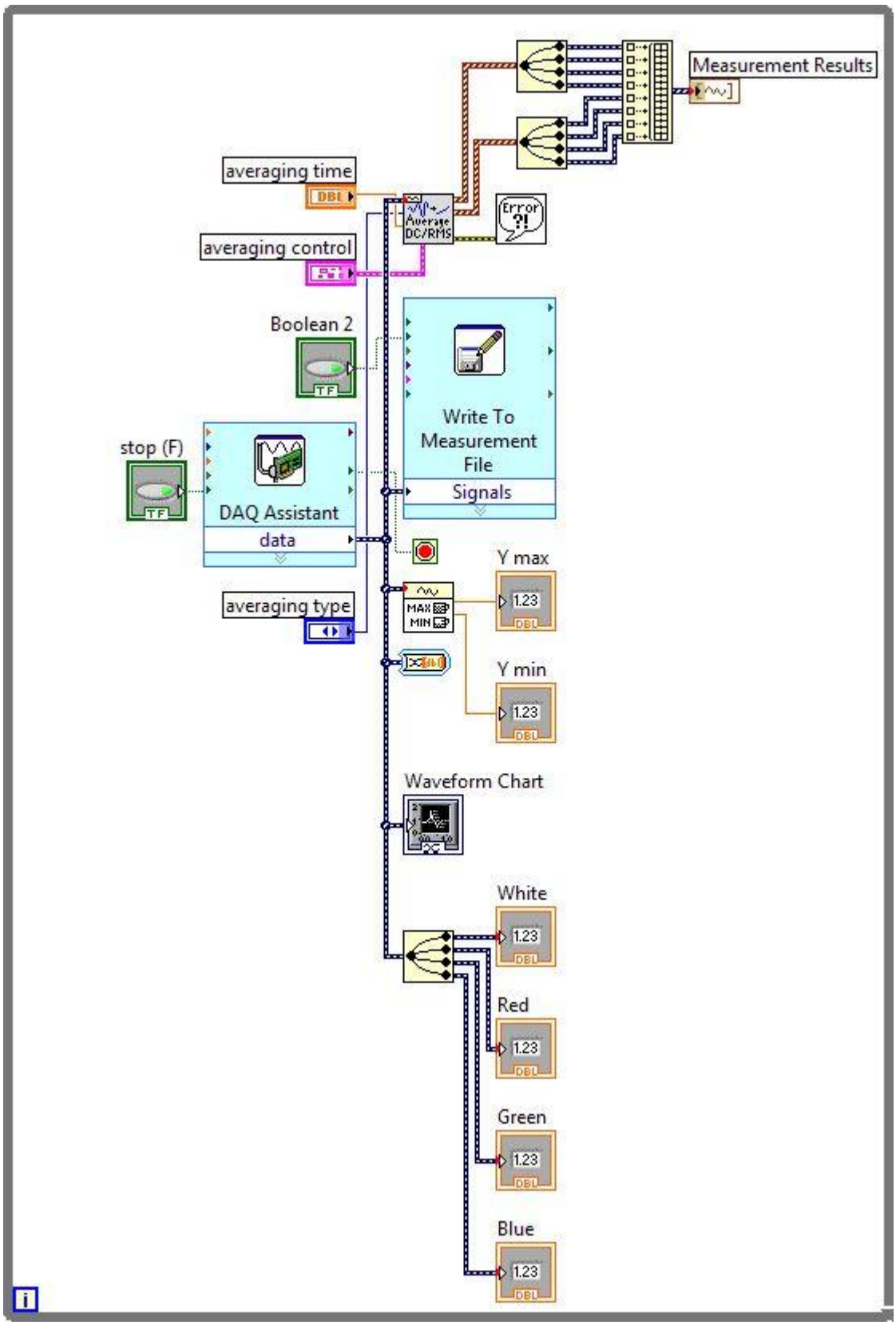

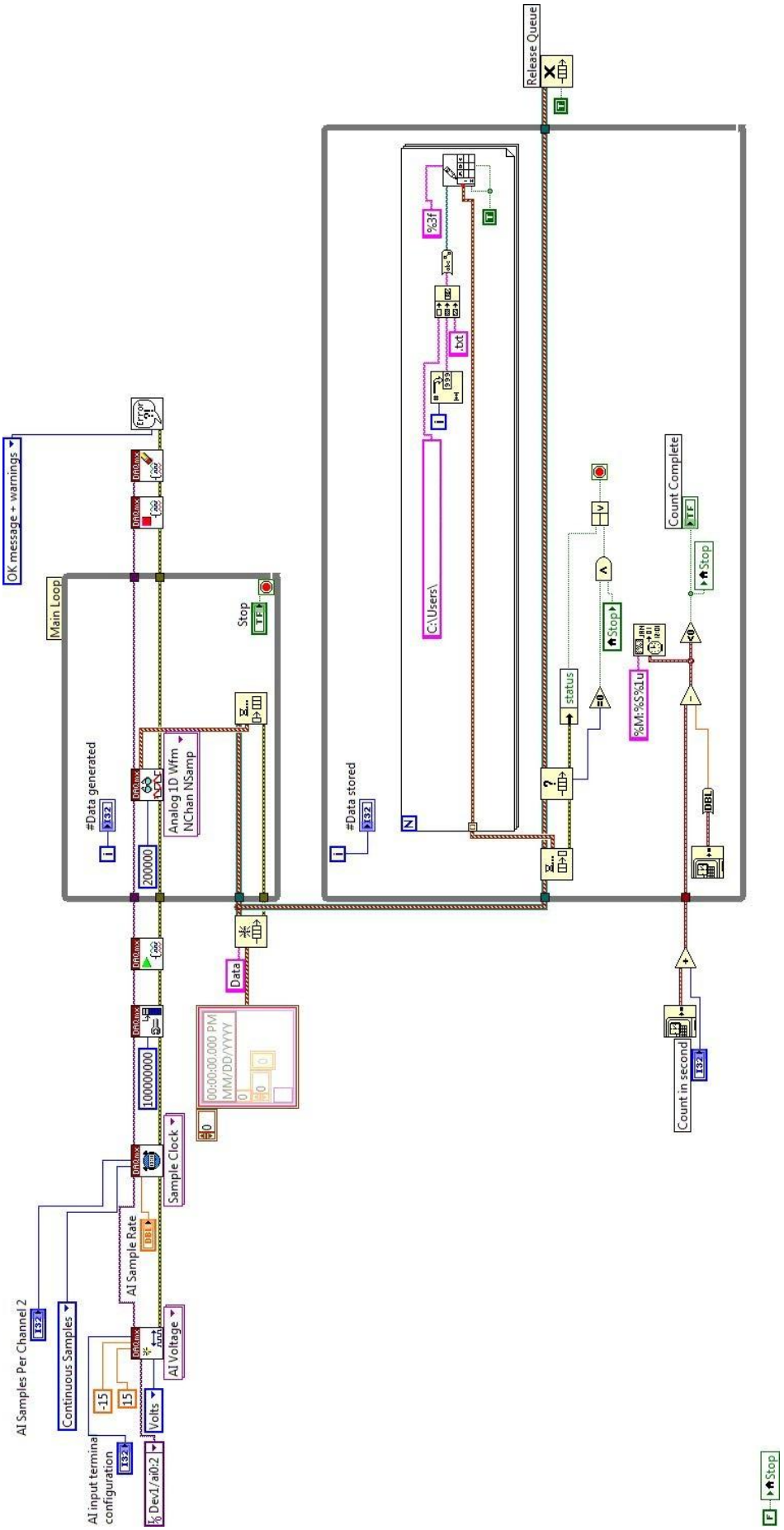
Release Queue
OK message + warnings
Main Loop
Stop
#Data generated
Analog 1D Wfm
NChan NSamp
200000
#Data stored
C:\Users\
.txt
%3f
status
Count Complete
Stop
%M:%S%1u
Data
10000000
Sample Clock
AI Sample Rate
AI Voltage
AI Samples Per Channel 2
Continuous Samples
-15
15
Volts
AI input termina
configuration
Dev1/ai0:2
Count in second
Stop

Appendix: MATLAB Codes design

```
% This is the main line script
% load 'F:\IMPORTANT\exp7\data4 - Copy (3)\passes (2)\aural0.txt'
% initialisation script
RMS1 = [];
STAT1 = [];
WAVELET1 = [];
n = 0;


% n = 0;
n = n + 1;
k = n;

[a b c d e] = split (data);
[a1 b1 c1 d1 e1] = filtering (a,b,c,d,e,k);
h = freq (a1,b1,c1,d1,e1,k);
h = wavelet (c);

[a2 b2 c2 d2 e2] = arhermes(a1,b1,c1,d1,e1,...
    0.0012*2000000, 0.0000005*2000000,k);

% RMS = [];
crms = size (RMS1,1);
crms = crms + 1;
RMS1 (crms, 1) = getrmsfeat(a1,128000,300);

% STAT = [];
cstat = size (STAT1,1);
cstat = cstat + 1;
STAT1 (cstat, :) = [ mean(c2) std(c2) var(c2)...
    max(c2) min(c2) range(c2) skewness(c2)...
    kurtosis(c2)];

% WAVELET = [];
cwav = size (WAVELET1,1);
cwav = cwav + 1;
WAVELET1 (cwav, :) = h;

if ishandle(1);
close figure 1;
close figure 2;
close figure 3;
end

clear a b c d e a1 b1 c1 d1 e1 a2 b2 c2 d2...
    e2 cstat cwav crms k h data
```

```
function [a, b, c, d, e] = split(data1)

%UNTITLED2 Summary of this function goes here
%   This script is used to extract features from the acoustic
%   emission data bundle from the data acquisition system
%
a = data1(10000001:10128000,1);
b = data1(11000001:11128000,1);
c = data1(12000001:12128000,1);
d = data1(13000001:13128000,1);
e = data1(14000001:14128000,1);

end

function [b1, b2, b3, b4, b5] = filtering(a1,a2,a3,a4,a5,k)

Fs = 2000000;               % Sampling Frequency
Fstop = 96000;              % Stopband Frequency
Fpass = 120000;             % Passband Frequency
Dstop = 0.00056234132519;   % Stopband Attenuation
Dpass = 0.057501127785;     % Passband Ripple
dens  = 20;                 % Density Factor

% Calculate the order from the parameters using FIRPMORD.
[N, Fo, Ao, W] = firpmord([Fstop, Fpass]/(Fs/2), [0 1], [Dstop, Dpass]);

% Calculate the coefficients using the FIRPM function.
b  = firpm(N, Fo, Ao, W, {dens});

b1 = filter(b,1,a1);
b2 = filter(b,1,a2);
b3 = filter(b,1,a3);
b4 = filter(b,1,a4);
b5 = filter(b,1,a5);

Tp=1/Fs;
tm=linspace(Tp,0.064,128000);

h = figure;
subplot (3,2,1); plot(tm,b1 )
xlabel('Time (Sec)')
ylabel('AE Signal (V)')
title('AE signal wave')
subplot (3,2,2); plot(tm,b2 )
xlabel('Time (Sec)')
ylabel('AE Signal (V)')
title('AE signal wave')
.
.

filename = [ 'C:\Users\Masters Research\Result\review\wave' num2str(k) ];
saveas (h,filename,'jpg');
end
```

```
function [ h ] = freq( a1,b1,c1,d1,e1,k )
% %UNTITLED8 Summary of this function goes here
% %   Detailed explanation goes here

% Fs = 2000000;
% Tp = 1/Fs;
% tm = linspace(Tp,0.064,128000);

Qa = fft(a1,2048);
Pya = Qa.*conj(Qa)/2048;
Qb = fft(b1,2048);
Pyb = Qb.*conj(Qb)/2048;
Qc = fft(c1,2048);
Pyc = Qc.*conj(Qc)/2048;
Qd = fft(d1,2048);
Pyd = Qd.*conj(Qd)/2048;
Qe = fft(e1,2048);
Pye = Qe.*conj(Qe)/2048;

fstep = 2000000/2048*(0:1015);

h = figure;
subplot (3,2,1); plot(fstep,Pya(1:1016));
xlabel('Frequency (MHz)');
ylabel('PSD(V^2/Hz)');
title('Power spectral density');
subplot (3,2,2); plot(fstep,Pyb(1:1016));
xlabel('Frequency (MHz)');
ylabel('PSD(V^2/Hz)');
title('Power spectral density');
subplot (3,2,3); plot(fstep,Pyc(1:1016));
xlabel('Frequency (MHz)');
ylabel('PSD(V^2/Hz)');
title('Power spectral density');
subplot (3,2,4); plot(fstep,Pyd(1:1016));
xlabel('Frequency (MHz)');
ylabel('PSD(V^2/Hz)');
title('Power spectral density');
subplot (3,2,5); plot(fstep,Pye(1:1016));
xlabel('Frequency (MHz)');
ylabel('PSD(V^2/Hz)');
title('Power spectral density');

filename = [ 'C:\Users\Masters Research\Result\review\freq' num2str(k) ];
saveas (h,filename,'jpg');

end
```

```
function [ay, by, cy, dy, ey] = arhermes(a3,b3,c3,d3,e3, windowlength, downsampling,k)
%UNTITLED9 Summary of this function goes here
%   Detailed explanation goes here

wgts = exp(-[1:6*windowlength]/windowlength);
b = wgts/windowlength;

a3 = a3.^2; % Square the samples
asignal_averaged = filter(b,[1],a3); amm = [1:downsampling:length(a3)];
saa = asignal_averaged(amm); ay = sqrt(saa);

b3 = b3.^2; % Square the samples
bsignal_averaged = filter(b,[1],b3); bmm = [1:downsampling:length(b3)];
sab = bsignal_averaged(bmm); by = sqrt(sab);

c3 = c3.^2; % Square the samples
csignal_averaged = filter(b,[1],c3); cmm = [1:downsampling:length(c3)];
sac = csignal_averaged(cmm); cy = sqrt(sac);

d3 = d3.^2; % Square the samples
dsignal_averaged = filter(b,[1],d3); dmm = [1:downsampling:length(d3)];
sad = dsignal_averaged(dmm); dy = sqrt(sad);

e3 = e3.^2; % Square the samples
esignal_averaged = filter(b,[1],e3); emm = [1:downsampling:length(e3)];
sae = esignal_averaged(emm); ey = sqrt(sae);

Fs = 2000000; Tp=1/Fs; tm=linspace(Tp,0.064,128000);

h = figure;
subplot (3,2,1); plot(tm,ay);
xlabel('Time (Sec)'); ylabel('AE Signal (V)')
title('AE signal wave')
subplot (3,2,2); plot(tm,by)
xlabel('Time (Sec)'); ylabel('AE Signal (V)')
title('AE signal wave')
subplot (3,2,3); plot(tm,cy)
xlabel('Time (Sec)'); ylabel('AE Signal (V)')
title('AE signal wave')
subplot (3,2,4); plot(tm,dy)
xlabel('Time (Sec)'); ylabel('AE Signal (V)')
title('AE signal wave')
subplot (3,2,5); plot(tm,ey)
xlabel('Time (Sec)'); ylabel('AE Signal (V)')
title('AE signal wave')
filename = [ 'C:\Users\Masters Research\Result\review\rms' num2str(k) ];
saveas (h,filename,'jpg');
end
```

```
function [ wav ] = wavelet( s )
% l_s = length(s);
[C,L]=wavedec(s,5,'db3');

% Do a multi-level analysis to five levels with the
% Daubechies-3 wavelet
A5=wrcoef('a',C,L,'db3',5);
D1=wrcoef('d',C,L,'db3',1);
D2=wrcoef('d',C,L,'db3',2);
D3=wrcoef('d',C,L,'db3',3);
D4=wrcoef('d',C,L,'db3',4);
D5=wrcoef('d',C,L,'db3',5);

Fs=2000000; Tp=1/Fs; tm=linspace(Tp,0.064,128000);

d1=D1.*D1; d2=D2.*D2; d3=D3.*D3; d4=D4.*D4; d5=D5.*D5; a5=A5.*A5;

% Feature Extraction by using
% sum of absolute divided by total sample

feat1 = sum(abs(s))/128000;
feat2 = sum(abs(D1))/128000;
feat3 = sum(abs(D2))/128000;
feat4 = sum(abs(D3))/128000;
feat5 = sum(abs(D4))/128000;
feat6 = sum(abs(D5))/128000;

featset1 =[feat1 feat2 feat3 feat4 feat5 feat6];

% Feature Extraction by using
% sum of energy components

energy_d1= trapz(tm,d1);
energy_d2= trapz(tm,d2);
energy_d3= trapz(tm,d3);
energy_d4= trapz(tm,d4);
energy_d5= trapz(tm,d5);
energy_a5= trapz(tm,a5);

G_Tot = energy_d1+energy_d2+energy_d3+energy_d4+...     % Sig=s.*s;
energy_d5+energy_a5;        % energy = trapz(tm,Sig);

wav (1, :) = [ feat1 feat2 feat3...
    feat4 feat5 feat6 G_Tot];

end
```

```
% ************************************************************************
% This part of the program is used to create a neural network for training
% with the following settings.

% NN training for deriving sensor data from process parameter and condition
% inputs of the NN: feed,speed,and time domain features
% outputs of the NN: wear condition, not worn, half worn, broken tool
% ************************************************************************

[PN,PS] = mapminmax(P); % Create your input data set e.g. P = a(:,1:5)';
[TN,TS] = mapminmax(T); % Create your target data set e.g. T = a(:,7:9)';

research = newff(minmax(Po),minmax(To),[20 20],{'logsig','logsig',...
    'logsig','logsig'},'traingdx');
research.trainParam.epochs = 1000;
research.trainParam.lr = 0.3;
research.trainParam.mc = 0.7;
research.layers{3}.dimensions = 3;
research.trainParam.show = 50;
research.divideFcn = '';
research.performFcn = 'mse';

randn('seed',192736);
[research,tr]=train(research,Po,To);

z = Po (:,120);
test = sim(research, z);
bar(test,'DisplayName','test');figure(gcf);


% In line command

for i = 0:length(S)
    my_p(i+1) = correlate(i, speed, S);
end

% In line command as well "my_p = "

min_rho = min(my_p); max_rho = max(my_p);

if (abs(min_rho) > abs(max_rho))
    disp(sprintf('min correlation coeff: %5.4f', min_rho))
else
    disp(sprintf('max correlation coeff: %5.4f', max_rho))
end
```